RESEARCH REPORT **RR 89/149**

DEPARTMENT OF TRANSPORT

The use of the DRTT K-mould to determine the elastic and shear properties of pavement materials

April 1991

TITEL/TITLE: THE USE OF THE DRTT K-MOULD TO DETERMINE THE ELASTIC AND SHEAR PROPERTIES OF PAVEMENT MATERIALS

VERSLAG NR: **REPORT NO:** RR 89/149	**ISBN:**	**DATUM:** **DATE:** April 1991	**VERSLAGSTATUS:** **REPORT STATUS:** Final

NAVORSINGS NR/RESEARCH NO: RR 89/149

GEDOEN DEUR:
CARRIED OUT BY:
Division of Roads and Transport Technology, CSIR
P O Box 395
PRETORIA
0001

OPDRAGGEWER:
COMMISSIONED BY:
Director General : Transport
Private Bag X193
PRETORIA
0001

OUTEUR(S):
AUTHOR(S):
C J Semmelink

NAVRAE:
ENQUIRIES:
Department of Transport
Directorate : Transport Economic Analysis
Private Bag X193
PRETORIA
0001

SINOPSIS:

Die meganistiese plaveiselontwerptegnieke wat in Suid-Afrika gebruik word benodig waardes vir die materiaalparameters E_i, $E_d(M_R)$, ν, c en ϕ. Omdat dit relatief moeilik en duur is om hierdie parameters akkuraat te bepaal, word gewoonlik van geskatte waardes gebruik gemaak, wat aanleiding mag gee tot konserwatiewe plaveiselontwerpe. Die K-druksel is 'n eenvoudige apparaat waarmee hierdie parameters vinnig, effektief en relatief goedkoop bepaal kan word vanaf digtheidsmonsters wat gebruik word om voggehalte-digtheidskurwes vas te stel. Hierdie verslag bespreek kortliks die teoretiese agtergrond van die K-druksel, die ontwikkeling daarvan en die resultate wat daarmee verkry is op 'n aantal onbehandelde padbou-materiale.

SYNOPSIS:

The mechanistic pavement design methods employed in South Africa require input values for the material parameters E_i, $E_d(M_R)$, ν, c and ϕ. Because of the difficulty and cost involved to determine these parameters accurately use is often made of estimated values, which may lead to conservative pavement designs. The K-mould is a simple instrument with which these parameters can be determined rapidly, effectively and relatively inexpensively utilising samples compacted for establishing the moisture-density curves. This report briefly discusses the theoretical background of the K-mould, its development and the results obtained with it on a number of untreated roadbuilding materials.

TREFWOORDE:
KEYWORDS: K-mould, stress, elastic moduli, friction angle, cohesion

VERSLAGKOSTE:
REPORT COST:

DISCLAIMER

The views and opinions expressed in this report are those of the author and do not represent Department of Transport Policy.

LIST OF CONTENTS

LIST OF TABLES

LIST OF FIGURES

LIST OF SYMBOLS

E_1	=	elastic modulus of soil
$E_d(M_R)$	=	modulus of resilience
K_o-line	=	line through q vs p for soil subject to one dimensional strain
K_f-line	=	line through q vs p for soil subject to multi dimensional strain
ν	=	Poison's ratio
c	=	adhesion component of friction force of soil
ϕ	=	friction angle of soil
σ_1	=	the main axial stress (i.e vertical stress)
σ_3	=	the secondary axial stress (i.e radial stress)
σ_i	=	$-a.\tan\alpha = -c.\cot\phi$
σ'_1	=	$\sigma_1 - \sigma_i$
σ'_3	=	$\sigma_3 - \sigma_i$
a	=	intercept of q - p graph on q-axis
α	=	angle of the q versus p graph
q	=	$(\sigma_1 - \sigma_3)/2$
p	=	$(\sigma_1 + \sigma_3)/2$
ε_1	=	vertical strain
ε_3	=	radial strain

1. INTRODUCTION

The mechanistic pavement design models applied in South Africa require input values for the material design parameters E_l, $E_d(M_R)$, ν, c and ϕ . These parameters are mainly determined with triaxial compression tests or shear box tests in a laboratory but because of the expensive and time-consuming nature of such tests, estimated values are often accepted. Properties designed for and those achieved during construction are rarely correlated and quality control on site consists mostly of acceptance limits for the density, grading and Atterberg Limits of constructed layers.

A complicating factor in this situation is the fact that some concerns exist with regard to the validity of triaxial tests for determining soil properties. Handy et al comment that loading by a foundation or wheel load involves the application of a vertical load to the underlying supporting soil, that in turn must excite a simultaneous increase in the horizontal stress in that soil. The only conditions allowing a constancy of lateral stress in field loading is for materials with a Poisson's ratio of zero, such as peat, or situations where the soil is in failure and no additional horizontal restraint is available, as in a bearing capacity failure[1].

The K-mould is a mechanical device for rapidly testing a soil specimen and which automatically increases the lateral restraint as the specimen is being vertically loaded. Handy et al claimed that the K-test simulates an undrained, rapid field-loading situation and that it appears particularly applicable for transportation facilities[2].

2. DESCRIPTION OF THE K-MOULD AND ITS THEORETICAL BACKGROUND

The K-mould may be described as any of several mechanical devices that automatically increase the lateral restraint on a soil specimen as it is being vertically loaded. The result is a confined compression test but with a constant or controlled horizontal modulus rather than a constant or controlled horizontal stress. An advantage over the triaxial stress path method is that the horizontal stress need not be calculated in advance on the basis of elastic theory and an assumed K_o, but seeks its own value. Another advantage is that axially rigid but laterally flexing walls distribute strain uniformly through the specimen rather than to allow bulging in the middle, as typically occurs in the triaxial test[1].

"A unique feature of a K-test system is that by following along either a K_o consolidation stress path or K_f shear failure stress path or something in between, a travelling Mohr circle is obtained that traces the entire envelope from one test on a single specimen" (see Figure 2.1)[1]. The slope α of the graph readily converts to a friction-angle ϕ, as shown in Figure 2.2.

From Figure 2.2 follows :

$$\sin \phi = BD/AB = 0{,}5.(\sigma'_1 - \sigma'_3)/0{,}5.(\sigma'_1 + \sigma'_3) = (\sigma'_1 - \sigma'_3)/(\sigma'_1 + \sigma'_3)$$

$$\tan \alpha = BC/AB = 0{,}5.(\sigma'_1 - \sigma'_3)/0{,}5.(\sigma'_1 + \sigma'_3) = (\sigma'_1 - \sigma'_3)/(\sigma'_1 + \sigma'_3)$$

$$\therefore \quad \sin \phi = \tan \alpha = (\sigma_1 - \sigma_3)/(\sigma_1 + \sigma_3 - 2\sigma_i) \qquad \text{.....Eq.1}$$

Furthermore

$$-\sigma_i = a.\cot \alpha$$

$$-\sigma_i = c.\cot \phi$$

$$\therefore \quad c = -\sigma_i.\tan \phi$$

$$= a \cot \alpha.\tan \phi$$

$$= (a/\tan \alpha).\tan \phi$$

$$= (a/\sin \phi)(\sin \phi/\cos \phi)$$

$$= a.\sec \phi \qquad \text{.....Eq.2}$$

Apart from being able to determine c and ϕ the K-test allows simultaneous monitoring of vertical and lateral strain and volume change. From this data it is possible to determine the E-values as well as Poisson's ratio ν, assuming that the test sample is a homogenous, isotropic, elastic material :

$$E = \sigma_1 / \varepsilon_1 \qquad \text{.....Eq.3}$$

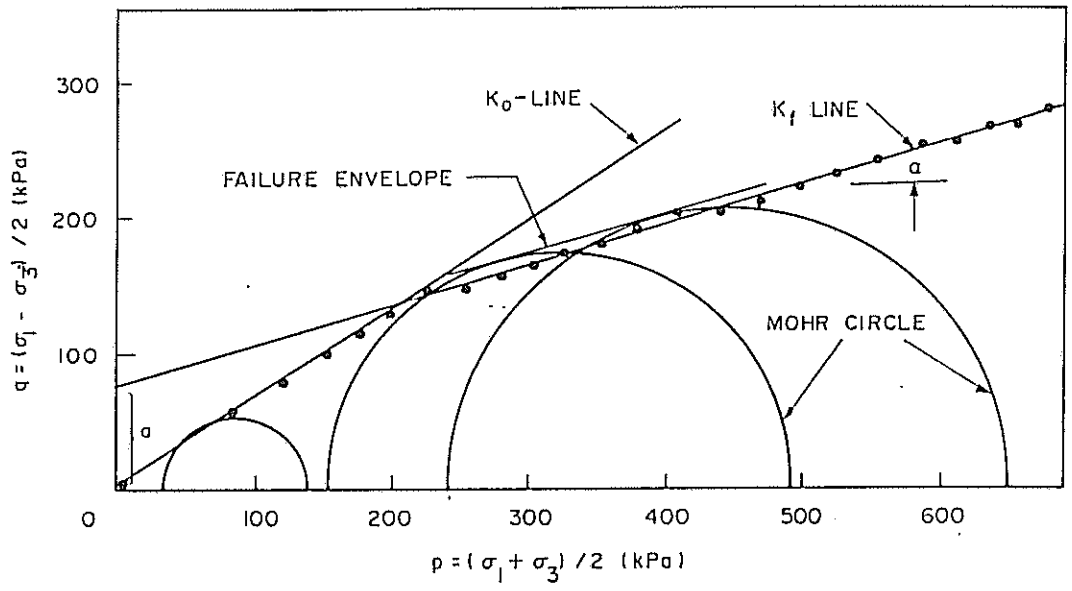

FIGURE 2.1 - STRESS PATH OF A COMPACTED SILTY CLAY FROM HANDY ET AL[1]

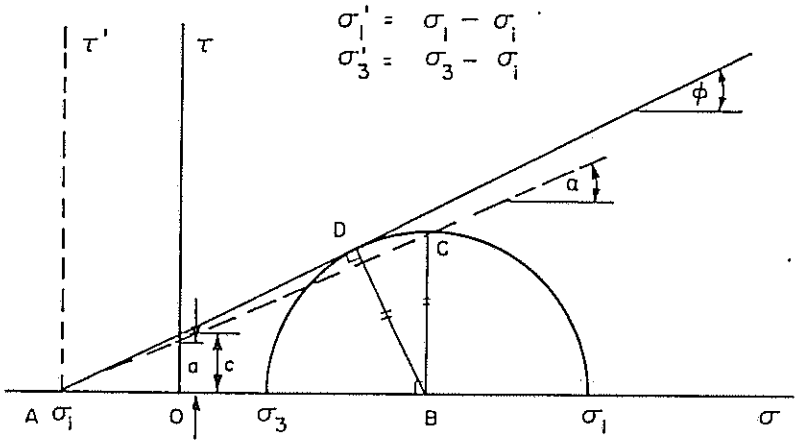

FIGURE 2.2 - RELATION BETWEEN α AND ϕ; AND a AND c

For the three-dimensional loading situation the following applies:

$$\varepsilon_1 = (1/E).(\sigma_1 - 2\nu.\sigma_3)$$

$$\varepsilon_3 = (1/E).(\sigma_3 - \nu.(\sigma_1 + \sigma_3))$$

where ε_1 = vertical strain

ε_3 = radial strain

σ_1 = vertical stress

σ_3 = radial stress

ν = Poisson's ratio

It can now be shown that :

$$E = (\sigma_1 - 2\nu.\sigma_3)/\varepsilon_1 = (\sigma_3 - \nu.(\sigma_1 + \sigma_3))/\varepsilon_3$$

And therefore

$$\varepsilon_3.(\sigma_1 - 2\nu.\sigma_3) = \varepsilon_1.(\sigma_3 - \nu.(\sigma_1 + \sigma_3))$$

Also,

$$\nu.(\varepsilon_1.(\sigma_1 + \sigma_3) - 2\,\varepsilon_3.\sigma_3) = \varepsilon_1.\sigma_3 - \varepsilon_3.\sigma_1$$

So that

$$\nu = (\varepsilon_1.\sigma_3 - \varepsilon_3.\sigma_1)/(\varepsilon_1.(\sigma_1 + \sigma_3) - 2\,\varepsilon_3.\sigma_3) \quad \text{.....Eq.4}$$

The K-test may be criticised as not measuring pore pressure (although pore pressures can be monitored), and therefore being more conducive to total stress than effective stress analysis. However, this appears appropriate for pavement design because of the rapid loading cycles and unpredictability of pore pressures under typical field loading conditions.[1]

The lateral stiffness of the K-mould has an effect on the measured parameters c, ϕ, E and ν. Handy et al, concluded that a "soft" K-system will tend to give failure shear parameters but with an initial stage of transfer from K_o to K_f conditions that may result in an overestimation of ϕ and an underestimation of c. Also a "stiff" K-test system will tend to give consolidation shear parameters with lower c and ϕ values than the maximums that can be developed during shear failure.[1]

For pavement design purposes the stiff system may therefore be the more preferable, particularly as the dilatancy (i.e. the expansion of deformed masses of granular material, such as sand due to the rearrangement of the component grains) that contributes to peak strength parameters also weakens the soil to resist successive repeated load cycles.

The K-mould can also be used for repeated loading tests. The modulus of resilience (M_R) is then obtained. Insertion of a K-test module into a cyclical load frame allows vertical and lateral deformations and lateral stress to be recorded versus repetitions of a preset load.[1]

3. DEVELOPMENT OF THE K-MOULD

The original concept of the K-mould was developed at the Iowa State University under the guidance of professor R L Handy. The current American version consists of a 100 mm (4 inch) diameter mould to take normal Proctor samples. Since local practice uses 152,4 mm diameter samples, it was felt that the right approach would be to develop a K-mould of similar diameter so that the sample used to determine moisture-density curves can also be utilized to determine the parameters E_1, $E_d(M_R)$, ν, c and ϕ.

Professor Handy was kind enough to send some design drawings for the basic manufacture of a 152,4 mm diameter K-mould. This design has not been tried and tested as yet in the USA.

The first prototype K-mould developed by the Division of Roads and Transport Technology (DRTT) varies slightly from the proposed design of professor Handy but is based on the original 100 mm diameter Handy K-mould (see Figure 3.1). It was machined from high-quality steel and case-hardened to prevent grooving of the internal mould surface by hard rock particles during the tests. This is necessary to limit material-to-steel friction forces which may yield erroneous results. Because the mould was slightly deformed by the heat treatment it was rebored to an internal diameter of 152,4 mm diameter.

The second prototype K-mould (see Figure 3.2) developed at the DRTT consists of an internal thick-walled cylinder (with an internal diameter of 152,4 mm) made up of eight equal case-hardened circular segments. Each segment is mounted on two horizontal shafts which fit into two radially mounted linear ball bearings to allow each segment to move freely in a radial direction. The linear bearings are mounted on an outer thick-walled cylinder which also support sixteen mountings housing the springs which apply radial forces to the internal segmented cylinder.

The main advantage of this model is that the stiffness of the mould is infinitely variable and can therefore be adjusted to simulate the inherent lateral support of the material in its natural state. It is even possible to laterally preload the sample to any required level before any vertical load is applied, by ensuring that the springs are already slightly compressed when the spring mountings are in their locked position (tightened). The level of preloading is controlled by the adjustable spring mounting whereby the amount of initial compression of the springs can be set. The mould allows the material to deform radially and, because of its eight segments, also allows substantially larger total deformations than is possible with the original model. Furthermore, because the lateral spring force can be totally removed by unlocking of the spring mountings, it is far easier to load and remove the material samples.

As a supplementary measure to reduce the material-to-steel friction as far as possible, the internal surfaces of the top and bottom end plates and the internal surfaces of both K-moulds are sprayed with the lubricant WD-40 before testing. This is done instead of using a thin Teflon lining which would be more costly.

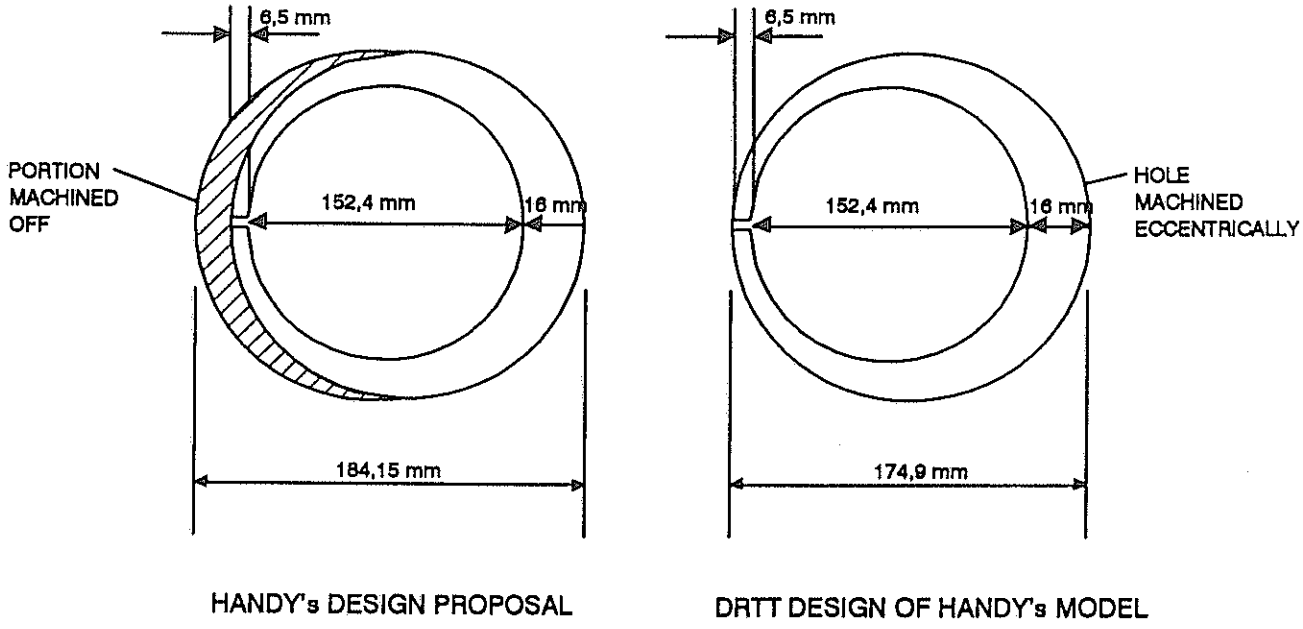

FIGURE 3.1 - COMPARISON OF TWO K-MOULD DESIGNS OF HANDY'S MODEL

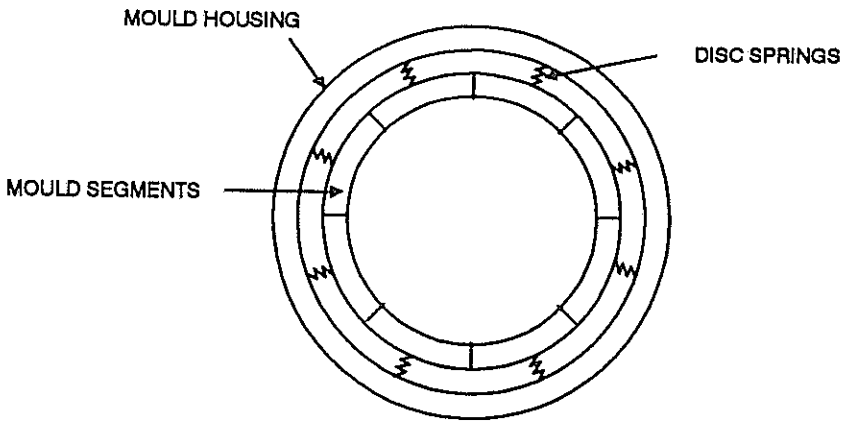

FIGURE 3.2 - SCHEMATIC PRESENTATION OF THE DRTT K-MOULD

4. MEASURING APPARATUS

Vertical loads applied to the mould are measured with two electronic load cells. The bottom load cell is contained in a base mounting plate in such a way that the vertical force on the sample itself at the bottom is measured by the load cell but the material-to-steel friction force is not picked up. The benefits of this approach are discussed elsewhere.[1] The vertical deformation is measured on the top end plate by three linear potentiometers mounted at 120° intervals on a circular plate, in order to determine the average vertical deformation (see Figure 4.1).

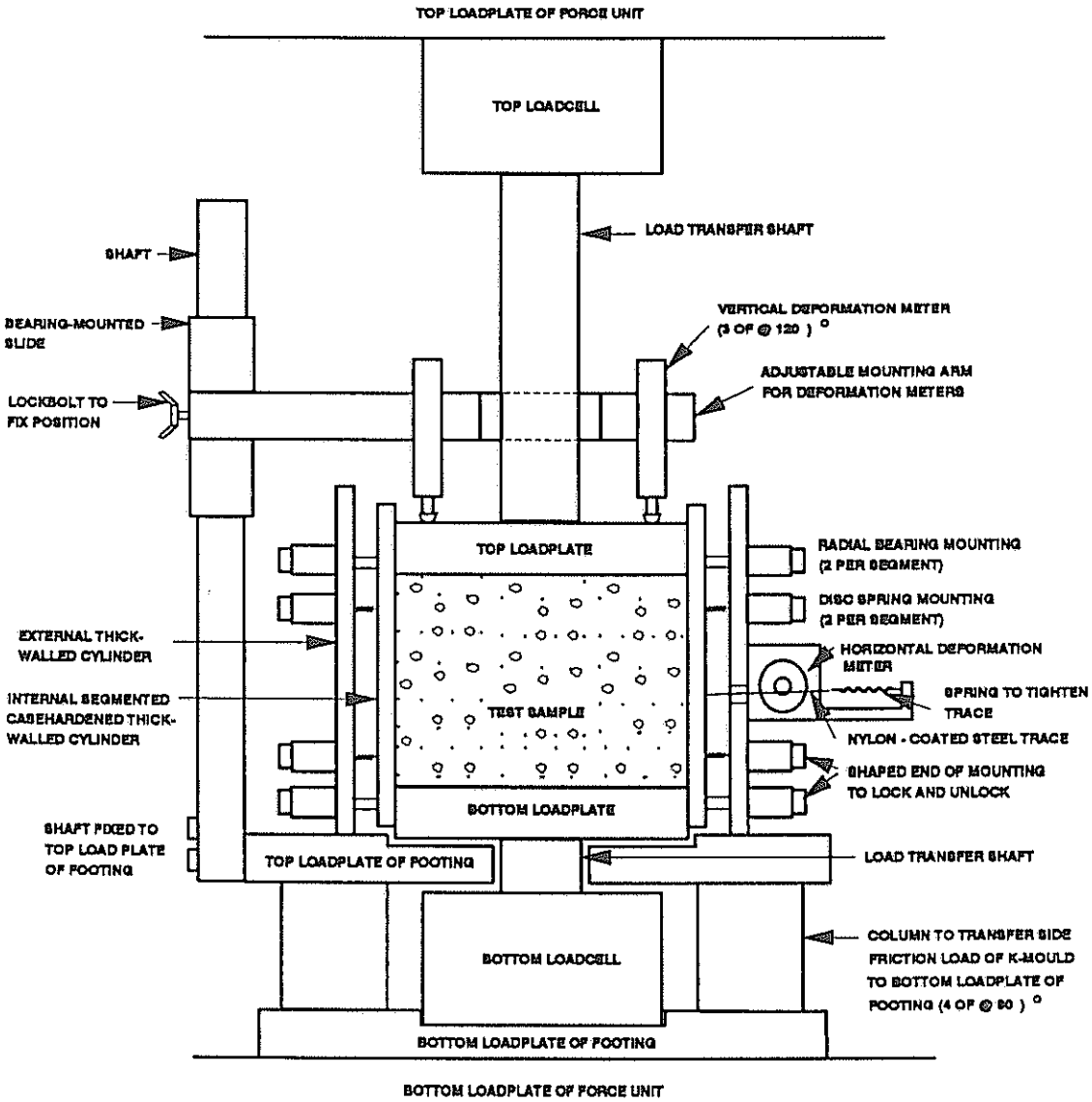

FIGURE 4.1 - SCHEMATIC SIDE VIEW OF K-MOULD SET-UP

In the centre of this plate a large enough hole allows a steel shaft of 50 mm diameter to transfer the load to the sample freely. The lateral deformation is measured with a circular potentiometer which captures the movement of a thin spring-loaded nylon-coated stainless steel cable which is wrapped once around the internal cylinder and fixed to the outer thick-walled cylinder of the mould. This movement is then converted to a radial expansion. The signals of the load cells and potentiometers are simultaneously recorded on a multi-channel analogue cassette recorder and transferred to computer memory with an analogue-to-digital interface which allows for rapid transfer of data. The load force is being applied by either a 300 kN or 1 300 kN Baldwin press. The load cells can measure a maximum load of 200 kN.

Because the load cell output signals are very small, use is made of two amplifiers to improve the accuracy of the data. Both the load cells and potentiometers were properly calibrated before use.

5. THE CALIBRATION OF THE LATERAL MOULD STIFFNESS

To calibrate the Handy model of the K-mould use is made of a very soft silicone rubber dummy sample for which it is assumed that σ_3 is equal to the σ_1. The lateral mould stiffness (E_3) is then determined by dividing σ_1 by the lateral strain (ε_3). An appropriate silicone rubber could not be obtained locally and had to be imported from the USA. This method was also used to calibrate the original 100 mm diameter models. For similarity it was decided to use the same approach with the DRTT model. Loading was repeated a number of times and the calculated average E_3 was assumed to be the stiffness of the mould. For the DRTT model, the stiffness clearly changed as the spring configuration was changed.

The springs used in the DRTT model consist of small disc springs (which look like dome shaped washers) which make it possible to vary the stiffness by varying their stacking pattern and the number of discs used (the length of the spring). Different stacking patterns were evaluated for one disc size (12 mm outer diameter, 4,2 diameter central hole, 0,6 mm material thickness and 1,0 mm height). The results are given in Table 5.1 (dummy sample height = 105,1 mm). The stiffness can be further varied by the use of different disc sizes.

TABLE 5.1 - MOULD STIFFNESSES OF DRTT MODEL FOR DIFFERENT STACKING PATTERNS OF DISC SPRINGS AND HANDY'S MODEL

STACK HEIGHT (DISCS PER STACK)	NUMBER OF STACKS PER SPRING	TOTAL DISCS PER SPRING	MEASURED E3 kPA	STIFFNESS RATIO (MEASURED)*	STIFFNESS RATIO (THEORETI-CAL)**
7	2	14	112 237	23,70	(7/1)(14/2) = 49,00
4	3	12	85 116	17,98	(4/1)(14/3) = 18,67
2	7	14	15 905	3,36	(2/1)(14/9) = 4,00
1	7	7	9 575	2,02	(1/1)(14/7) = 2,00
1	14	14	4 735	1	1
Handy's model	-	-	58 800	-	-

* Measured stiffness ratio = (Measured E_3)/4735 (= measured mould stiffness / mould stiffness of weakest spring)

** Theoretical stiffness ratio = (Stack height/1) x (14/Number of stacks per spring)

6. MATERIALS EVALUATED IN THE RESEARCH PROJECT

Because a substantial amount of information had been collected on the materials used in the research project on the compactability of roadbuilding materials[4], and because these materials covered a very wide range of roadbuilding materials, it was decided to use some of these materials in this research project. This would also cut out unnecessary duplication of testing.

For the sake of convenience, the materials were divided into three main groups, as follows:

- fine materials
- natural gravels
- crushed stone materials

Four materials were selected from each group for the initial analysis (see Table 6.1).

Apart from these twelve materials, four G2 materials being used in the research project on the compactability of G2 crushed stone materials using the CPA specification requirements were also evaluated. (See Table 6.1)

Two materials from the HVS site at Bultfontein were also evaluated to see whether the results obtained with the K-mould tie in with the E-moduli which were determined from the back calculation of the multi-depth deflectometer measurements. The materials were the G1 crushed stone base material and the in-situ ferricrete material. For comparison purposes the K-mould samples were tested at density levels and moisture contents approximately similar to those recorded on site at the time when the multi-depth deflectometer measurements were recorded.

TABLE 6.1 - LIST OF MATERIALS AND THEIR BASIC DESCRIPTION

MATERIAL CATEGORY	SAMPLE	MATERIAL TYPE	TRB-PRA CLASSIFICATION
Fine material	KBAB	Black clay (montmorrillonite)	A-7-6 (17)
Fine material	SPK	Red sandy clay	A-6 (5)
Fine material	SILK	Silty sand	A-2-4 (0)
Fine material	KDW	Slightly plastic sand	A-2-4 (0)
Natural gravel	DENS7	Dolomitic soil	A-2-6 (0)
Natural gravel	LENC	Red chert soil	A-2-4 (0)
Natural gravel	NPAB	Decomposed dolerite	A-2-7 (0)
Natural gravel	TP2	Quartzite gravel	A-2-4 (0)
Crushed stone	FERRO	Quartzite crushed stone (G1)	A-1-a (0)
Crushed stone	ROSS	Granite crushed stone (G1)	A-1-a (0)
Crushed stone	NPAA	Dolerite crushed stone (G1)	A-1-a (0)
Crushed stone	NPAE	Tillite crushed stone (G1)	A-2-4 (0)
G2 material	CPA4	Crushed alluvial gravel	A-1-1 (0)
G2 material	CPA5	Crushed granite	A-1-a (0)
G2 material	CPA7	Crushed dolerite	A-1-a (0)
G2 material	CPA9	Crushed hornfels	A-1-a (0)

7. METHOD OF TESTING

The research project on the compactability of materials[2] clearly showed that the bearing capacity of materials is strongly influenced by the density level and the moisture content of the materials. It was therefore decided to evaluate each of the materials in this study at different levels of density and moisture contents. The density levels chosen for the fine materials and natural gravels were 90 %, 95 % and 100 % mod.AASHTO, expressed as a percentage of the "solid" density. The density levels for the crushed stone were approximately equivalent to 95 %, 100% and 105 % mod.AASHTO (see Table 7.1).

Because the compaction study also showed that there is a critical moisture content (CMC) for each material at which the highest CBR values are achieved for any level of density, it was decided to evaluate the materials at moisture contents of 0,75 CMC, CMC, 1,25 CMC, 1,50 CMC and 1,75 CMC. Some of the materials, such as the black clay samples, were also evaluated at moisture contents equal to or greater than 2,00 CMC to achieve a totally saturated sample (see Table 7.2).

TABLE 7.1 - EXPRESSION OF DIFFERENT LEVELS OF mod.AASTHO DENSITY IN TERMS OF "SOLID" DENSITY

MATERIAL SAMPLE	DENSITY LEVELS			
	90 % * mod.AASHTO (% AD)	95 % * mod.AASHTO (% AD)	100 % * mod.AASHTO (% AD)	MDD (vibratory) (% AD)
KBAB	53,62	56,60	59,58	59,11
SPK	62,19	65,40	69,10	71,01
SILK	63,38	66,90	70,42	73,72
KDW	68,78	72,60	76,42	78,12
DENS7	71,83	75,82	79,81	84,28
LENC	67,40	71,15	74,89	79,59
NPAB	68,45	72,25	76,05	77,44
TP2	69,48	73,34	77,20	82,14
FERRO	76,82	81,12	85,34	86,79
ROSS	78,38	82,77	87,07	86,64
NPAA	77,87	82,23	86,51	88,04
NPAE	80,99	85,52	89,97	88,33

* Respective density levels for crushed stone are approximately 95 %, 100 % and 105 % mod.AASHTO

TABLE 7.2 - SAMPLE NUMBER FOR DIFFERENT COMBINATIONS OF DENSITY AND MOISTURE CONTENT

MOISTURE CONTENT % CMC *	DENSITY LEVEL		
	90 % mod.AASHTO **	95 % mod.AASHTO **	100 % mod.AASHTO **
75	1	6	11
100	2	7	12
125	3	8	13
150	4	9	14
175	5	10	15
≥ 200	16	17	18

* CMC = Critical Moisture Content
** Respective density levels for crushed stone are approximately 95 %, 100 % and 105 % mod.AASHTO

The amount of dry material was calculated for a compacted sample height of 100 mm. To control the compacted sample height, use was made of an infra red sensor, which automatically switches off the vibratory compaction table as soon as the set height is reached (100 mm for fine materials and natural gravels, and 95 mm for crushed stone material). For most of the materials, it is virtually impossible to compact to the required density level when the moisture content of the material is approximately equal to the CMC of the material. To limit degradation of these materials during compaction, the compaction period was limited to four minutes maximum, if the required height had not been reached by then.

Immediately after compaction the average sample heights were determined by taking four measurements at 90° intervals with a vernier height gauge. In some cases the CBRs at moulding moisture content were also determined. In these cases the top surface of the samples were then scarified and levelled after which the samples were again briefly compacted (15 seconds) to give a firm level surface for testing the samples in the K-mould. In these cases the height measurement was then repeated.

The samples were then transferred from the compaction-mould to the K-mould by means of a special extruder press. This is normally only used in the case of dry, granular materials, where the sample tends to fall apart if removed without lateral support. In the case of more cohesive samples which don't collapse when the lateral support is removed, the sample was transferred manually. The side wall as well as the top and bottom end plates of the K-mould were lubricated with a silicon lubricant spray prior to transferring each sample.

The K-mould plus sample was then transferred to a Baldwin press where all the sensors and load cells are connected to an analogue cassette recorder. Each sample was then loaded once while the top and bottom loads and vertical and lateral deformations were recorded continuously during the whole loading cycle. After completion of the loading cycle the sample was removed from the K-mould and oven dried to determine its moisture content.

The analogue data was transferred to the computer by means of an analogue digital interface. Once this had been done, the data was processed to correct the mV signals to loads (kN) and deformations (mm). These values were then processed to determine the E-values of the material.

In the case of the G2 materials the approach was slightly different, in that the samples were all compacted for three minutes and the height of the samples were not controlled to reach specific density levels. The test in the K-mould was performed in the normal manner.

In the case of the materials from the HVS site at Bultfontein, the sample preparation also varied slightly. Because extremely high densities were measured on site, particularly in the G1 material (i.e 91 % AD) it was important to compact the crushed stone material as densely as possible on the vibratory table. This is only possible in the case of G1 materials if the sample is totally saturated. However, the field moisture content was much lower; therefore the samples had to be air-dried after compaction before testing in the K-mould.

8. THEORETICAL APPROACH OF DATA EVALUATION

In general it was found that the plot of σ_1 (Sigma-1) and σ_d (Sigma-d) against ε_1 (Epsilon-1) were well described by a third degree function of ε_1 (see Figure 8.1). The r^2-values for this relation for almost every sample evaluated was above 0,99 (see Examples in Appendix A).

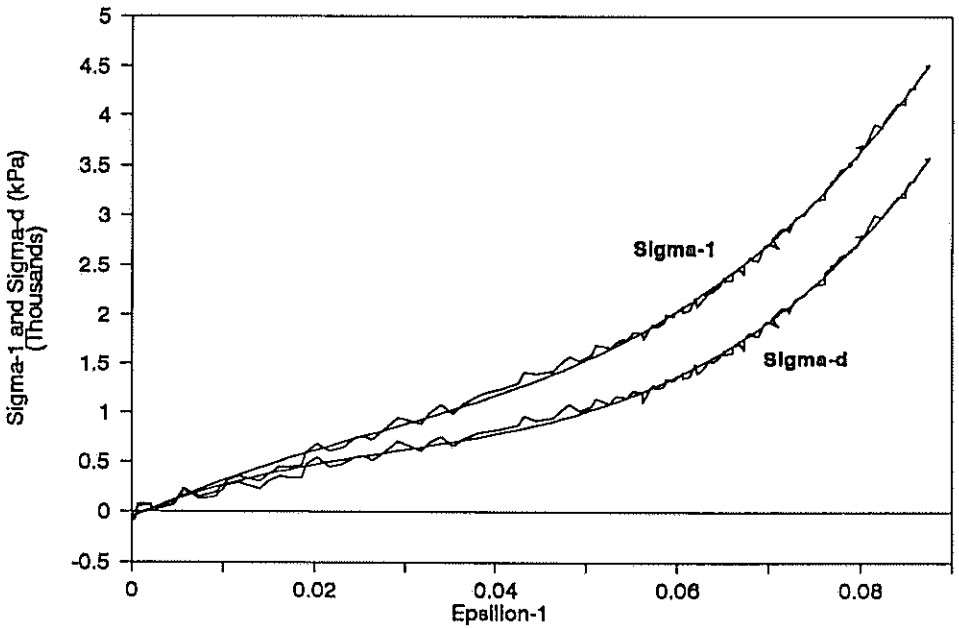

FIGURE 8.1 - EXAMPLE OF THE RELATION BETWEEN σ_1, σ_d AND ε_1

The smooth lines in Figure 8.1 are the best fitting curves of the respective third degree functions. The elastic modulus (E_1) and modulus of resilience (M_R)(E_d) as they are known in road engineering are actually the slopes of these curves ($=d\sigma/d\varepsilon_1$). Strictly speaking, M_R is defined as the material stiffness as measured under dynamic loading (to simulate wheelloading). Furthermore, the deviator stress, σ_d, is assumed to be equal to the total stress σ_1 minus the lateral confining stress σ_3, because in the case of the normal triaxial test σ_3 is also applied to the top end platen of the sample. For the K-mould this is different, in that the sample is not enclosed in a pressure cell and σ_3 is therefore not applied to the top end of the sample. For the purpose of discussion of this document it is assumed that M_R and E_d are approximately the same.

From Figure 8.1, it follows that

$$\sigma = A.\varepsilon_1 + B.\varepsilon_1^2 + C.\varepsilon_1^3 + D \quad \text{..... Eq.5}$$

where σ = stress level (kPa) (either σ_1 or $\sigma_d = \sigma_1 - \sigma_3$)

ε_1 = vertical deformation

A..D = regression constants

and $$E = d\sigma/d\varepsilon_1 = A + 2B.\varepsilon_1 + 3C.\varepsilon_1^2 \quad \text{..... Eq.6}$$

The values of A, B and C for Equation 6 are the same as for Equation 5 and are determined through regression analyses of the data.

Because the sample mass, moisture content, height and diameter are known at the start of the loading cycle, it is possible to determine the percentage of "solid" density of the material on a continuous basis as the sample height and diameter changes with loading. As was mentioned in the compaction study[2] the "solid" density of the materials depends on the nature of the material. For most materials the apparent density is used (ie AD = ARD x 1000 kg/m^3), but for porous materials, for which there is a substantial difference in the values of the bulk relative density (BRD) and the apparent relative density (ARD), the dry bulk density is used (ie DBD = BRD x 1000 kg/m^3).

By plotting E_1 and E_d against dry density (% AD or % DBD) it is possible to see what effect density has on the elastic moduli of the materials (see Figure 8.2).

It is evident from the smooth curves in Figure 8.2 that a very good relationship exists between the E-values and the dry density (% AD or % DBD) at a particular moisture content. The curves are generally parabolic in nature. Therefore, by doing a regression analysis between these parameters, it may be possible to estimate E-values from the dry density and moisture content (see Figure 8.3).

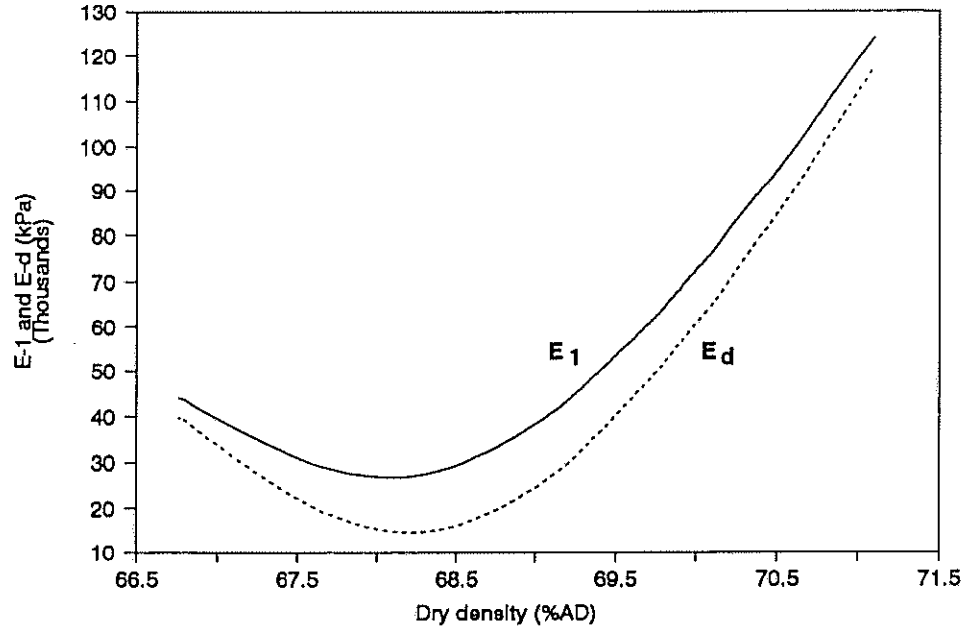

FIGURE 8.2 - EXAMPLE OF THE RELATIONSHIP BETWEEN E_1 AND E_d AND DRY DENSITY (% AD)

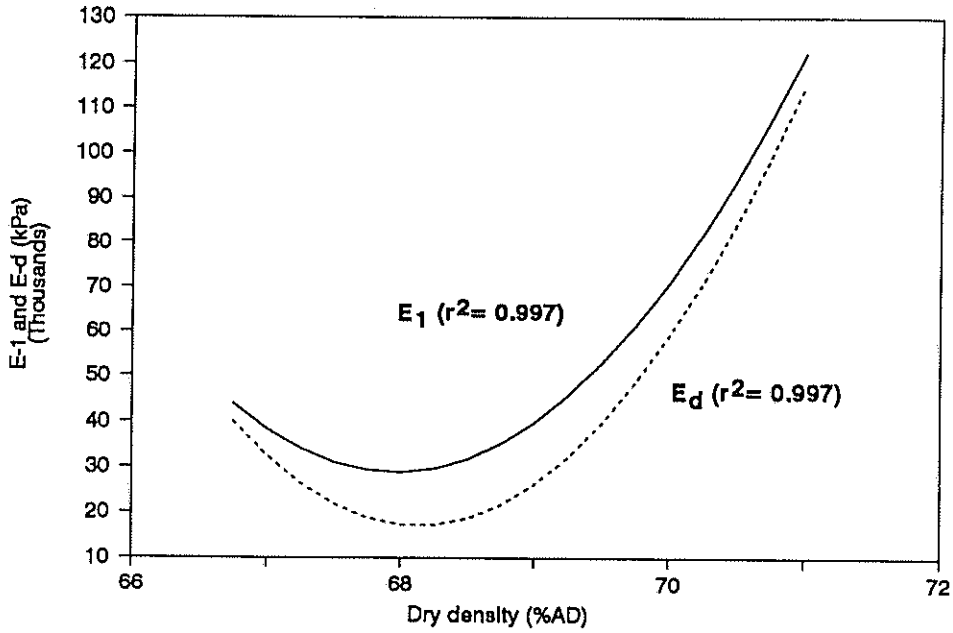

FIGURE 8.3 - EXAMPLE OF THE THEORETICAL RELATIONSHIP BETWEEN E_1 AND E_d ($E = f(DD, DD^2)$) AND DRY DENSITY (% AD) FOR FIGURE 8.2

9. DISCUSSION OF THE RESULTS

9.1 THE ELASTIC MODULI (E_1 AND E_d)

Originally the vertical stress was to be calculated from the average vertical load as determined by the top and bottom load cells of the K-mould. However, at the start of the testing programme the bottom load cell failed and for the greater part of the research project the vertical load had to be calculated from the top load only. When the crushed stone materials were tested, the bottom load cell had been replaced and the average vertical stress could be calculated. Because the E-values using the average stress for the crushed stone materials seemed low, they were recalculated using the top load only. This increased their E-values by approximately a third (see Figures 9.1(a) and 9.1(b))(Example). This is also in agreement with the triaxial test.

However, it came to our notice very recently that Maree[3] had found that the E-moduli as determined by the repeated loading triaxial compression test gave higher values than the E-moduli of the material in the road itself as determined by means of back calculation of the E-moduli from the deflection measurements. The difference in value is also approximately a third. This means that the E-moduli as calculated from the average vertical stresses of the K-mould are actually closer to the real E-moduli in the road than those measured by the repeated loading triaxial compression test.

Using the average vertical stress for the determination of the E-moduli for the material from the Bultfontein HVS site, the estimated E-moduli determined with the K-mould tied in very well with the back calculated E-moduli of 1000 MPa for the G1 material at a dry density of 91 % AD (see Figure 9.2(a) and 9.2(b) (see Appendix A for regression analysis results). The E-moduli of the in-situ ferricrete ranged from about 20 MPa to 186 MPa with the K-mould while the back calculated E-moduli ranged from 42 MPa to 186 MPa (see Figure 9.3).

As mentioned earlier, density levels and moisture content were again shown to have a very definite effect on the elastic modulus of the materials (see Figure 9.4 to 9.19 as examples). By comparing the E-values at the same dry densities (% AD or % DBD) it is clear what tremendous effect a small change in moisture content can have on the strength of materials.

In general the E-values as measured with the DRTT K-mould seem to tie in well with presently listed values for materials[4] (see Table 9.1).

Most of the curves of E-moduli against dry density seem to have a fairly flat slope at low density levels. This is most probably the area in which there is a difference between the actual dry density and

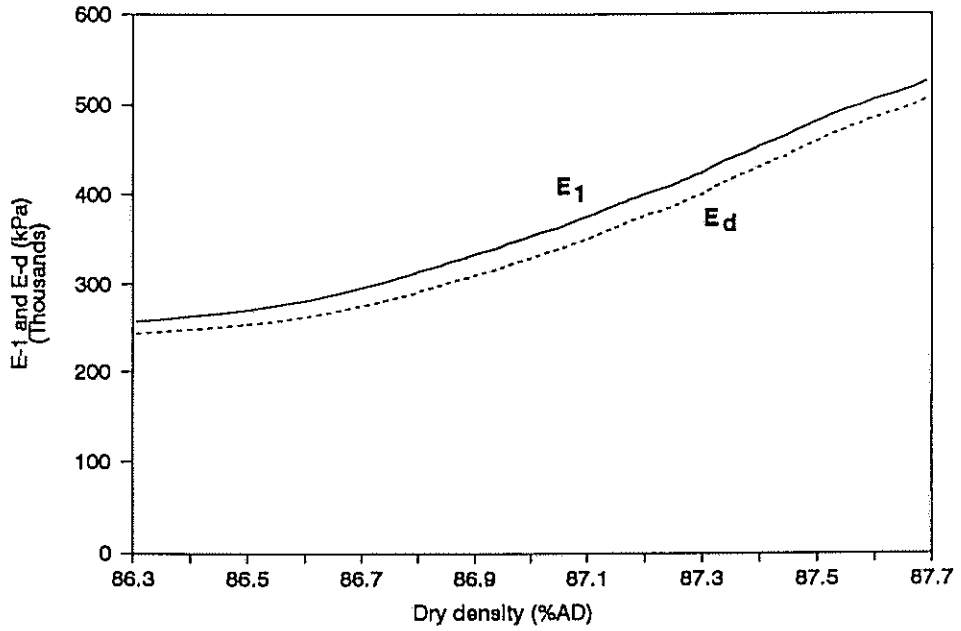

FIGURE 9.1(a) - MEASURED VALUES FOR E_1 AND E_d AGAINST DRY DENSITY (% AD) FOR QUARTZITE CRUSHED STONE USING THE TOP VERTICAL STRESS (MC = 5,29 %)

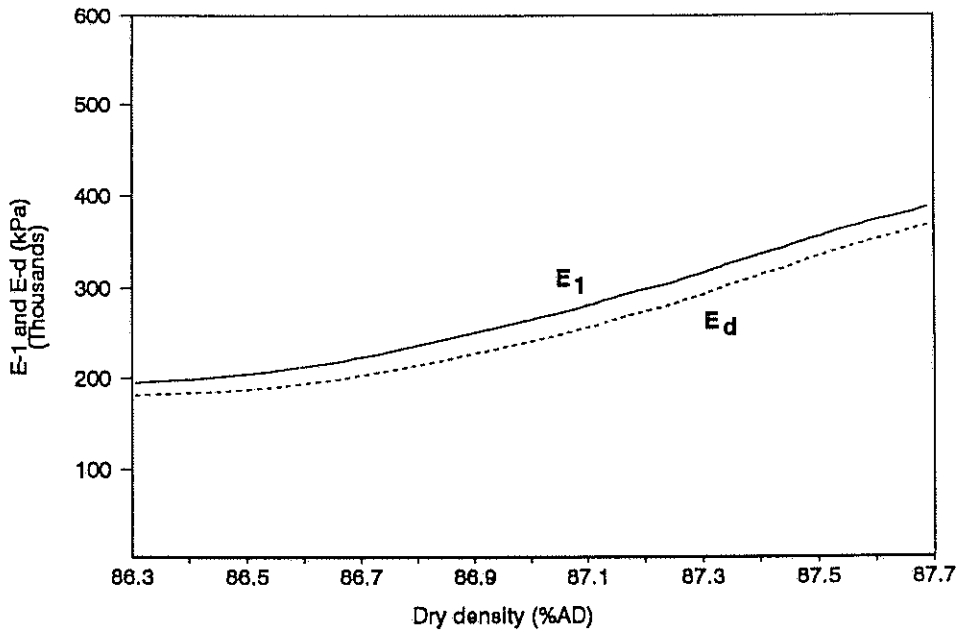

FIGURE 9.1(b) - MEASURED VALUES FOR E_1 AND E_d AGAINST DRY DENSITY (% AD) FOR QUARTZITE CRUSHED STONE USING THE MEAN VERTICAL STRESS (MC = 5,29 %)

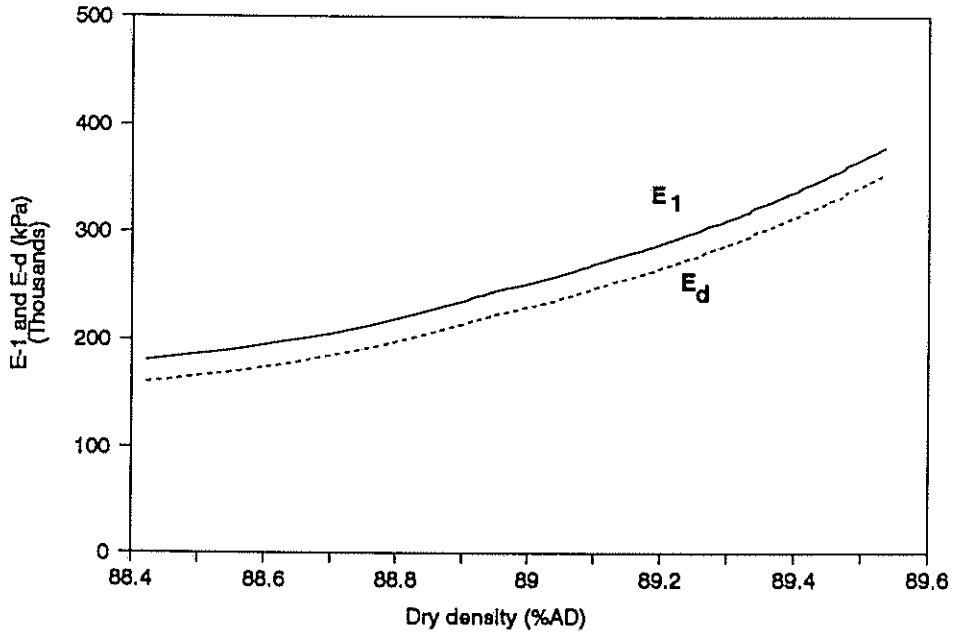

FIGURE 9.2(a) - MEASURED VALUES FOR E_1 AND E_d AGAINST DRY DENSITY (% AD) FOR G1 MATERIAL FROM BULTFONTEIN HVS SITE

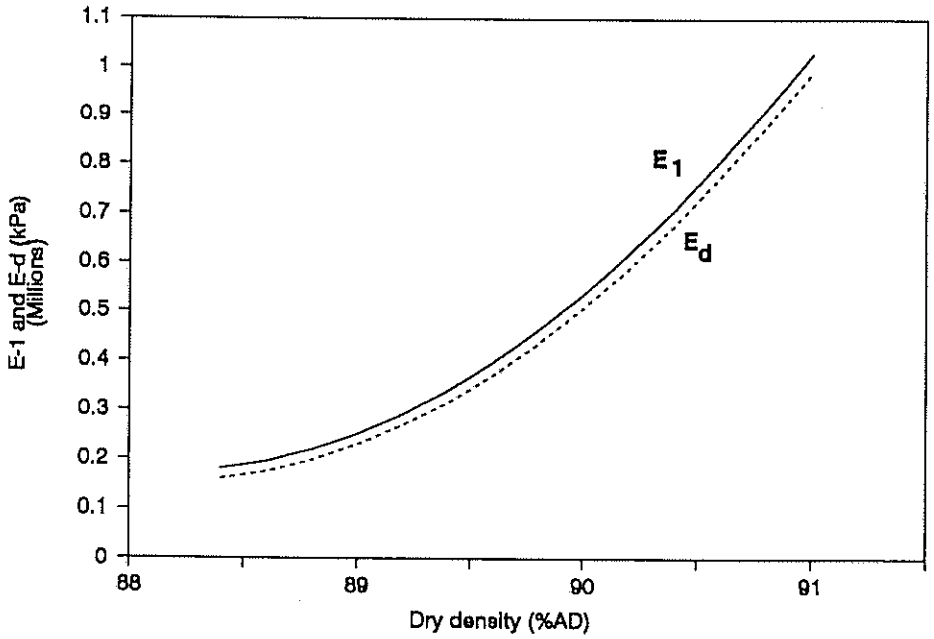

FIGURE 9.2(b) - CALCULATED VALUES FOR E_1 AND E_d ($E = f(DD,DD^2)$) AND DRY DENSITY (% AD) FOR G1 MATERIAL FROM BULTFONTEIN HVS SITE AS DETERMINED FROM THE INFORMATION USED FOR FIGURE 9.2(a)

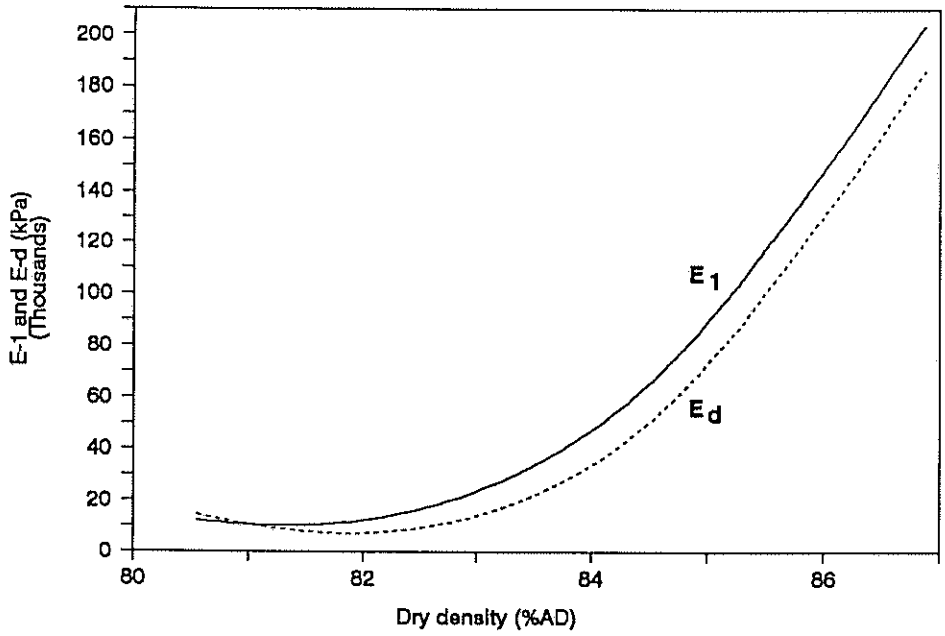

FIGURE 9.3 - MEASURED VALUES FOR E_1 AND E_d AGAINST DRY DENSITY (% AD) FOR IN-SITU FERRICRETE MATERIAL FROM BULTFONTEIN HVS SITE

the maximum dry density (MDD) (see Table 7.1). Under the repeated load triaxial system this would be attributed to "plastic deformation" of the material. It is therefore clear that the "plastic deformation" of soils is generally due to the density of the materials being lower than MDD. Once this has been taken up the relation between the E-moduli and dry density is virtually a straight line.

This is also confirmed by plots of log (E_d) against log ($\sigma_1 + 2.\sigma_3$) (see Figures 9.20 and 9.21 as examples) (more figures are given in Appendix B). Figure 9.20 for the crushed stone material from Bultfontein HVS site has two straight lined sections. The slope of the first section is very flat. This is the section during which further densification of the material take place. The second section has a much steeper slope; thus is the section where the material has reached maximum dry density. Similarly Figure 9.21 for the in-situ ferricrete from the Bultfontein HVS site has two sections. The slope of the first section is negative (stress-softening). This means that the elastic moduli of these types of materials (fine materials in general) are actually decreasing while further densification is taking place. The second section has a much greater positive slope, clearly showing much greater strength once the material has reached maximum dry density.

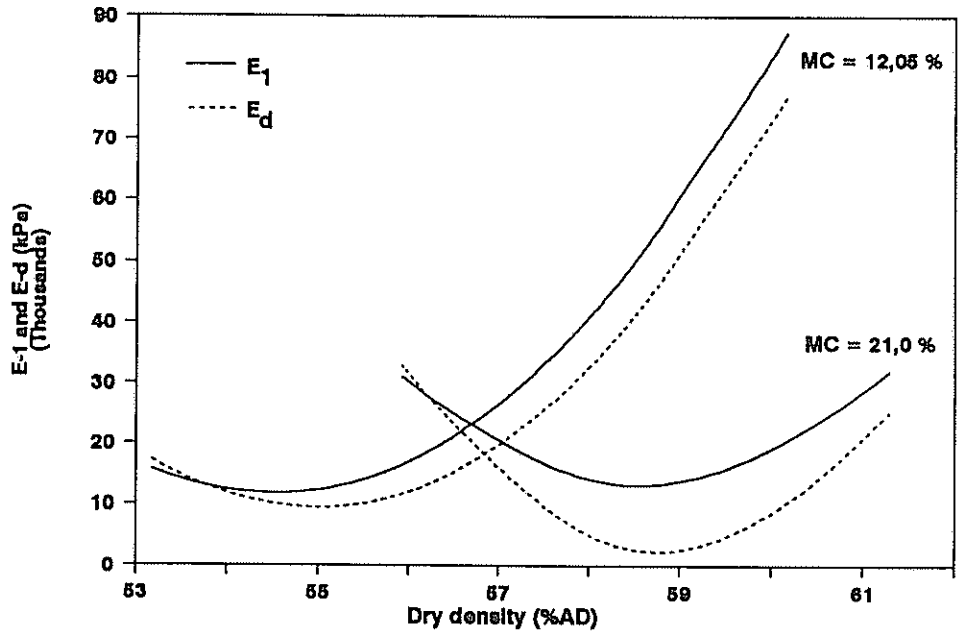

FIGURE 9.4 - MEASURED VALUES FOR E_1 AND E_d AGAINST DRY DENSITY (% AD) FOR BLACK CLAY FOR DIFFERENT MOISTURE CONTENTS

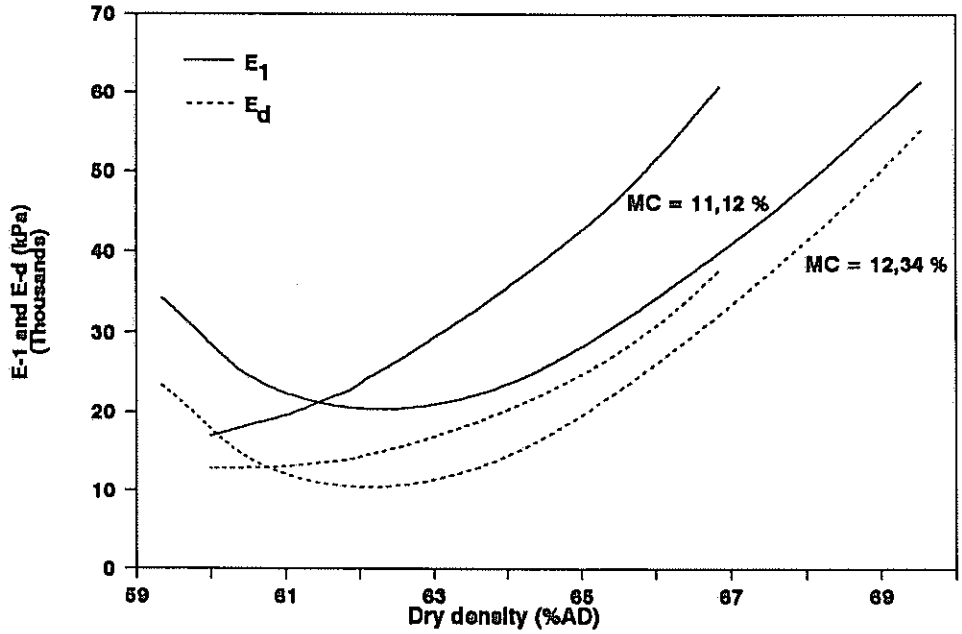

FIGURE 9.5 - MEASURED VALUES FOR E_1 AND E_d AGAINST DRY DENSITY (% AD) FOR RED SANDY CLAY FOR DIFFERENT MOISTURE CONTENTS

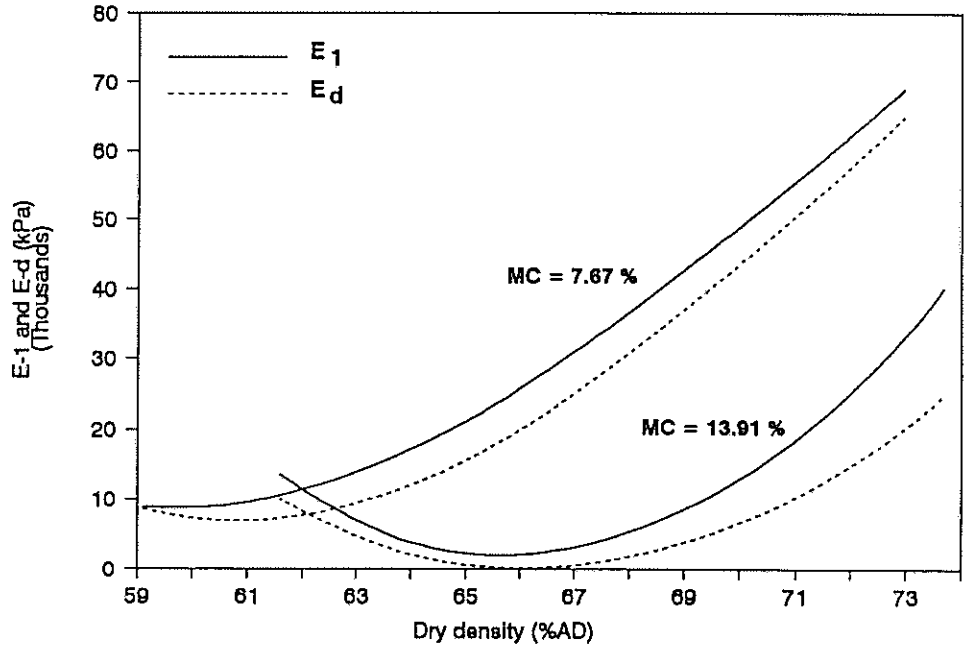

FIGURE 9.6 - MEASURED VALUES FOR E_1 AND E_d AGAINST DRY DENSITY (% AD) FOR SILTY SAND FOR DIFFERENT MOISTURE CONTENTS

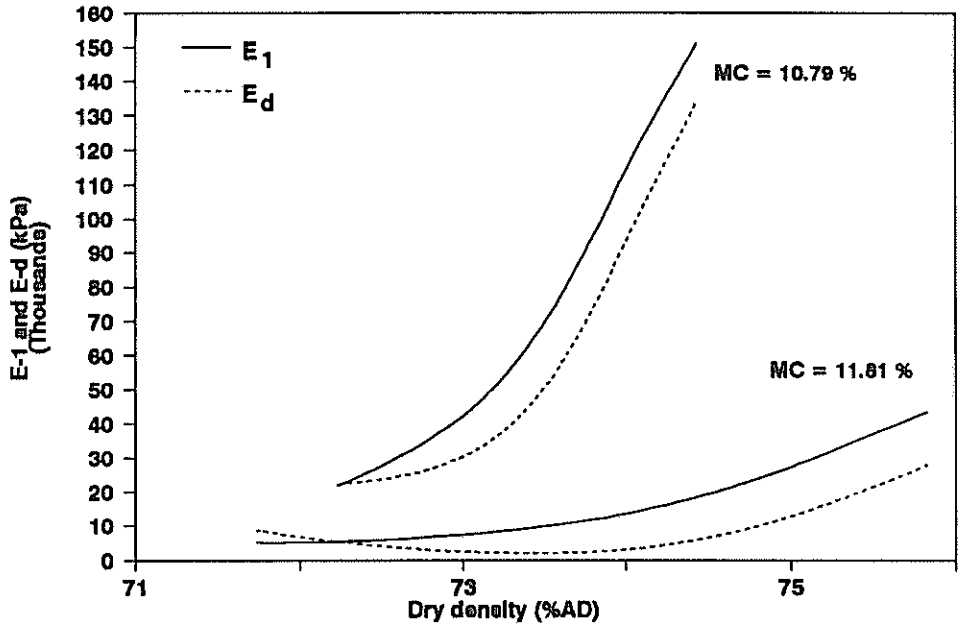

FIGURE 9.7 - MEASURED VALUES FOR E_1 AND E_d AGAINST DRY DENSITY (% AD) FOR SILTY PLASTIC SAND FOR DIFFERENT MOISTURE CONTENTS

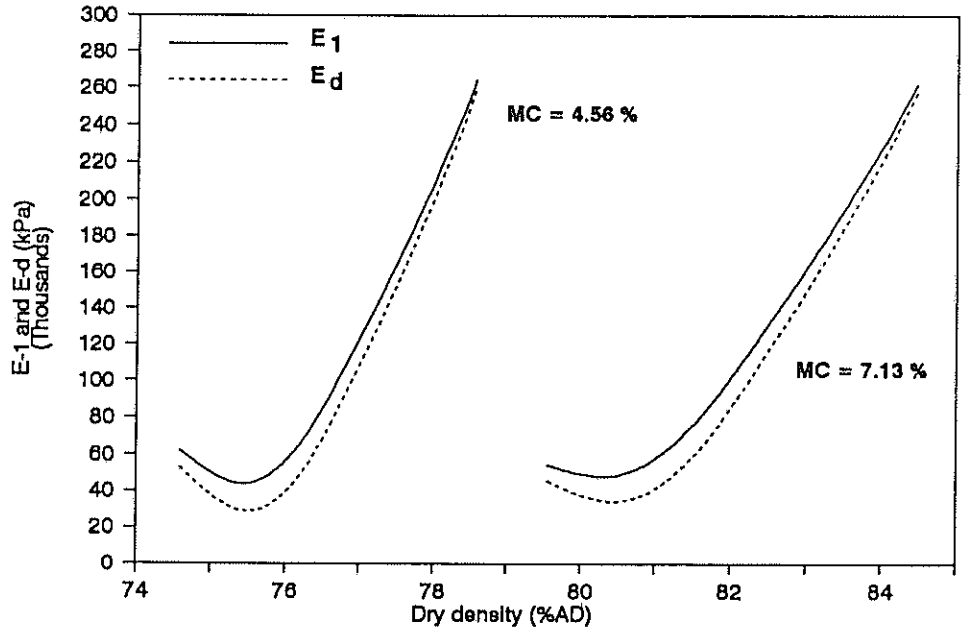

FIGURE 9.8 - MEASURED VALUES FOR E_1 AND E_d AGAINST DRY DENSITY (% AD) FOR DOLERITE SOIL FOR DIFFERENT MOISTURE CONTENTS

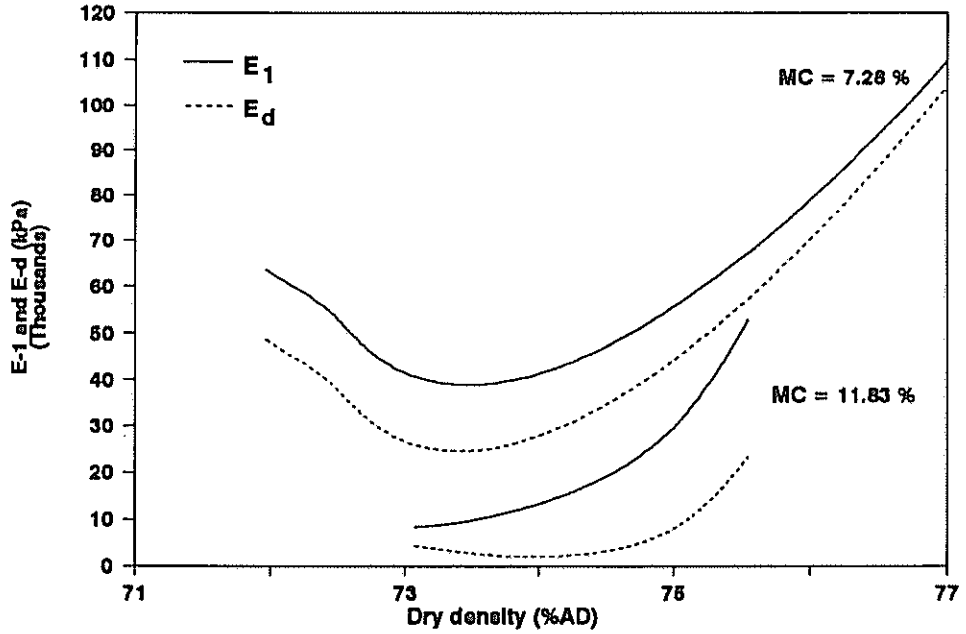

FIGURE 9.9 - MEASURED VALUES FOR E_1 AND E_d AGAINST DRY DENSITY (% AD) FOR RED CHERT SOIL FOR DIFFERENT MOISTURE CONTENTS

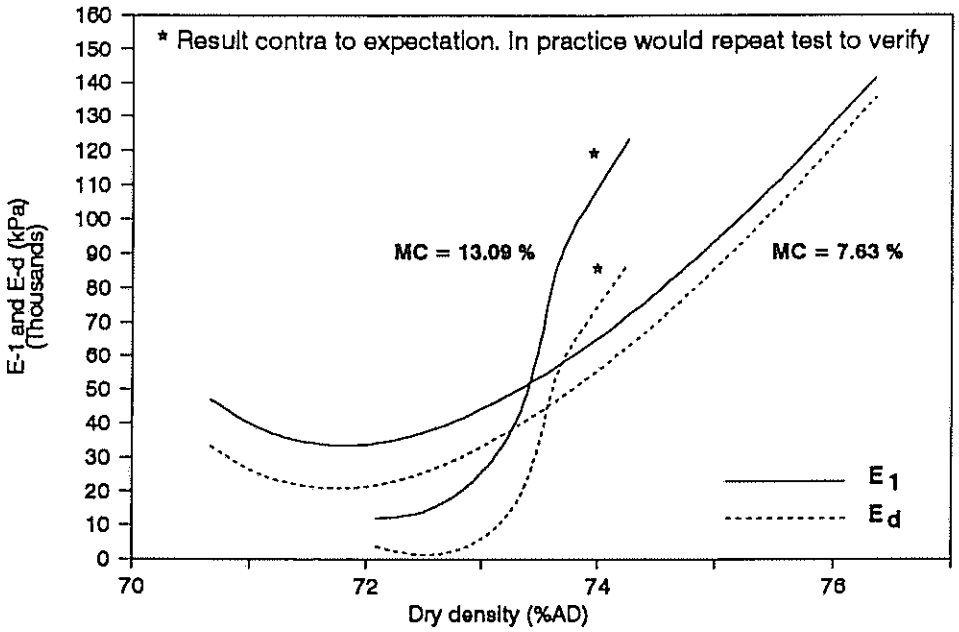

FIGURE 9.10 - MEASURED VALUES FOR E_1 AND E_d AGAINST DRY DENSITY (% AD) FOR DECOMPOSED DOLERITE FOR DIFFERENT MOISTURE CONTENTS

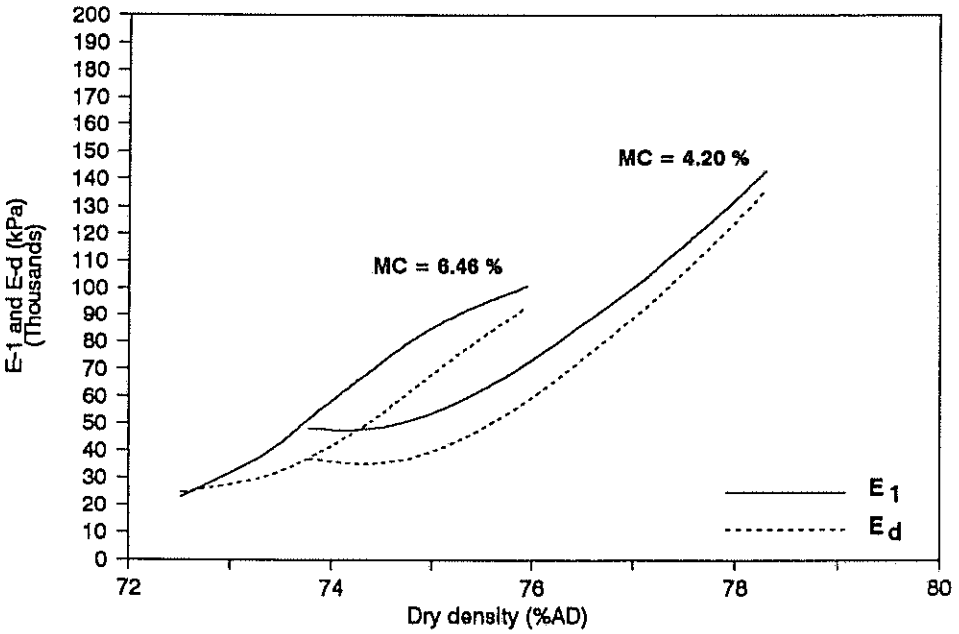

FIGURE 9.11 - MEASURED VALUES FOR E_1 AND E_d AGAINST DRY DENSITY (% AD) FOR QUARTZITE GRAVEL FOR DIFFERENT MOISTURE CONTENTS

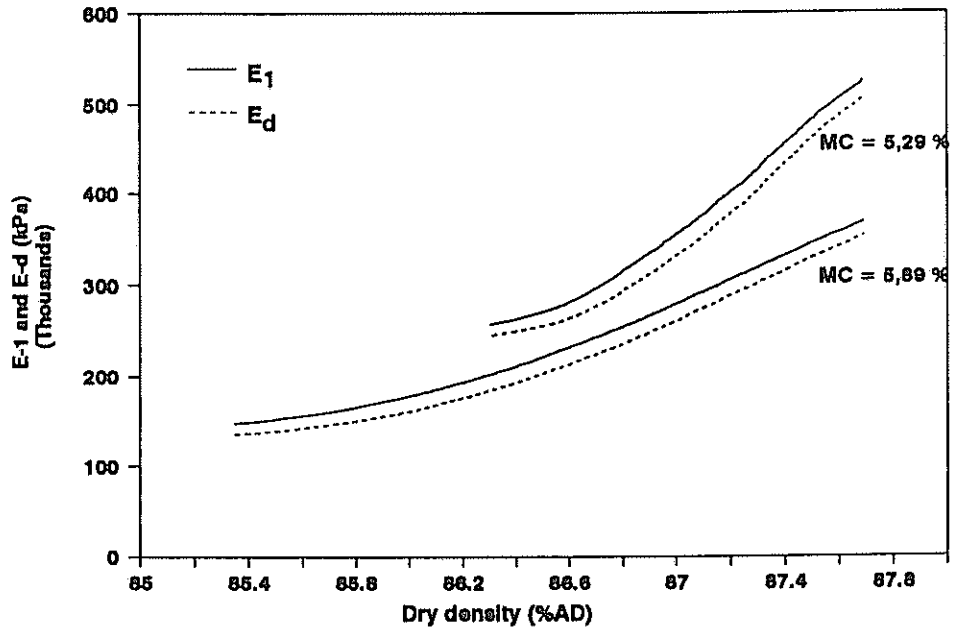

FIGURE 9.12 - MEASURED VALUES FOR E_1 AND E_d AGAINST DRY DENSITY (% AD) FOR QUARTZITE CRUSHED STONE (G1) FOR DIFFERENT MOISTURE CONTENTS

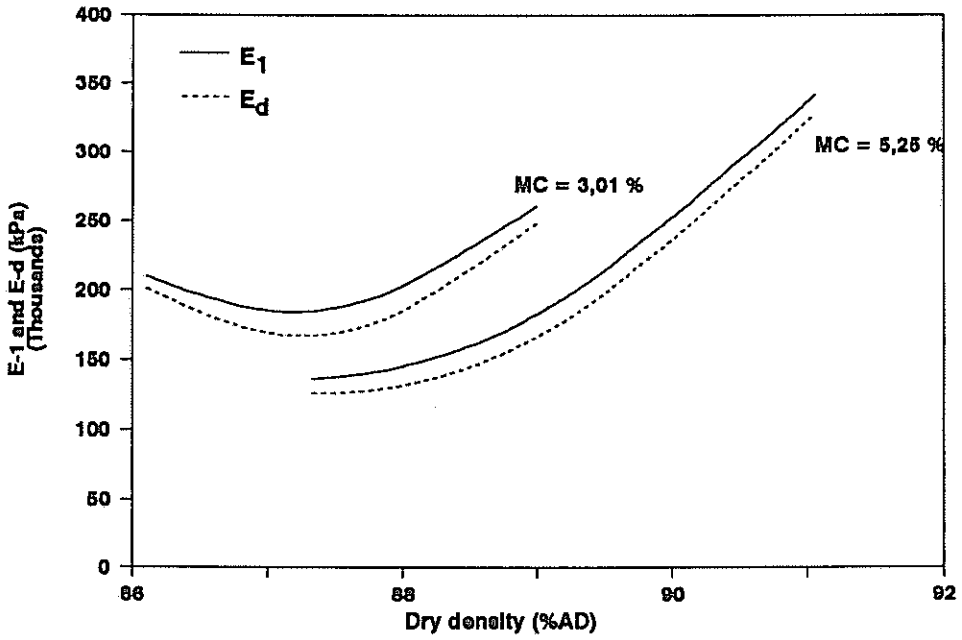

FIGURE 9.13 - MEASURED VALUES FOR E_1 AND E_d AGAINST DRY DENSITY (% AD) FOR GRANITE CRUSHED STONE (G1) FOR DIFFERENT MOISTURE CONTENTS

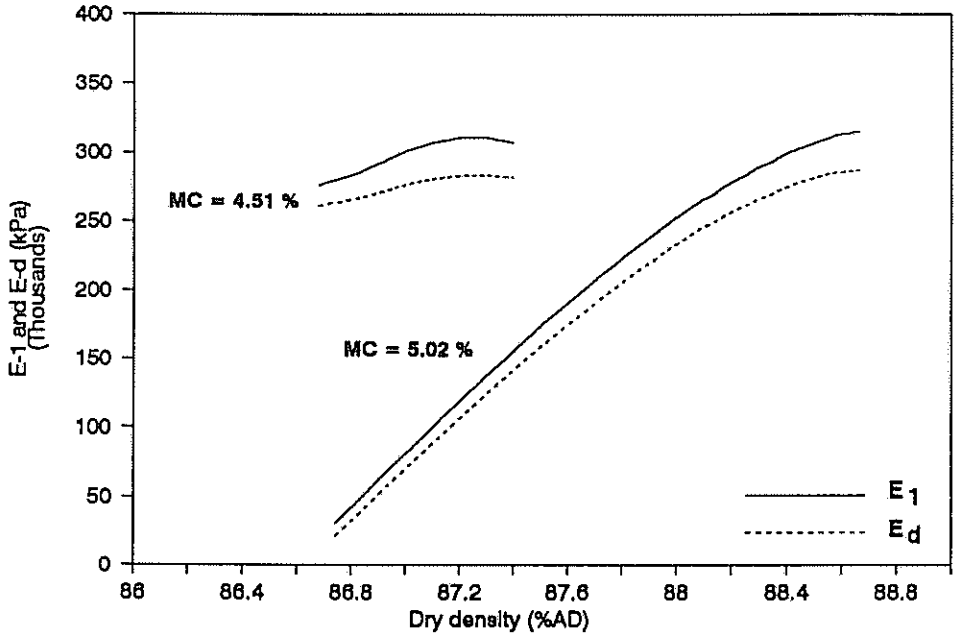

FIGURE 9.14 - MEASURED VALUES FOR E_1 AND E_d AGAINST DRY DENSITY (% AD) FOR DOLERITE CRUSHED STONE (G1) FOR DIFFERENT MOISTURE CONTENTS

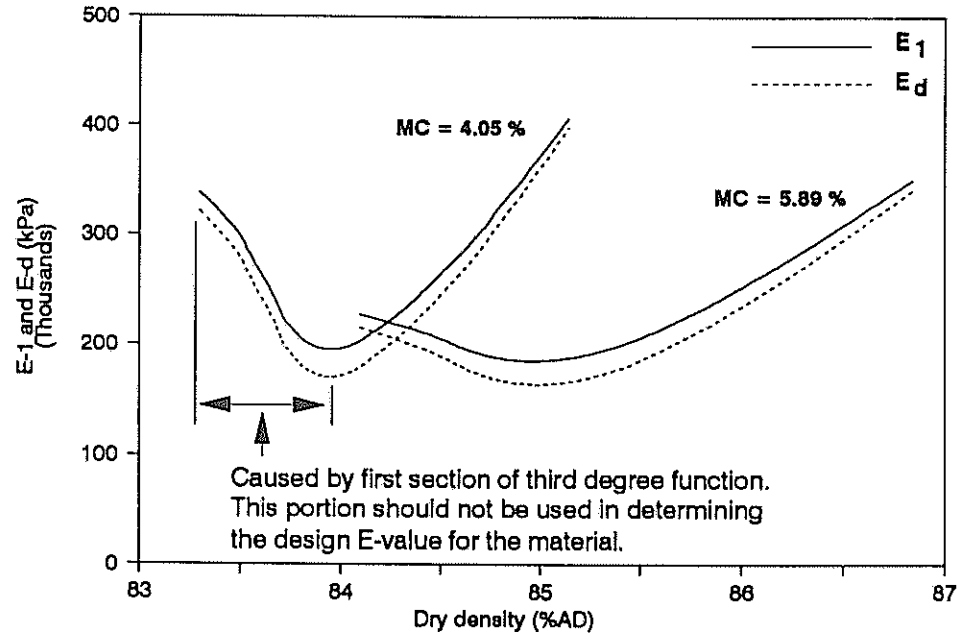

FIGURE 9.15 - MEASURED VALUES FOR E_1 AND E_d AGAINST DRY DENSITY (% AD) FOR TILLITE CRUSHED STONE (G1) FOR DIFFERENT MOISTURE CONTENTS

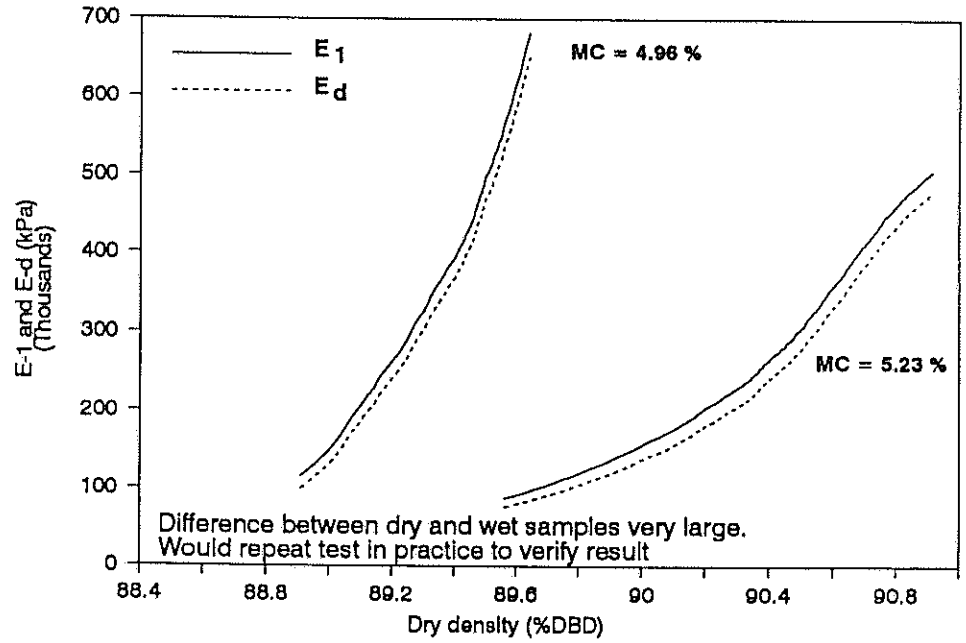

FIGURE 9.16 - MEASURED VALUES FOR E_1 AND E_d AGAINST DRY DENSITY (% DBD) FOR CRUSHED ALLUVIAL GRAVEL (G2) FOR DIFFERENT MOISTURE CONTENTS

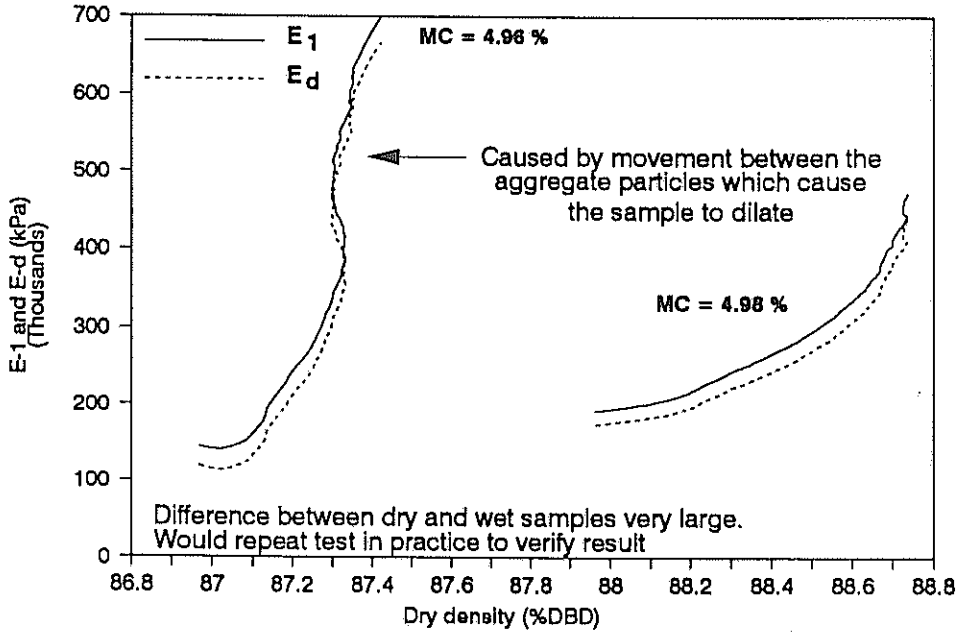

FIGURE 9.17 - MEASURED VALUES FOR E_1 AND E_d AGAINST DRY DENSITY (% DBD) FOR CRUSHED GRANITE (G2) FOR DIFFERENT MOISTURE CONTENTS

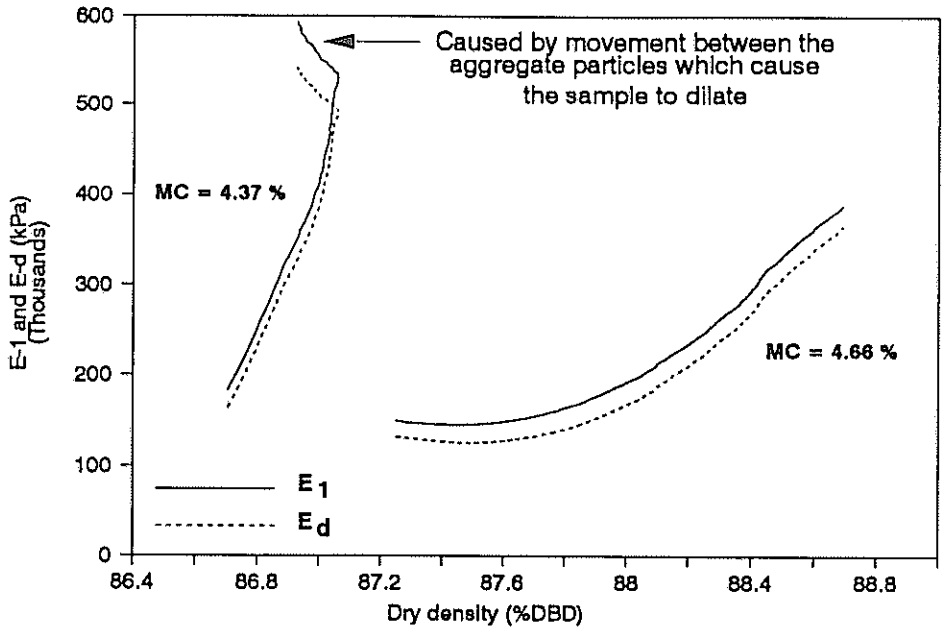

FIGURE 9.18 - MEASURED VALUES FOR E_1 AND E_d AGAINST DRY DENSITY (% DBD) FOR CRUSHED DOLERITE (G2) FOR DIFFERENT MOISTURE CONTENTS

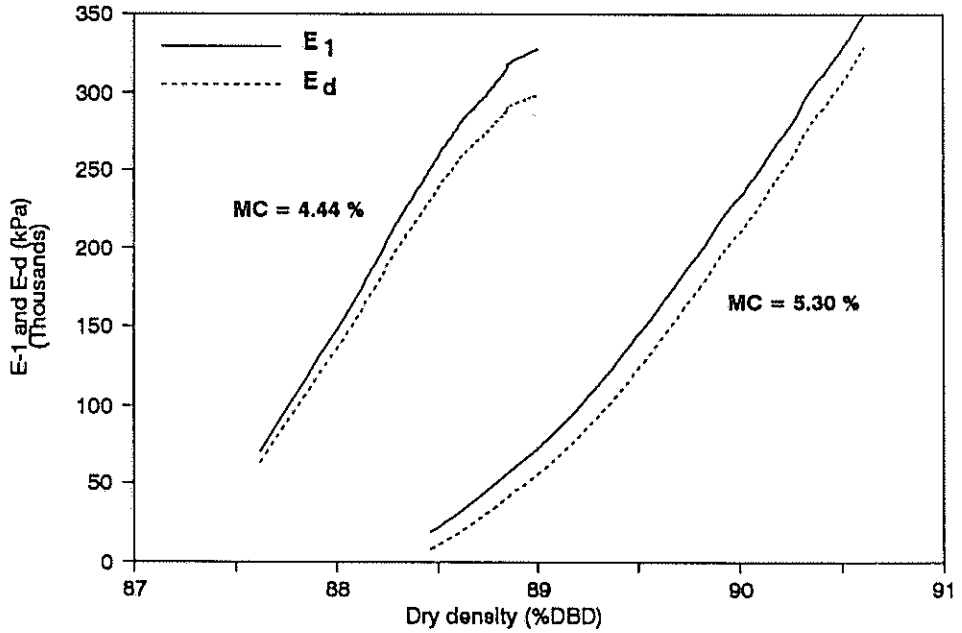

FIGURE 9.19 - MEASURED VALUES FOR E_1 AND E_d AGAINST DRY DENSITY (% DBD) FOR CRUSHED HORNFELS (G2) FOR DIFFERENT MOISTURE CONTENTS

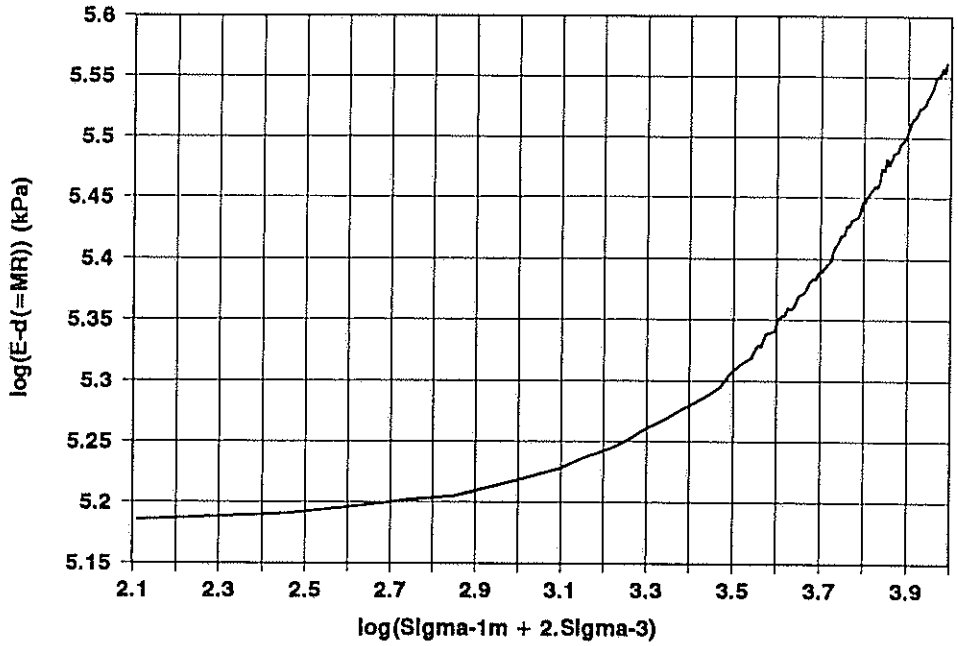

FIGURE 9.20 - LOG (E_d) AGAINST LOG ($\sigma_{1m} + 2.\sigma_3$) FOR THE G1 CRUSHED STONE MATERIAL FROM BULTFONTEIN HVS SITE

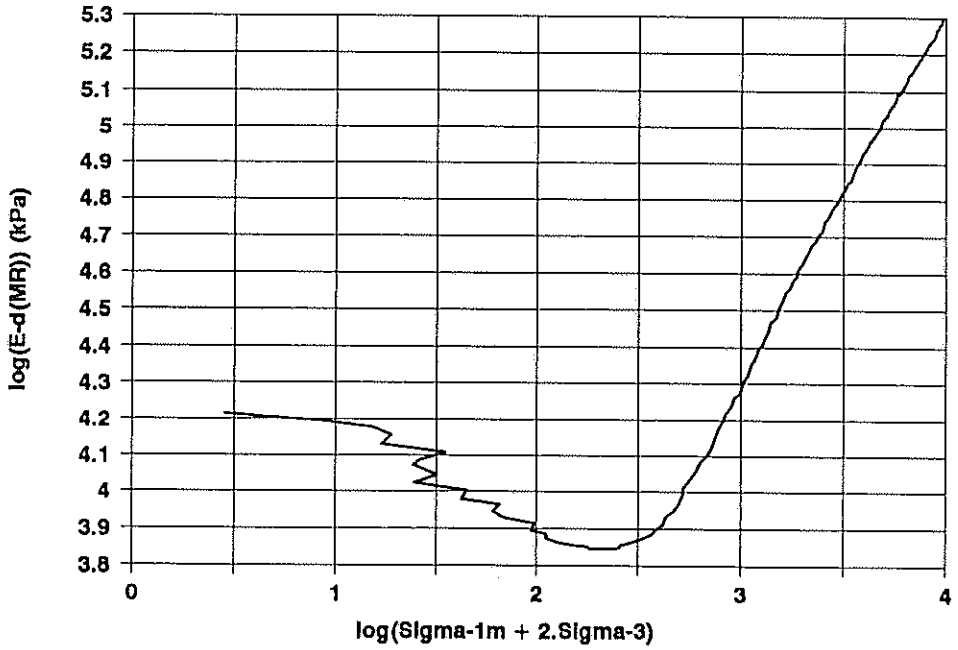

FIGURE 9.21 - LOG (E_d) AGAINST LOG ($\sigma_{1m} + 2.\sigma_3$) FOR THE IN-SITU FERRICRETE MATERIAL FROM THE BULTFONTEIN HVS SITE

TABLE 9.1 - COMPARISON OF E-VALUES FROM K-MOULD WITH STANDARD E-VALUES*

MATERIAL	ESTIMATED SOAKED CBR	STANDARD E-VALUES * (MPa)		K-MOULD E-VALUES (MPa)		
FINE MATERIAL		**WET**	**DRY**	**WET**	**DRY**	**SATU-RATED**
KBAB	3	45	90	30	70	10
SPK	7	70	140	70	95	25
SILK	10	90	180	40	140	20
KDW	12	90	180	100	180	20
NATURAL GRAVELS		**Mini-mum**	**Maxi-mum**	**100 % mod**	**Mini-mum**	**Maxi-mum**
DENS7	36	50	300	180 - 260 +	30	200
LENC	7	30	150	40	3	100
NPAB	16	50	250	50 - 70	0	180
TP2	20	50	250	50 - 80	20	150
G1 MATERIALS		**Mini-mum**	**Maxi-mum**	**86 % AD**	**Mini-mum****	**Maxi-mum**
FERRO	200 +	175	1 000	250 - 300	100	500
ROSS	200 +	175	1 000	120 - 270	45	330
NPAA	200 +	175	1 000	160 - 230	30	285
NPAE	200 +	175	1 000	175 - 200	30	400
G2 MATERIALS		**Mini-mum**	**Maxi-mum**		**Mini-mum**	**Maxi-mum**
CPA4	200 + (85) +	150	800	-	90 (81,2)+	650 (90)+
CPA5	200 + (85)	150	800	-	50 (82,3)	650 (88,8)
CPA7	200 + (85)	150	800	-	50 (80,5)	500 (88,0)
CPA9	200 + (85)	150	800	-	60 (82,6)	330 (90,5)

* See reference 4 - Tables 2, A1 and A5

** Minimum densities around 74 % AD to 78 % AD

\+ Densities as % DBD

9.2 THE DETERMINATION OF ϕ AND c FROM THE q VERSUS p GRAPHS.

As mentioned under discussion of the theoretical background (see section 2) it is possible to determine both ϕ and c from the q versus p graphs (see Figures 9.22 as an example).

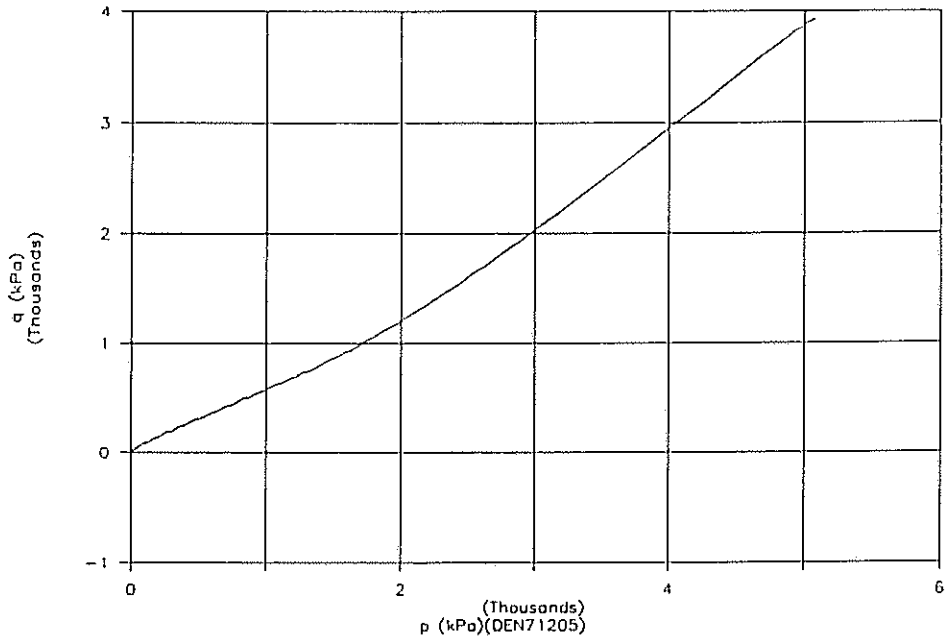

FIGURE 9.22 - EXAMPLE OF A q VERSUS p GRAPH

For the samples tested up till now the slope of the q-p graph can usually be divided into at least two sections; an initial section with a slope which is slightly flatter than the slope of the second section of the graph. The first section coincides with the section where the material is further densified, while the second section coincides with the section where the material has reached maximum density. Using equations (1) and (2) the values for ϕ and c can be calculated for these sections separately (see Table 9.2 as an example of these results).

Note from Table 9.2 that the ϕ-values compare favourably with those measured in the triaxial compression test. Although c is mostly positive for the first section, it sometimes changes to a negative value in the second portion, showing the effect of pore water pressure. This negative adhesion component can have a substantial effect on the effective friction angle (see third regression analysis in Table 9.2 where c = 0). Drops in the effective friction angle of more than ten degrees were recorded during the testing with the K-mould.

Examples of the ϕ and c values for the different classes of material are listed in Appendix B and examples of q versus p graphs for different materials are given in Appendix E.

TABLE 9.2 - EXAMPLE OF RESULTS FOR ϕ AND c OBTAINED FROM THE q VERSUS p GRAPH SHOWN IN FIGURE 9.22

DENS712 (MC=4.56%)(corrected)(Sigma-1m)

phi and c (intercept computed)(0<p<1800kPa)

Regression Output:			
Constant	23.42084		
Std Err of Y Est	9.757645		
R Squared	0.999012		
No. of Observations	57		
Degrees of Freedom	55		
		phi	c
X Coefficient(s)	0.565748	34.45425	28.40343
Std Err of Coef.	0.002398		

phi and c (intercept computed)(1800<p<5071kPa)

Regression Output:			
Constant	-625.904		
Std Err of Y Est	27.34530		
R Squared	0.999182		
No. of Observations	39		
Degrees of Freedom	37		
		phi	c
X Coefficient(s)	0.896611	63.71620	-1413.45
Std Err of Coef.	0.004217		

phi and c (intercept zero)(1800<p<5071kPa)

Regression Output:			
Constant	0		
Std Err of Y Est	190.6554		
R Squared	0.959163		
No. of Observations	39		
Degrees of Freedom	38		
		phi	c
X Coefficient(s)	0.725307	46.49447	0
Std Err of Coef.	0.008752		

phi and c (intercept computed)(0<p<5071kPa)

Regression Output:			
Constant	-145.467		
Std Err of Y Est	125.6821		
R Squared	0.987859		
No. of Observations	96		
Degrees of Freedom	94		
		phi	c
X Coefficient(s)	0.759974	49.46194	-223.812
Std Err of Coef.	0.008689		

9.3 THE DETERMINATION OF POISSON'S RATIO ν

Poisson's ratio for the material can also be determined by using equation (4) (see section 2). The values determined in this manner were fairly constant in general for a particular sample. However, the value of ν was not constant at 0,35 but ranged from about 0,4 to 0,2 (see Figures 9.23 and 9.24 as examples). Further examples are given in Appendix E.

In his doctoral dissertation Sweere[5] found that ν was stress dependent. He plotted ν against the cyclic deviator stress over confining stress. The graphs show values as high as 0,7 starting from about 0,35. He observed "For $\nu < 0,5$ the model only predicts specimen compression ($\varepsilon_{v,r} > 0$) and for $\nu > 0,5$ only specimen dilation ($\varepsilon_{v,r} < 0$) is obtained from the model, irrespective of the stress ratio applied". (p.262) It should be mentioned that Sweere used dynamic loaded triaxial compression tests with constant confining pressures in his test programme.

To verify whether the materials tested with the K-mould reacted similarly, ν was plotted against (σ_d/σ_3) for a number of different materials for the first loading cycle. In all cases the maximum value of ν was less than 0,5. However, ν tended to increase from a very low value (< 0,1) to a maximum value somewhere in the order of 0,35, after which it started dropping again (see Figures 9.25 and 9.26 as examples). During the elastic phase ν is relatively constant but during the plastic phase there is a rapid rise in the value of ν. This is mainly due to the rapid change in σ_3.

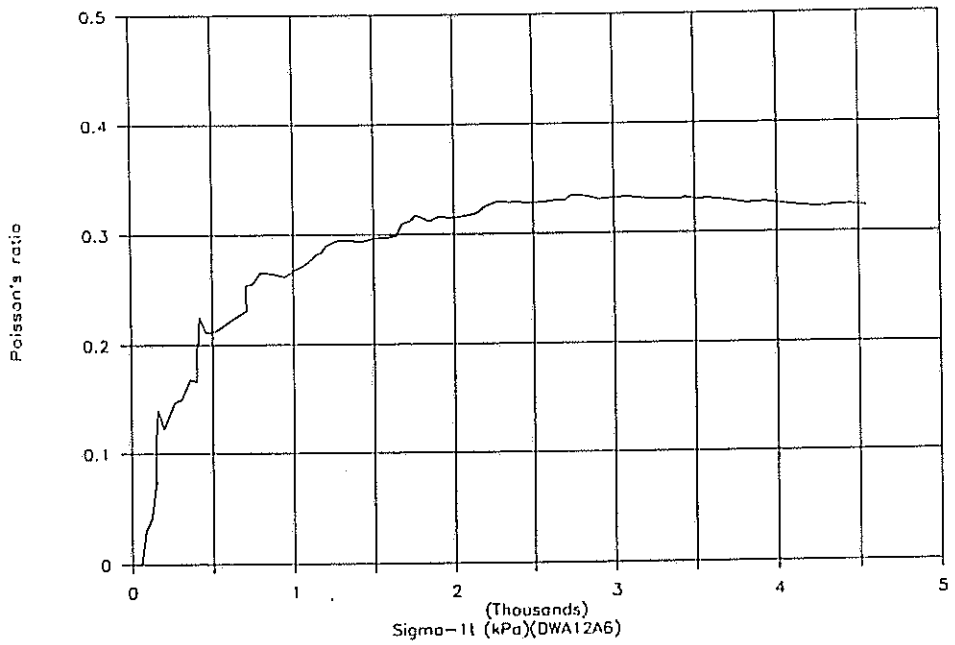

FIGURE 9.23 - POISSON'S RATIO AGAINST σ_{1t} FOR SLIGHTLY PLASTIC SAND (MC = 10,74 %)

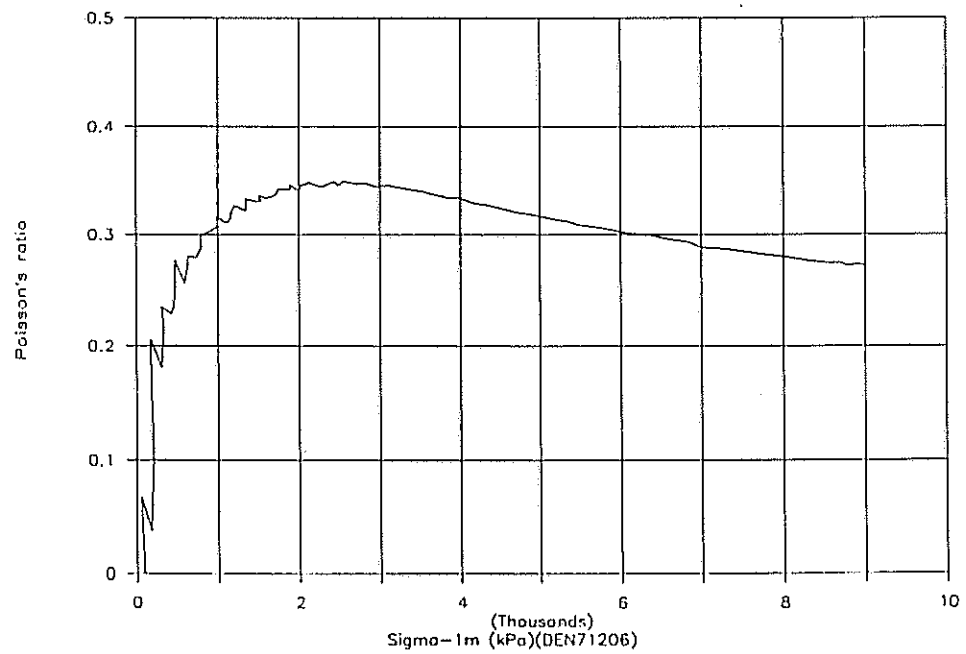

FIGURE 9.24 - POISSON'S RATIO AGAINST σ_{1m} FOR DOLOMITIC SOIL (MC = 4,56 %)

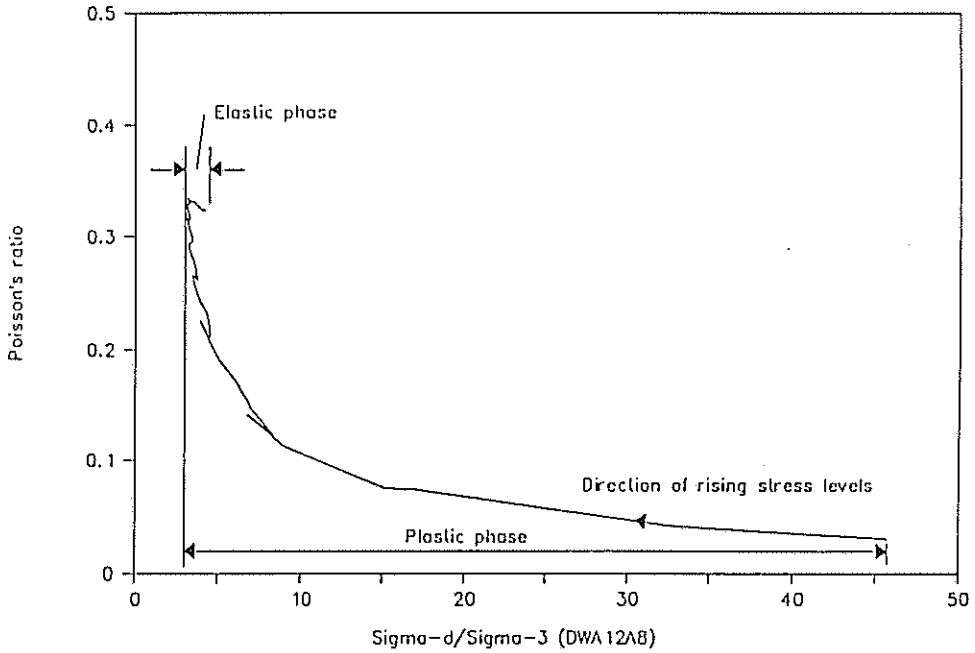

FIGURE 9.25 - POISSON'S RATIO AGAINST σ_d/σ_3 FOR SLIGHTLY PLASTIC SAND (MC = 10,74 %)

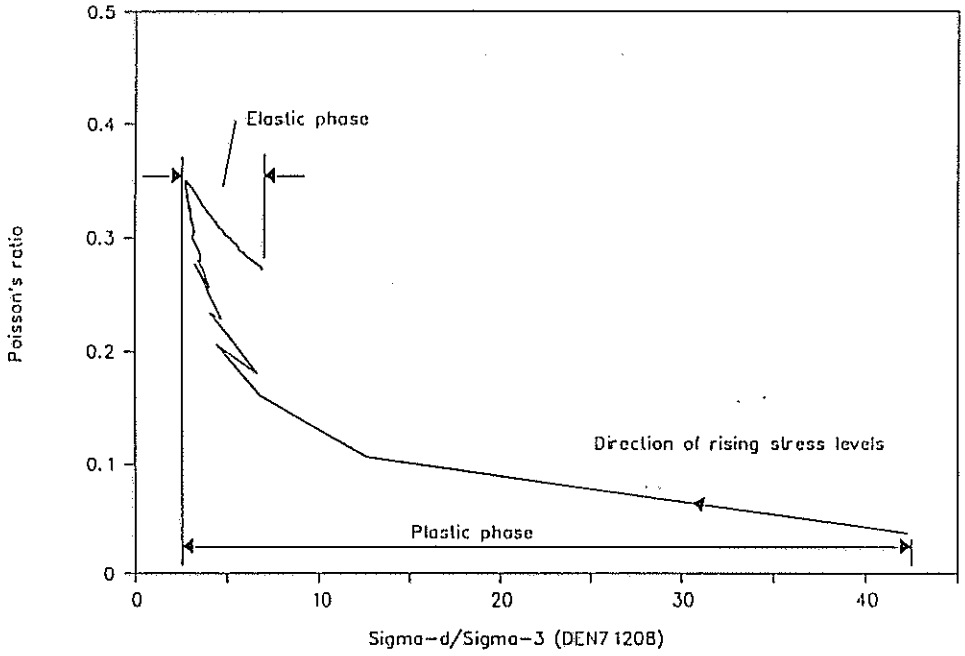

FIGURE 9.26 - POISSON'S RATIO AGAINST σ_d/σ_3 FOR DOLOMITIC SOIL (MC = 4,56 %)

10. CONCLUSIONS AND RECOMMENDATIONS

It is possible to determine the material parameters E_i, $E_d(M_R)$, ν, c and ϕ for all untreated roadbuilding materials with a great degree of accuracy with the K-mould in a single loading cycle. The high r^2-values also obtained between the E-moduli and the dry density (see Appendix A for values) show that the density of the material has a tremendous influence on the elastic performance of the material. The different E-moduli at the same densities for different moisture contents also show the detrimental effect of high moisture contents.

The modulus of resilience (M_R) which is determined by dividing the deviator stress by the elastic component of the deformation only, is the elastic modulus which is normally used for mechanistic design. To determine the plastic component of the deformation it is general practice to subject the sample to repeated loading cycles (as many as 20 000). However, the greater the number of load cycles the longer a test takes and the more expensive it becomes.

In the latest AASHTO specification (AASHTO T274) this has already been reduced to 200 load cycles and in research by others[6] it is suggested that the number of load cycles can safely be reduced to 50. Another source[7] proposes that the load be kept on the sample for five minutes, after which the plastic component of the deformation can be determined and the rest of the deformation is attributed to elastic deformation. From both sources it is clear that the number of loading cycles necessary can be drastically reduced.

Maree[3] also found that the rate of loading, the duration of loading pulse and the frequency of the loading pulse had little or no effect on E-moduli of G1 materials. On the other hand he found that the number of repetitions and particularly the change in density and the in-situ moisture content had a tremendous influence on the E-moduli of G1 materials.

These findings confirm our observations with the K-mould that the plastic component of deformation is actually caused by the densification of under-compacted materials and that the E-moduli can probably be determined in a single loading cycle.

All roadbuilding materials should therefore be compacted to the highest density practically possible. A maximum allowable moisture content during construction should be specified and proper precautions for surface and subsurface drainage (where required) should be taken on all roadbuilding projects to ensure optimal performance from the road.

construct more optimally.

Compared to the back-calculated E-values from the the multi-depth-delectometer measurements on the HVS site at Bultfontein (ie M_R for crushed stone = 1000 MPa at a dry density = 91 % AD and M_R ranged from 42 MPa to 186 MPa for the in situ ferricrete), the K-mould seems to tie in with practice as shown by the K-mould results on the materials from the Bultfontein HVS site (see Figures 9.2(b) and 9.3). It is therefore strongly recommended that more evaluation of materials from as many HVS sites as possible should be done. This will give greater confidence in the reliability of the K-mould and will supply the input data for the development of a model to predict likely pavement behaviour under varying conditions. This is absolutely essential if we are to construct and maintain an effective road network in South Africa in the future.

Only when we can quantify material behaviour more accurately, will it be possible to design and construct more optimally. This should be our main aim with the limited budgets to our disposal.

It is also felt that the K-mould can be used to determine the material parameters E_i, $E_d(M_R)$, ν, c and ϕ for treated roadbuilding materials such as lime or cement stabilized materials as well as asphalts. No work has yet been done on these materials with the K-mould.

Seeing that both the elastic modulus and the bearing capacity (CBR) are functions of dry density (% AD or % DBD) and moisture content, it would seem possible to determine elastic modulus indirectly from bearing capacity. It would then be relatively easy to verify during construction whether the design criteria (with respect to E-values) are satisfied, by doing in-situ CBR determinations on the finished layerwork. If the design criteria are not satisfied the design can then timeously be adjusted to prevent future failure or alternatively, this procedure could be included in acceptance control systems.

Although CBR results were measured on all samples before the actual K-mould tests, too little information is available presently to make definite statements about the relation between the elastic modulus and the CBR.

11. REFERENCES

1. Handy R L and Fox D E, K-tests for subgrade and base evaluation. ATC Proceedings, 3 - 7 August 1987, Session 4A, Page VI, ISBN 0798842148.

2. Semmelink C J An index for describing the compactability of untreated roadbuilding materials Research Report DPVT-141, Division of Roads and Transport Technology, CSIR, 1990.

3. Maree J H Aspekte van die ontwerp en gedrag van plaveisels met korrelmateriaalkroonlae D.Sc. Eng Thesis, University of Pretoria, May 1982

4. Freeme C R Evaluation of pavement behaviour for major rehabilitation of roads Research Report RP/19/83, National Institute for Transport and Road Research, CSIR, 1983.

5. Sweere G T H Unbound granular bases for roads Doctoral Thesis, Technical University of Delft, September 1990

6. Elliot R P and Thornton S I Simplification of subgrade resilient modulus testing Transportation Research Record 1192, Transportation Research Board, National Research Council, Washington, DC 1988, ISBN 0-309-04770-6

7. Sweere GTH and Galjaard P J Repeated Static Loading Triaxial Tests for determination of resilient properties of sands, Transportation Research Record 1192, Transportation Research Board, National Research Council, Washington DC 1988, ISBN 0-309-04770-6

12. LIST OF INTERIM REPORTS

1. Semmelink C J - The K-mould : its theory and application for determining design parameters for roadbuilding materials. DPVT-137, April 1990.

2. Semmelink C J - The development and calibration of the K-mould to determine the soil engineering properties of roadbuilding materials. DPVT-146, March 1990.

3. Semmelink C J - Elastic moduli of four fine-graded materials as determined with the DRTT K-mould, October 1990.

4. Semmelink C J - Elastic moduli of four natural gravel materials as determined with DRTT K-mould, November 1990.

5. Semmelink C J - Elastic moduli of four G1 materials as determined with DRTT K-mould, January 1991.

APPENDIX A - Examples of regression analysis results for E-moduli for different classes of materials

DWA12A (MC=10.79%)(corrected)(91/03/26)
Sigma-1 vs Epsilon-1
Regression Output:

Constant	-12.3980
Std Err of Y Est	54.41656
R Squared	0.998493
No. of Observations	84
Degrees of Freedom	80

X Coefficient(s)	14648.98	581707.1	6402405.
Std Err of Coef.	3452.998	125287.4	1304652.

Sigma-d vs Epsilon-1
Regression Output:

Constant	-29.0454
Std Err of Y Est	55.00833
R Squared	0.997518
No. of Observations	84
Degrees of Freedom	80

X Coefficient(s)	21640.58	-79364.7	11565616
Std Err of Coef.	3490.549	126649.8	1318840.

E-1 vs DD(%AD)(72.2-74.4)
Regression Output:

Constant	1.3E+08
Std Err of Y Est	1842.476
R Squared	0.997685
No. of Observations	75
Degrees of Freedom	72

X Coefficient(s)	-3496548	24255.18
Std Err of Coef.	91799.76	625.1182

E-d vs DD(%AD)(72.2-74.4)
Regression Output:

Constant	1.7E+08
Std Err of Y Est	1682.547
R Squared	0.997627
No. of Observations	75
Degrees of Freedom	72

X Coefficient(s)	-4685209	32293.66
Std Err of Coef.	83831.39	570.8569

SILK2 (MC=7.67%)
Sigma-1 vs Epsilon-1

Regression Output:

Constant	-88.3086
Std Err of Y Est	47.27895
R Squared	0.999421
No. of Observations	110
Degrees of Freedom	106

X Coefficient(s)	9218.291	-25101.9	509187.3
Std Err of Coef.	708.0675	7466.274	21755.06

Sigma-d vs Epsilon-1

Regression Output:

Constant	-90.1237
Std Err of Y Est	46.88669
R Squared	0.999178
No. of Observations	110
Degrees of Freedom	106

X Coefficient(s)	9571.457	-70366.1	617796.5
Std Err of Coef.	702.1929	7404.328	21574.56

E-1 vs DD(%AD)(59-73)

Regression Output:

Constant	898990.6
Std Err of Y Est	665.6074
R Squared	0.998869
No. of Observations	101
Degrees of Freedom	98

X Coefficient(s)	-30965.7	268.7530
Std Err of Coef.	560.6670	4.251135

E-d vs DD(%AD)(59-73)

Regression Output:

Constant	1244199.
Std Err of Y Est	774.3452
R Squared	0.998340
No. of Observations	101
Degrees of Freedom	98

X Coefficient(s)	-41353.3	345.5631
Std Err of Coef.	652.2612	4.945627

DENS712 (MC=4.56%)(corrected)(Sigma-1m)
Sigma-1 vs Epsilon-1

Regression Output:

Constant	-211.213
Std Err of Y Est	116.1938
R Squared	0.998087
No. of Observations	96
Degrees of Freedom	92

X Coefficient(s)	72135.53	-1260495	18629955
Std Err of Coef.	4518.839	117164.3	858991.5

Sigma-d vs Epsilon-1

Regression Output:

Constant	-177.868
Std Err of Y Est	114.5072
R Squared	0.997534
No. of Observations	96
Degrees of Freedom	92

X Coefficient(s)	64939.47	-1504218	20656235
Std Err of Coef.	4453.247	115463.6	846522.9

E-1 vs DD(%AD)(74.5-78.5)

Regression Output:

Constant	1.1E+08
Std Err of Y Est	6009.493
R Squared	0.992052
No. of Observations	87
Degrees of Freedom	84

X Coefficient(s)	-2852029	18992.87
Std Err of Coef.	85285.05	556.8999

E-d vs DD(%AD)(74.5-78.5)

Regression Output:

Constant	1.2E+08
Std Err of Y Est	6519.032
R Squared	0.991356
No. of Observations	87
Degrees of Freedom	84

X Coefficient(s)	-3225948	21444.94
Std Err of Coef.	92516.28	604.1189

NPAB12 (MC=7.63%)(corrected)
Sigma-1 vs Epsilon-1

Regression Output:

Constant	52.73181
Std Err of Y Est	52.00024
R Squared	0.999276
No. of Observations	119
Degrees of Freedom	115

X Coefficient(s)	51024.94	-575445.	6204174.
Std Err of Coef.	1439.890	30101.43	177589.2

Sigma-d vs Epsilon-1

Regression Output:

Constant	74.83382
Std Err of Y Est	52.69858
R Squared	0.998917
No. of Observations	119
Degrees of Freedom	115

X Coefficient(s)	37208.07	-563188.	6360237.
Std Err of Coef.	1459.227	30505.67	179974.1

E-1 vs DD(%AD)(70.7-76.3)

Regression Output:

Constant	25858804
Std Err of Y Est	2272.580
R Squared	0.995033
No. of Observations	110
Degrees of Freedom	107

X Coefficient(s)	-720649.	5027.864
Std Err of Coef.	12977.16	88.38579

E-d vs DD(%AD)(70.7-76.3)

Regression Output:

Constant	26124620
Std Err of Y Est	2314.017
R Squared	0.995505
No. of Observations	110
Degrees of Freedom	107

X Coefficient(s)	-729584.	5098.305
Std Err of Coef.	13213.79	89.99740

NPAA13 (MC=4.51%)(corrected)
Sigma-1 vs Epsilon-1

Regression Output:	
Constant	22.66592
Std Err of Y Est	65.08575
R Squared	0.999356
No. of Observations	81
Degrees of Freedom	77

X Coefficient(s)	268517.8	2003548.	-3.1E+07
Std Err of Coef.	8346.088	662567.9	14901843

Sigma-d vs Epsilon-1

Regression Output:	
Constant	28.69268
Std Err of Y Est	60.54121
R Squared	0.999339
No. of Observations	81
Degrees of Freedom	77

X Coefficient(s)	257059.4	1200813.	-1.8E+07
Std Err of Coef.	7763.331	616304.8	13861338

E-1 vs DD(%AD)(86.68-87.38)

Regression Output:	
Constant	-7.6E+08
Std Err of Y Est	1438.573
R Squared	0.979465
No. of Observations	72
Degrees of Freedom	69

X Coefficient(s)	17457213	-99977.8
Std Err of Coef.	820079.0	4709.723

E-d vs DD(%AD)(86.68-87.38)

Regression Output:	
Constant	-4.3E+08
Std Err of Y Est	850.1812
R Squared	0.982193
No. of Observations	72
Degrees of Freedom	69

X Coefficient(s)	9776866.	-55968.1
Std Err of Coef.	484657.5	2783.394

FERRT14 (MC=5.29%)(corrected)
Sigma-1 vs Epsilon-1

Regression Output:

Constant	-297.639
Std Err of Y Est	106.9418
R Squared	0.999400
No. of Observations	107
Degrees of Freedom	103

X Coefficient(s)	247853.2	1354823.	32089289
Std Err of Coef.	8870.646	464528.8	6930697.

Sigma-d vs Epsilon-1

Regression Output:

Constant	-276.023
Std Err of Y Est	100.3358
R Squared	0.999402
No. of Observations	107
Degrees of Freedom	103

X Coefficient(s)	237186.1	807454.1	39253060
Std Err of Coef.	8322.684	435833.7	6502571.

E-1 vs DD(%AD)(86.3-87.7)

Regression Output:

Constant	5.7E+08
Std Err of Y Est	3269.069
R Squared	0.998174
No. of Observations	98
Degrees of Freedom	95

X Coefficient(s)	-1.3E+07	78129.83
Std Err of Coef.	453843.4	2606.224

E-d vs DD(%AD)(86.3-87.7)

Regression Output:

Constant	7.1E+08
Std Err of Y Est	3264.190
R Squared	0.998161
No. of Observations	98
Degrees of Freedom	95

X Coefficient(s)	-1.7E+07	96250.51
Std Err of Coef.	453166.0	2602.334

FERRT15 (MC=5.89%)(corrected)
Sigma-1 vs Epsilon-1

Regression Output:

Constant	-226.251
Std Err of Y Est	96.12600
R Squared	0.999219
No. of Observations	118
Degrees of Freedom	114

X Coefficient(s)	142406.6	542951.0	20455450
Std Err of Coef.	6272.704	252364.4	2962150.

Sigma-d vs Epsilon-1

Regression Output:

Constant	-229.740
Std Err of Y Est	94.51632
R Squared	0.999123
No. of Observations	118
Degrees of Freedom	114

X Coefficient(s)	132980.0	261126.0	23335937
Std Err of Coef.	6167.665	248138.4	2912547.

E-1 vs DD(%AD)(85.3-87.7)

Regression Output:

Constant	1.8E+08
Std Err of Y Est	1764.403
R Squared	0.999214
No. of Observations	109
Degrees of Freedom	106

X Coefficient(s)	-4254472	25155.17
Std Err of Coef.	80305.99	463.6180

E-d vs DD(%AD)(85.3-87.7)

Regression Output:

Constant	2.1E+08
Std Err of Y Est	1799.556
R Squared	0.999177
No. of Observations	109
Degrees of Freedom	106

X Coefficient(s)	-4907362	28920.14
Std Err of Coef.	81905.96	472.8549

CPA424 (MC=4.96%)(corrected)
Sigma-1 vs Epsilon-1

Regression Output:

Constant	12.18569
Std Err of Y Est	98.21562
R Squared	0.999061
No. of Observations	81
Degrees of Freedom	77

X Coefficient(s)	8824.963	9193608.	31618522
Std Err of Coef.	14015.65	862057.8	15790277

Sigma-d vs Epsilon-1

Regression Output:

Constant	26.25524
Std Err of Y Est	93.75909
R Squared	0.999025
No. of Observations	81
Degrees of Freedom	77

X Coefficient(s)	-2075.33	8697208.	35176029
Std Err of Coef.	13379.69	822942.0	15073794

E-1 vs DD(%AD)(88.95-89.65)

Regression Output:

Constant	5.8E+09
Std Err of Y Est	9778.752
R Squared	0.995658
No. of Observations	72
Degrees of Freedom	69

X Coefficient(s)	-1.3E+08	741136.6
Std Err of Coef.	5956798.	33349.86

E-d vs DD(%AD)(88.95-89.65)

Regression Output:

Constant	5.8E+09
Std Err of Y Est	9688.656
R Squared	0.995497
No. of Observations	72
Degrees of Freedom	69

X Coefficient(s)	-1.3E+08	738137.0
Std Err of Coef.	5901916.	33042.60

CPA925 MC=5.3% (corrected)
Sigma-1 vs Epsilon-1

Regression Output:

Constant	5.647550
Std Err of Y Est	43.68476
R Squared	0.999704
No. of Observations	145
Degrees of Freedom	141

X Coefficient(s)	4513.566	2512236.	14602556
Std Err of Coef.	2955.635	129383.8	1631222.

Sigma-d vs Epsilon-1

Regression Output:

Constant	17.79449
Std Err of Y Est	40.28736
R Squared	0.999681
No. of Observations	145
Degrees of Freedom	141

X Coefficient(s)	-4175.84	2108760.	18478935
Std Err of Coef.	2725.773	119321.5	1504361.

E-1 vs DD(%AD)(88.5-90.6)

Regression Output:

Constant	2.1E+08
Std Err of Y Est	2339.819
R Squared	0.999420
No. of Observations	136
Degrees of Freedom	133

X Coefficient(s)	-4746748	27390.40
Std Err of Coef.	109414.8	610.3294

E-d vs DD(%AD)(88.5-90.6)

Regression Output:

Constant	2.5E+08
Std Err of Y Est	2203.419
R Squared	0.999462
No. of Observations	136
Degrees of Freedom	133

X Coefficient(s)	-5677117	32558.45
Std Err of Coef.	103036.5	574.7503

BULTG1A4 - MC=2.75% (corrected)
Sigma-1 vs Epsilon-1

Regression Output:

Constant	-102.427
Std Err of Y Est	62.61707
R Squared	0.999267
No. of Observations	92
Degrees of Freedom	88

X Coefficient(s)	171112.3	925494.5	47927141
Std Err of Coef.	8198.411	537261.9	10063390

Sigma-d vs Epsilon-1

Regression Output:

Constant	-96.7265
Std Err of Y Est	59.21912
R Squared	0.999219
No. of Observations	92
Degrees of Freedom	88

X Coefficient(s)	151773.5	872284.8	47262752
Std Err of Coef.	7753.520	508107.1	9517296.

E-1 vs DD(%AD)(88.4-89.5)

Regression Output:

Constant	8.2E+08
Std Err of Y Est	1513.593
R Squared	0.999275
No. of Observations	83
Degrees of Freedom	80

X Coefficient(s)	-1.9E+07	105101.2
Std Err of Coef.	330489.5	1855.794

E-d vs DD(%AD)(88.4-89.5)

Regression Output:

Constant	8.0E+08
Std Err of Y Est	1478.761
R Squared	0.999272
No. of Observations	83
Degrees of Freedom	80

X Coefficient(s)	-1.8E+07	103551.1
Std Err of Coef.	322884.0	1813.087

BULTIA5 - MC=8.13%

Sigma-1 vs Epsilon-1

Regression Output:

Constant	-63.5897
Std Err of Y Est	37.20388
R Squared	0.999720
No. of Observations	162
Degrees of Freedom	158

X Coefficient(s)	13939.58	-300254.	7814607.
Std Err of Coef.	979.1084	20818.04	125983.6

Sigma-d vs Epsilon-1

Regression Output:

Constant	-84.8277
Std Err of Y Est	41.70626
R Squared	0.999481
No. of Observations	162
Degrees of Freedom	158

X Coefficient(s)	17831.66	-528463.	8616685.
Std Err of Coef.	1097.599	23337.43	141230.1

E-1 vs DD(%AD)(80.5-86.9)

Regression Output:

Constant	47988016
Std Err of Y Est	1811.115
R Squared	0.999160
No. of Observations	153
Degrees of Freedom	150

X Coefficient(s)	-1175547	7200.590
Std Err of Coef.	8564.685	51.05142

E-d vs DD(%AD)(80.5-86.9)

Regression Output:

Constant	51864584
Std Err of Y Est	1919.752
R Squared	0.998890
No. of Observations	153
Degrees of Freedom	150

X Coefficient(s)	-1265103	7715.418
Std Err of Coef.	9078.426	54.11367

APPENDIX B - Examples of regression analysis results for ϕ and c for different classes of materials

DWA12A (MC=10.79%)(corrected)(91/03/26)

phi and c (intercept computed)(0<p<1500kPa)

Regression Output:

Constant		23.61802	
Std Err of Y Est		8.329118	
R Squared		0.999073	
No. of Observations		57	
Degrees of Freedom		55	
		phi	c
X Coefficient(s)	0.597822	36.71411	29.46255
Std Err of Coef.	0.002454		

phi and c (intercept computed)(1500<p<2714kPa)

Regression Output:

Constant		-255.843	
Std Err of Y Est		11.02786	
R Squared		0.998678	
No. of Observations		27	
Degrees of Freedom		25	
		phi	c
X Coefficient(s)	0.767437	50.12430	-399.053
Std Err of Coef.	0.005583		

phi and c (intercept zero)(1500<p<2714kPa)

Regression Output:

Constant		0	
Std Err of Y Est		47.20457	
R Squared		0.974820	
No. of Observations		27	
Degrees of Freedom		26	
		phi	c
X Coefficient(s)	0.650676	40.59263	0
Std Err of Coef.	0.004211		

phi and c (intercept computed)(0<p<2714kPa)

Regression Output:

Constant		-5.32788	
Std Err of Y Est		33.46514	
R Squared		0.996234	
No. of Observations		84	
Degrees of Freedom		82	
		phi	c
X Coefficient(s)	0.648138	40.40141	-6.99635
Std Err of Coef.	0.004400		

SILK2 (MC=7.67%)

phi and c (intercept computed)(0<p<1500kPa)

Regression Output:

Constant		3.367663	
Std Err of Y Est		8.569279	
R Squared		0.998840	
No. of Observations		72	
Degrees of Freedom		70	
		phi	c
X Coefficient(s)	0.524786	31.65388	3.956214
Std Err of Coef.	0.002136		

phi and c (intercept computed)(1500<p<2648kPa)

Regression Output:

Constant		-337.634	
Std Err of Y Est		5.895889	
R Squared		0.999553	
No. of Observations		38	
Degrees of Freedom		36	
		phi	c
X Coefficient(s)	0.760915	49.54496	-520.357
Std Err of Coef.	0.002680		

phi and c (intercept zero)(1500<p<2648kPa)

Regression Output:

Constant		0	
Std Err of Y Est		57.80525	
R Squared		0.955891	
No. of Observations		38	
Degrees of Freedom		37	
		phi	c
X Coefficient(s)	0.604146	37.16745	0
Std Err of Coef.	0.004416		

phi and c (intercept computed)(0<p<2648kPa)

Regression Output:

Constant		-37.6941	
Std Err of Y Est		47.52463	
R Squared		0.992011	
No. of Observations		110	
Degrees of Freedom		108	
		phi	c
X Coefficient(s)	0.612062	37.73879	-47.6652
Std Err of Coef.	0.005285		

DENS712 (MC=4.56%)(corrected)(Sigma-1m)

phi and c (intercept computed)(0<p<1800kPa)

Regression Output:

Constant	23.42084		
Std Err of Y Est	9.757645		
R Squared	0.999012		
No. of Observations	57		
Degrees of Freedom	55		
		phi	c
X Coefficient(s)	0.565748	34.45425	28.40343
Std Err of Coef.	0.002398		

phi and c (intercept computed)(1800<p<5071kPa)

Regression Output:

Constant	-625.904		
Std Err of Y Est	27.34530		
R Squared	0.999182		
No. of Observations	39		
Degrees of Freedom	37		
		phi	c
X Coefficient(s)	0.896611	63.71620	-1413.45
Std Err of Coef.	0.004217		

phi and c (intercept zero)(1800<p<5071kPa)

Regression Output:

Constant	0		
Std Err of Y Est	190.6554		
R Squared	0.959163		
No. of Observations	39		
Degrees of Freedom	38		
		phi	c
X Coefficient(s)	0.725307	46.49447	0
Std Err of Coef.	0.008752		

phi and c (intercept computed)(0<p<5071kPa)

Regression Output:

Constant	-145.467		
Std Err of Y Est	125.6821		
R Squared	0.987859		
No. of Observations	96		
Degrees of Freedom	94		
		phi	c
X Coefficient(s)	0.759974	49.46194	-223.812
Std Err of Coef.	0.008689		

NPAB12 (MC=7.63%)(corrected)

phi and c (intercept computed)(0<p<1800kPa)

Regression Output:

Constant	27.50908		
Std Err of Y Est	21.42046		
R Squared	0.992998		
No. of Observations	69		
Degrees of Freedom	67		
		phi	c
X Coefficient(s)	0.507125	30.47253	31.91781
Std Err of Coef.	0.005202		

phi and c (intercept computed)(1800<p<4175kPa)

Regression Output:

Constant	-592.738		
Std Err of Y Est	20.11248		
R Squared	0.998841		
No. of Observations	50		
Degrees of Freedom	48		
		phi	c
X Coefficient(s)	0.856823	58.96180	-1149.58
Std Err of Coef.	0.004212		

phi and c (intercept zero)(1800<p<4175kPa)

Regression Output:

Constant	0		
Std Err of Y Est	140.9622		
R Squared	0.941890		
No. of Observations	50		
Degrees of Freedom	49		
		phi	c
X Coefficient(s)	0.657863	41.13712	0
Std Err of Coef.	0.006880		

phi and c (intercept computed)(0<p<4175kPa)

Regression Output:

Constant	-143.907		
Std Err of Y Est	103.0893		
R Squared	0.983143		
No. of Observations	119		
Degrees of Freedom	117		
		phi	c
X Coefficient(s)	0.698806	44.33132	-201.181
Std Err of Coef.	0.008459		

NPAA13 (MC=4.51%)(corrected)

phi and c (intercept computed)(0<p<3500kPa)

Regression Output:

Constant	35.31784
Std Err of Y Est	11.17904
R Squared	0.999824
No. of Observations	62
Degrees of Freedom	60

		phi	c
X Coefficient(s)	0.855169	58.77848	68.13537
Std Err of Coef.	0.001464		

phi and c (intercept computed)(3500<p<4712kPa)

Regression Output:

Constant	56.64416
Std Err of Y Est	3.329627
R Squared	0.999899
No. of Observations	19
Degrees of Freedom	17

		phi	c
X Coefficient(s)	0.843162	57.47554	105.3532
Std Err of Coef.	0.002048		

phi and c (intercept computed)(0<p<4712kPa)

Regression Output:

Constant	44.83646
Std Err of Y Est	12.59411
R Squared	0.999881
No. of Observations	81
Degrees of Freedom	79

		phi	c
X Coefficient(s)	0.848081	58.00357	84.61843
Std Err of Coef.	0.001037		

FERRT14 (MC=5.29%)(corrected)

phi and c (intercept computed)(p<=4000kPa)

Regression Output:

Constant	15.40399
Std Err of Y Est	7.643164
R Squared	0.999945
No. of Observations	67
Degrees of Freedom	65

		phi	c
X Coefficient(s)	0.836784	56.80209	28.13347
Std Err of Coef.	0.000769		

phi and c (intercept computed)(p>4000kPa)

Regression Output:

Constant	-181.524
Std Err of Y Est	6.903145
R Squared	0.999853
No. of Observations	41
Degrees of Freedom	39

		phi	c
X Coefficient(s)	0.885693	62.33695	-390.988
Std Err of Coef.	0.001715		

phi and c (intercept zero)(p>4000kPa)

Regression Output:

Constant	0
Std Err of Y Est	23.63471
R Squared	0.998241
No. of Observations	41
Degrees of Freedom	40

		phi	c
X Coefficient(s)	0.850399	58.25520	0
Std Err of Coef.	0.000723		

phi and c (intercept computed)(0<p<6123kPa)

Regression Output:

Constant	-11.1316
Std Err of Y Est	21.24101
R Squared	0.999796
No. of Observations	107
Degrees of Freedom	105

		phi	c
X Coefficient(s)	0.850742	58.29257	-21.1797
Std Err of Coef.	0.001184		

FERRT15 (MC=5.89%)(corrected)

phi and c (intercept computed)(0<p<2500kPa)

Regression Output:

Constant	-19.1445		
Std Err of Y Est	5.724049		
R Squared	0.999889		
No. of Observations	65		
Degrees of Freedom	63		
		phi	c
X Coefficient(s)	0.794220	52.58168	-31.5069
Std Err of Coef.	0.001054		

phi and c (intercept computed)(2500<p<5069kPa)

Regression Output:

Constant	-201.565		
Std Err of Y Est	12.50724		
R Squared	0.999648		
No. of Observations	53		
Degrees of Freedom	51		
		phi	c
X Coefficient(s)	0.860910	59.41901	-396.193
Std Err of Coef.	0.002261		

phi and c (intercept zero)(2500<p<5069kPa)

Regression Output:

Constant	0		
Std Err of Y Est	42.82286		
R Squared	0.995795		
No. of Observations	53		
Degrees of Freedom	52		
		phi	c
X Coefficient(s)	0.808561	53.95564	0
Std Err of Coef.	0.001559		

phi and c (intercept computed)(0<p<5069kPa)

Regression Output:

Constant	-19.5319		
Std Err of Y Est	5.831364		
R Squared	0.999888		
No. of Observations	66		
Degrees of Freedom	64		
		phi	c
X Coefficient(s)	0.794633	52.62065	-32.1731
Std Err of Coef.	0.001049		

CPA424 (MC=4.96%)(corrected)

phi and c (intercept computed)(0<p<2000kPa)

Regression Output:

Constant	-31.2876
Std Err of Y Est	14.03974
R Squared	0.999180
No. of Observations	36
Degrees of Freedom	34

		phi	c
X Coefficient(s)	0.833177	56.42656	-56.5775
Std Err of Coef.	0.004092		

phi and c (intercept computed)(2000<p<6484kPa)

Regression Output:

Constant	-154.485
Std Err of Y Est	7.377755
R Squared	0.999959
No. of Observations	45
Degrees of Freedom	43

		phi	c
X Coefficient(s)	0.899423	64.08245	-353.452
Std Err of Coef.	0.000876		

phi and c (intercept zero)(2000<p<6484kPa)

Regression Output:

Constant	0
Std Err of Y Est	52.33327
R Squared	0.997898
No. of Observations	45
Degrees of Freedom	44

		phi	c
X Coefficient(s)	0.860909	59.41884	0
Std Err of Coef.	0.002061		

phi and c (intercept computed)(0<p<6484kPa)

Regression Output:

Constant	-82.8309
Std Err of Y Est	28.40944
R Squared	0.999632
No. of Observations	81
Degrees of Freedom	79

		phi	c
X Coefficient(s)	0.881078	61.77278	-175.129
Std Err of Coef.	0.001899		

CPA925 MC=5.3% (corrected)

phi and c (intercept computed)(0<p<1200kPa)

Regression Output:			
Constant	-31.5621		
Std Err of Y Est	18.96970		
R Squared	0.992583		
No. of Observations	53		
Degrees of Freedom	51		
		phi	c
X Coefficient(s)	0.600444	36.90170	-39.4690
Std Err of Coef.	0.007267		

phi and c (intercept computed)(1200<p<3577kPa)

Regression Output:			
Constant	-282.584		
Std Err of Y Est	11.02550		
R Squared	0.999615		
No. of Observations	92		
Degrees of Freedom	90		
		phi	c
X Coefficient(s)	0.816338	54.71993	-489.261
Std Err of Coef.	0.001687		

phi and c (intercept zero)(1200<p<3577kPa)

Regression Output:			
Constant	0		
Std Err of Y Est	76.73204		
R Squared	0.981174		
No. of Observations	92		
Degrees of Freedom	91		
		phi	c
X Coefficient(s)	0.709493	45.19370	0
Std Err of Coef.	0.003138		

phi and c (intercept computed)(0<p<3577kPa)

Regression Output:			
Constant	-114.531		
Std Err of Y Est	51.91474		
R Squared	0.996345		
No. of Observations	145		
Degrees of Freedom	143		
		phi	c
X Coefficient(s)	0.751707	48.73848	-173.665
Std Err of Coef.	0.003807		

BULTG1A4 - MC=2.75% (corrected)

phi and c (intercept computed)(0<p<2000kPa)

Regression Output:

Constant	-10.0416		
Std Err of Y Est	5.388210		
R Squared	0.999906		
No. of Observations	31		
Degrees of Freedom	29		
		phi	c
X Coefficient(s)	0.815201	54.60729	-17.3378
Std Err of Coef.	0.001466		

phi and c (intercept computed)(2000<p<4526kPa)

Regression Output:

Constant	-99.3172		
Std Err of Y Est	6.500881		
R Squared	0.999896		
No. of Observations	61		
Degrees of Freedom	59		
		phi	c
X Coefficient(s)	0.861429	59.47748	-195.553
Std Err of Coef.	0.001139		

phi and c (intercept zero)(2000<p<4526kPa)

Regression Output:

Constant	0		
Std Err of Y Est	22.93045		
R Squared	0.998694		
No. of Observations	61		
Degrees of Freedom	60		
		phi	c
X Coefficient(s)	0.832289	56.33469	0
Std Err of Coef.	0.000882		

phi and c (intercept computed)(0<p<4526kPa)

Regression Output:

Constant	-45.6445		
Std Err of Y Est	16.40906		
R Squared	0.999754		
No. of Observations	92		
Degrees of Freedom	90		
		phi	c
X Coefficient(s)	0.845179	57.69122	-85.3996
Std Err of Coef.	0.001394		

BULTIA5 - MC=8.13%

phi and c (intercept computed)(0<p<1500kPa)

Regression Output:

Constant		-11.5987	
Std Err of Y Est		16.18934	
R Squared		0.995749	
No. of Observations		87	
Degrees of Freedom		85	
		phi	c
X Coefficient(s)	0.563963	34.33032	-14.0454
Std Err of Coef.	0.003996		

phi and c (intercept computed)(1500<p<2500kPa)

Regression Output:

Constant		-223.339	
Std Err of Y Est		5.646449	
R Squared		0.999320	
No. of Observations		35	
Degrees of Freedom		33	
		phi	c
X Coefficient(s)	0.721674	46.19287	-322.636
Std Err of Coef.	0.003276		

phi and c (intercept computed)(2500<p<4244kPa)

Regression Output:

Constant		-514.934	
Std Err of Y Est		5.789872	
R Squared		0.999825	
No. of Observations		40	
Degrees of Freedom		38	
		phi	c
X Coefficient(s)	0.837956	56.92500	-943.558
Std Err of Coef.	0.001797		

phi and c (intercept computed)(0<p<4244kPa)

Regression Output:

Constant		-83.6488	
Std Err of Y Est		74.91155	
R Squared		0.993219	
No. of Observations		162	
Degrees of Freedom		160	
		phi	c
X Coefficient(s)	0.695514	44.06820	-116.419
Std Err of Coef.	0.004543		

APPENDIX C - Examples of regression analysis results for $\log(E_d)$ versus $\log(\sigma_1 + 2.\sigma_3)$ for different classes of materials

DWA12A (MC=10.79%)(corrected)(91/03/26)

log(E-d) vs log(Sigma-1t + 2.Sigma-3)(log(Sigma)>3.0)
Regression Output:

Constant	2.198077
Std Err of Y Est	0.018090
R Squared	0.989324
No. of Observations	58
Degrees of Freedom	56

X Coefficient(s)	0.772047
Std Err of Coef.	0.010716

log(E-d) vs log(Sigma-1t + 2.Sigma-3)(1.2<log(Sigma)<2.5)
Regression Output:

Constant	4.295784
Std Err of Y Est	0.012101
R Squared	0.400911
No. of Observations	8
Degrees of Freedom	6

X Coefficient(s)	0.024334
Std Err of Coef.	0.012144

SILK2 (MC=7.67%)

log(E-d) vs log(Sigma-1m + 2.Sigma-3)(log(Sigma)>3.5)

Regression Output:

Constant	0.236757
Std Err of Y Est	0.003297
R Squared	0.999670
No. of Observations	63
Degrees of Freedom	61

X Coefficient(s)	1.142725
Std Err of Coef.	0.002656

log(E-d) vs log(Sigma-1m + 2.Sigma-3)(1.8<log(Sigma)<2.5)

Regression Output:

Constant	4.043533
Std Err of Y Est	0.016808
R Squared	0.651030
No. of Observations	14
Degrees of Freedom	12

X Coefficient(s)	-0.07649
Std Err of Coef.	0.016166

DENS712 (MC=4.56%)(corrected)(Sigma-1m)

log(E-d) vs log(Sigma-1m + 2.Sigma-3)(log(Sigma)>3.4)

Regression Output:

Constant	-0.23195
Std Err of Y Est	0.021306
R Squared	0.994234
No. of Observations	59
Degrees of Freedom	57

X Coefficient(s)	1.408960
Std Err of Coef.	0.014211

log(E-d) vs log(Sigma-1m + 2.Sigma-3)(2.2<log(Sigma)<3.2)

Regression Output:

Constant	5.367566
Std Err of Y Est	0.012178
R Squared	0.980084
No. of Observations	21
Degrees of Freedom	19

X Coefficient(s)	-0.29070
Std Err of Coef.	0.009506

NPAB12 (MC=7.63%)(corrected)

log(E-d) vs log(Sigma-1t + 2.Sigma-3)(log(Sigma)>3.4)

Regression Output:

Constant	-0.91521
Std Err of Y Est	0.013434
R Squared	0.997080
No. of Observations	78
Degrees of Freedom	76

X Coefficient(s)	1.536501
Std Err of Coef.	0.009537

log(E-d) vs log(Sigma-1t + 2.Sigma-3)(2.5<log(Sigma)<3.25)

Regression Output:

Constant	5.389833
Std Err of Y Est	0.009927
R Squared	0.975801
No. of Observations	23
Degrees of Freedom	21

X Coefficient(s)	-0.32998
Std Err of Coef.	0.011339

NPAA13 (MC=4.51%)(corrected)

log(E-d) vs log(Sigma-1t + 2.Sigma-3)(3.1<log(Sigma)<3.8)

Regression Output:

Constant	5.299389
Std Err of Y Est	0.000454
R Squared	0.996486
No. of Observations	44
Degrees of Freedom	42

X Coefficient(s)	0.040203
Std Err of Coef.	0.000368

log(E-d) vs log(Sigma-1t + 2.Sigma-3)(2.2<log(Sigma)<2.6)

Regression Output:

Constant	5.390495
Std Err of Y Est	0.001455
R Squared	0.778824
No. of Observations	3
Degrees of Freedom	1

X Coefficient(s)	0.009412
Std Err of Coef.	0.005015

FERRT14 (MC=5.29%)(corrected)

log(E-d) vs log(Sigma-1t + 2.Sigma-3)(log(Sigma)>3.7)

Regression Output:

Constant	3.690470
Std Err of Y Est	0.007915
R Squared	0.987392
No. of Observations	83
Degrees of Freedom	81

X Coefficient(s)	0.475586
Std Err of Coef.	0.005971

log(E-d) vs log(Sigma-1t + 2.Sigma-3)(1.67<log(Sigma)<2.7)

Regression Output:

Constant	5.355061
Std Err of Y Est	0.001863
R Squared	0.894309
No. of Observations	6
Degrees of Freedom	4

X Coefficient(s)	0.011986
Std Err of Coef.	0.002060

FERRT15 (MC=5.89%)(corrected)

log(E-d) vs log(Sigma-1t + 2.Sigma-3)(log(Sigma)>3.7)

Regression Output:

Constant	2.942872
Std Err of Y Est	0.005344
R Squared	0.995967
No. of Observations	72
Degrees of Freedom	70

X Coefficient(s)	0.629620
Std Err of Coef.	0.004788

log(E-d) vs log(Sigma-1t + 2.Sigma-3)(2.07<log(Sigma)<2.87)

Regression Output:

Constant	5.076157
Std Err of Y Est	0.002417
R Squared	0.906665
No. of Observations	6
Degrees of Freedom	4

X Coefficient(s)	0.022786
Std Err of Coef.	0.003655

CPA424 (MC=4.96%)(corrected)

log(E-d) vs log(Sigma-1t + 2.Sigma-3)(total range)

Regression Output:

Constant	3.369876
Std Err of Y Est	0.023115
R Squared	0.991878
No. of Observations	80
Degrees of Freedom	78

X Coefficient(s)	0.601804
Std Err of Coef.	0.006166

CPA925 MC=5.3% (corrected)

log(E-d) vs log(Sigma-1t + 2.Sigma-3)(total range)

Regression Output:

Constant	2.584295
Std Err of Y Est	0.030271
R Squared	0.994295
No. of Observations	143
Degrees of Freedom	141

X Coefficient(s)	0.739706
Std Err of Coef.	0.004718

BULTG1A4 - MC=2.75% (corrected)

log(E-d) vs log(Sigma-1m + 2.Sigma-3)(log(Sigma)>3.5)

Regression Output:

Constant	3.384397
Std Err of Y Est	0.005972
R Squared	0.993160
No. of Observations	74
Degrees of Freedom	72

X Coefficient(s)	0.543605
Std Err of Coef.	0.005316

log(E-d) vs log(Sigma-1m + 2.Sigma-3)(2.11<log(Sigma)<2.8)

Regression Output:

Constant	5.129066
Std Err of Y Est	0.002365
R Squared	0.934292
No. of Observations	4
Degrees of Freedom	2

X Coefficient(s)	0.026166
Std Err of Coef.	0.004906

BULTIA5 - MC=8.13%

log(E-d) vs log(Sigma-1m + 2.Sigma-3)(log(Sigma)>2.7)

Regression Output:

Constant	1.224701
Std Err of Y Est	0.013943
R Squared	0.998560
No. of Observations	126
Degrees of Freedom	124

X Coefficient(s)	1.025345
Std Err of Coef.	0.003495

log(E-d) vs log(Sigma-1m + 2.Sigma-3)(0.9<log(Sigma)<2.3)

Regression Output:

Constant	4.493040
Std Err of Y Est	0.027390
R Squared	0.946136
No. of Observations	22
Degrees of Freedom	20

X Coefficient(s)	-0.29396
Std Err of Coef.	0.015683

APPENDIX D - Examples of graphs of log (E_d) versus log ($\sigma_1 + 2.\sigma_3$) for different classes of materials

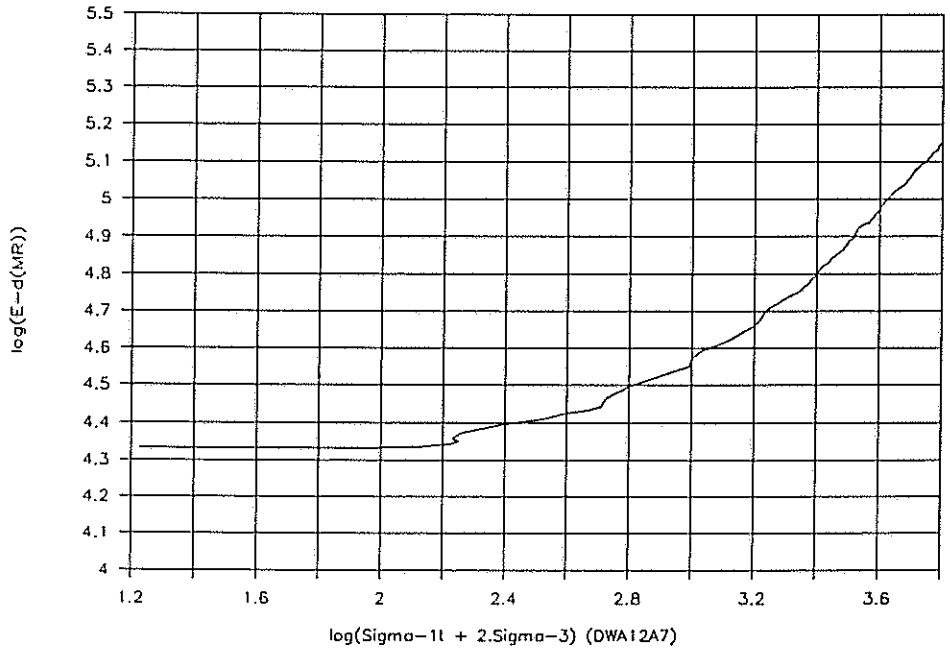

FIGURE D.1 - $\log(E_d)$ AGAINST $\log(\sigma_{1t} + 2.\sigma_3)$ FOR SLIGHTLY PLASTIC SAND, (MC = 10,79 %)

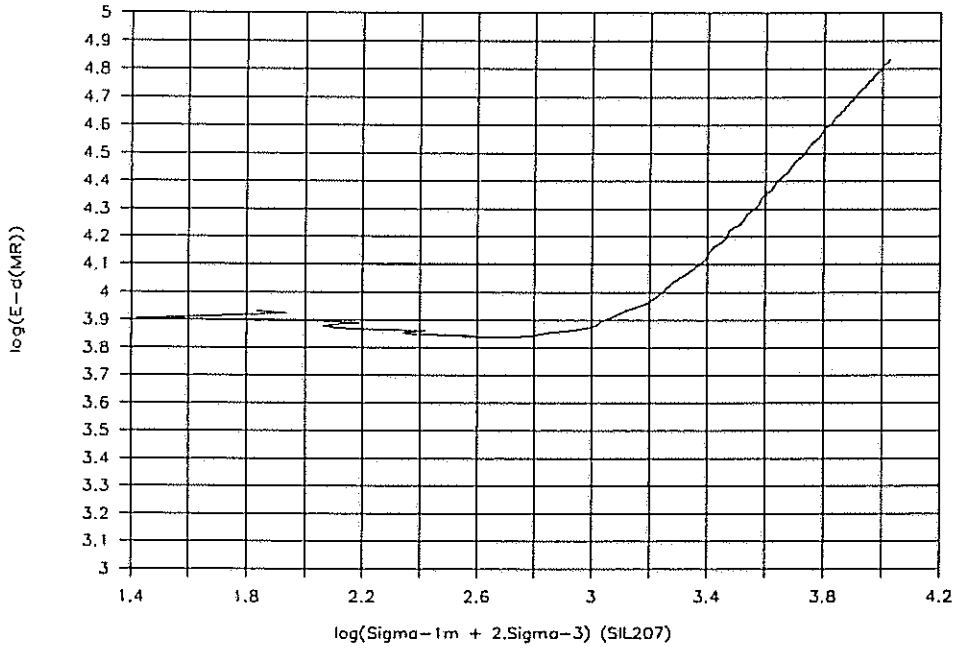

FIGURE D.2 - $\log(E_d)$ AGAINST $\log(\sigma_{1m} + 2.\sigma_3)$ FOR SILTY SAND (MC = 7,67%)

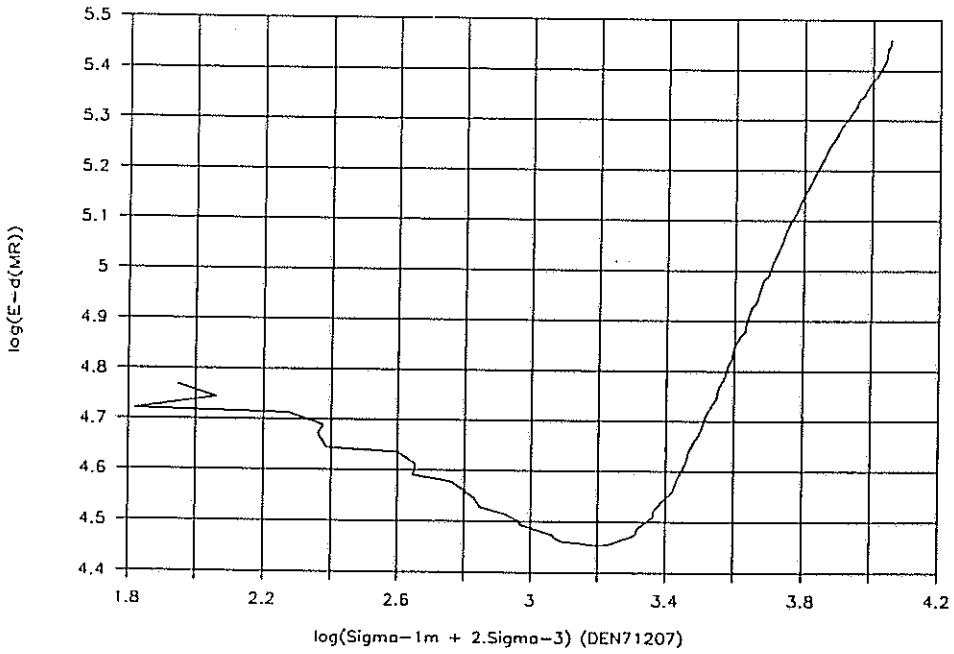

FIGURE D.3 - $\log(E_d)$ AGAINST $\log(\sigma_{1m} + 2.\sigma_3)$ FOR DOLOMITIC SOIL, (MC = 4,56 %)

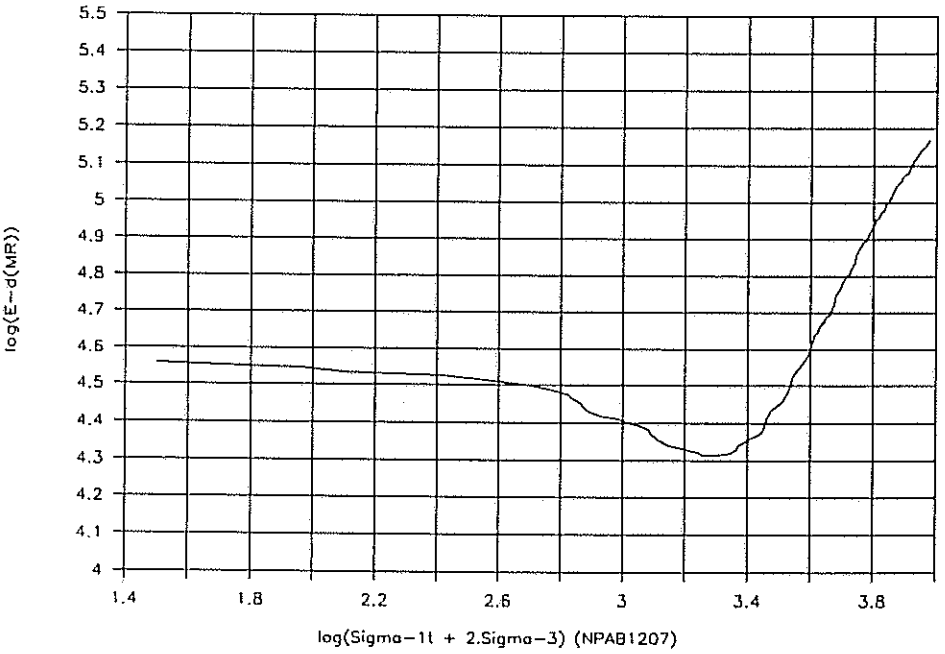

FIGURE D.4 - $\log(E_d)$ AGAINST $\log(\sigma_{1t} + 2.\sigma_3)$ FOR DECOMPOSED DOLERITE (MC = 7,63 %)

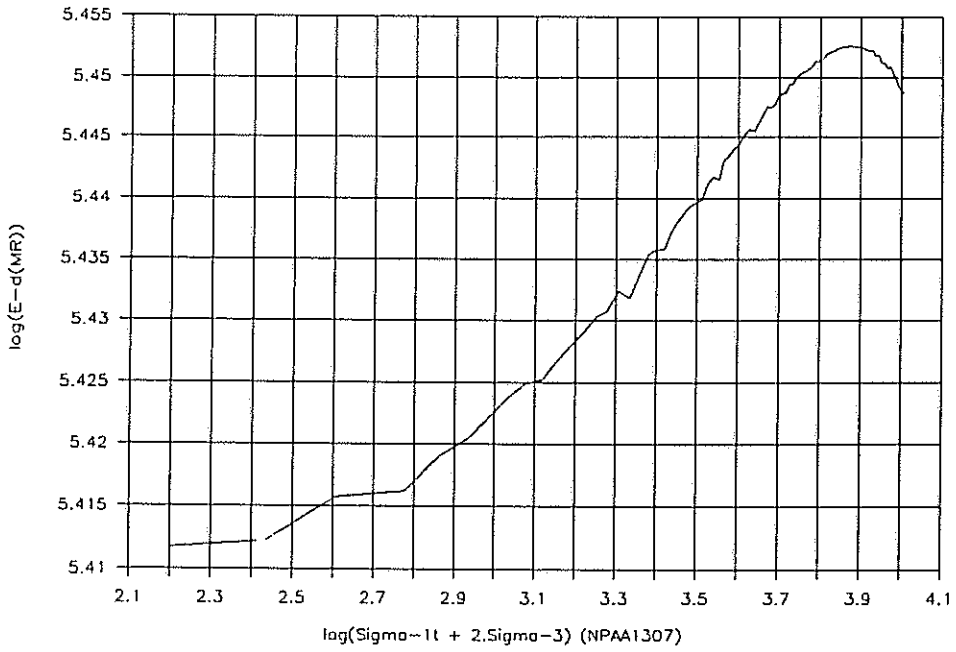

FIGURE D.5 - $\log(E_d)$ AGAINST $\log(\sigma_{1t} + 2.\sigma_3)$ FOR DOLERITE CRUSHED STONE (MC = 4,51 %)

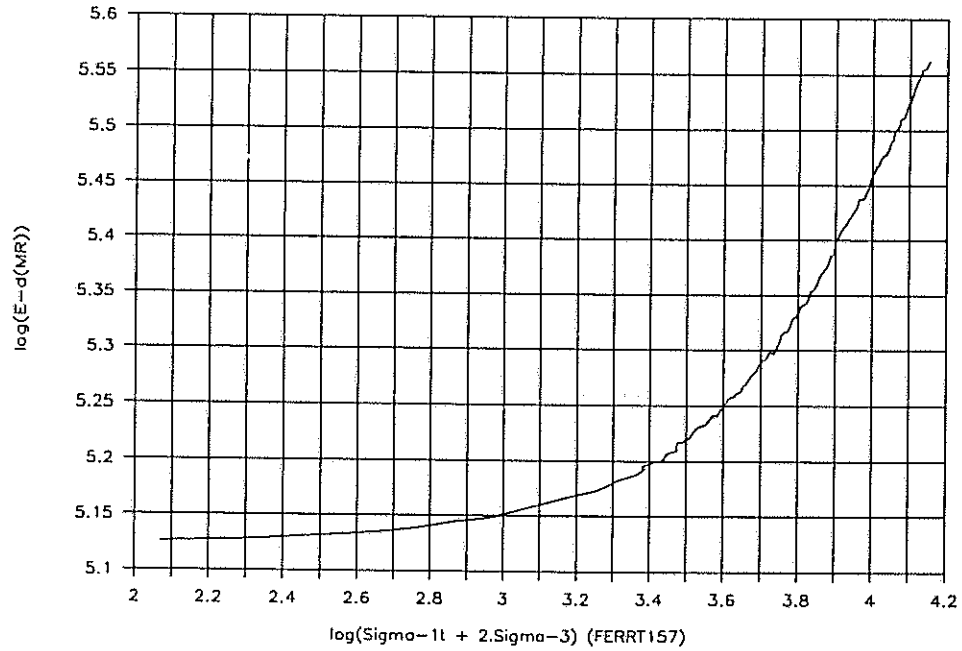

FIGURE D.6 - $\log(E_d)$ AGAINST $\log(\sigma_{1t} + 2.\sigma_3)$ FOR QUARTZITE CRUSHED STONE (MC = 5,29 %)

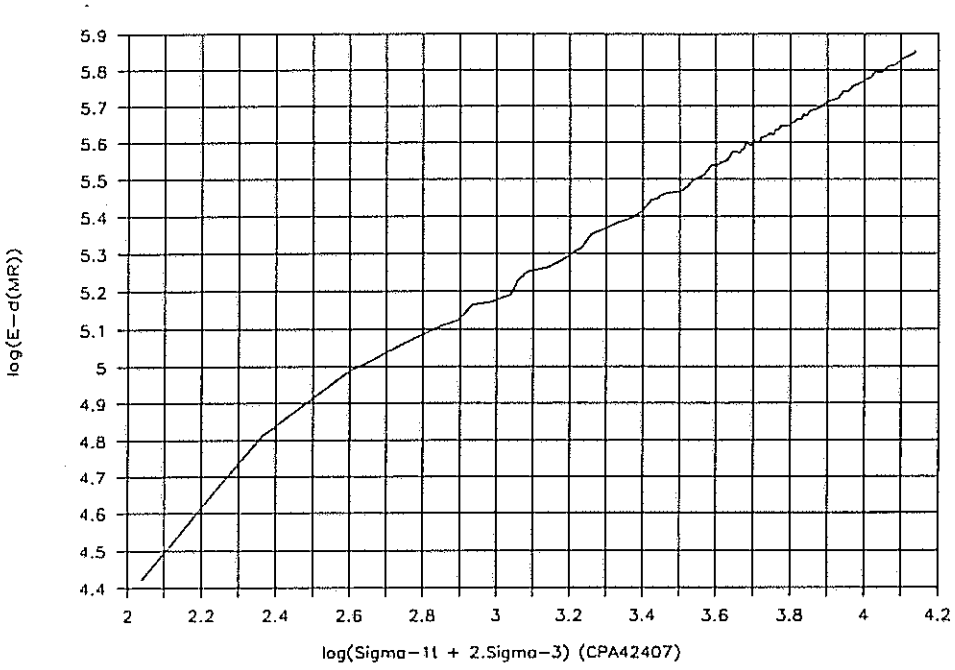

FIGURE D.7 - $\log(E_d)$ AGAINST $\log(\sigma_{1t} + 2.\sigma_3)$ FOR CRUSHED ALLUVIAL GRAVEL (MC = 4,96 %)

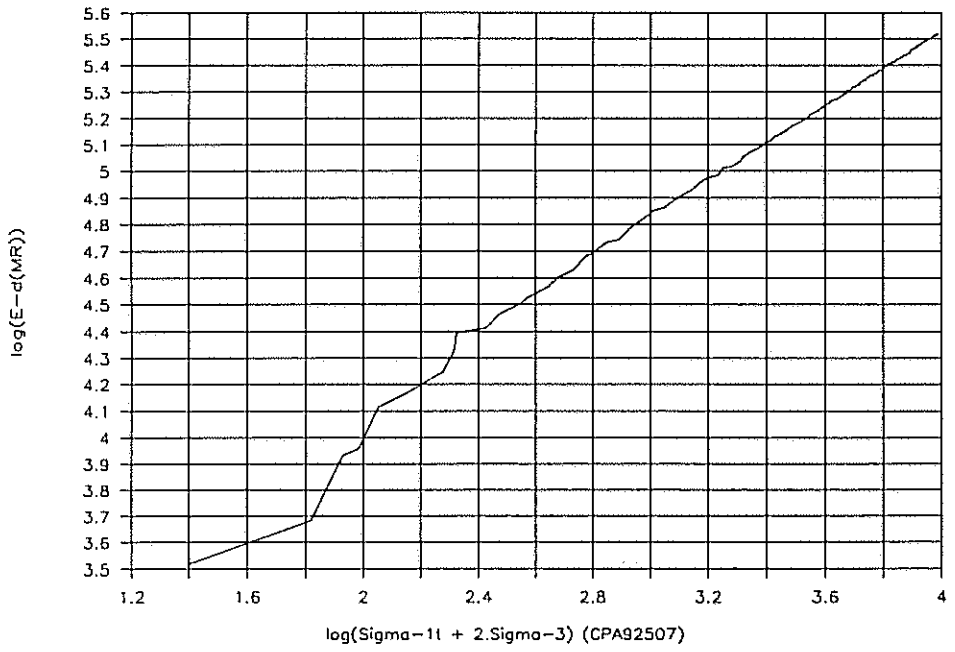

FIGURE D.8 - $\log(E_d)$ AGAINST $\log(\sigma_{1t} + 2.\sigma_3)$ FOR CRUSHED HORNFELS (MC = 5,3 %)

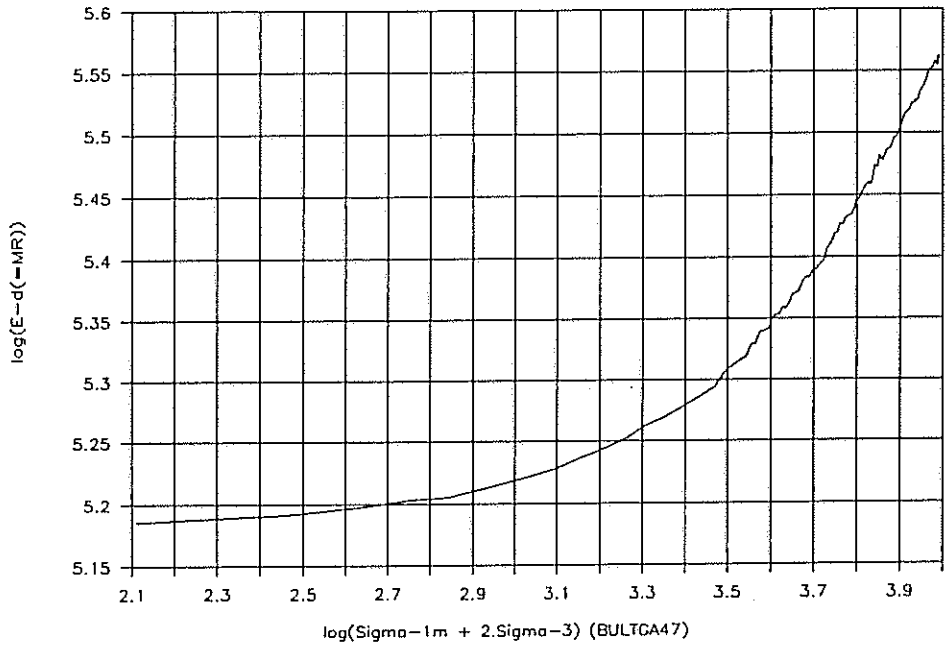

FIGURE D.9 - $\log(E_d)$ AGAINST $\log(\sigma_{1m} + 2.\sigma_3)$ FOR BULTFONTEIN G1 MATERIAL (MC = 2,75 %)

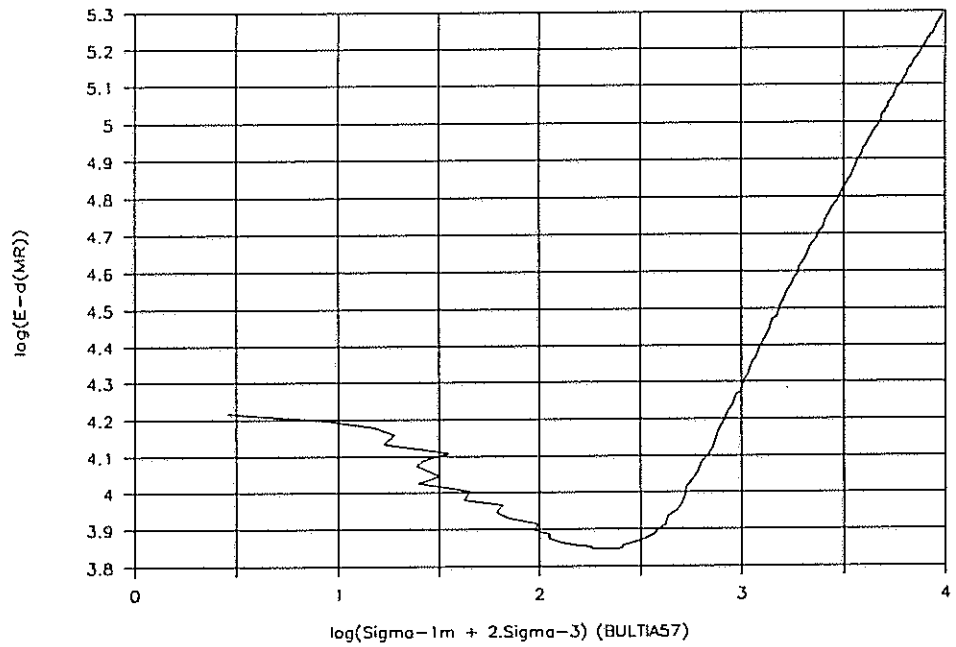

FIGURE D.10 - $\log(E_d)$ AGAINST $\log(\sigma_{1m} + 2.\sigma_3)$ FOR BULTFONTEIN IN-SITU FERRICRETE MATERIAL (MC = 8,13 %)

APPENDIX E - Examples of graphs of q versus p for different classes of materials

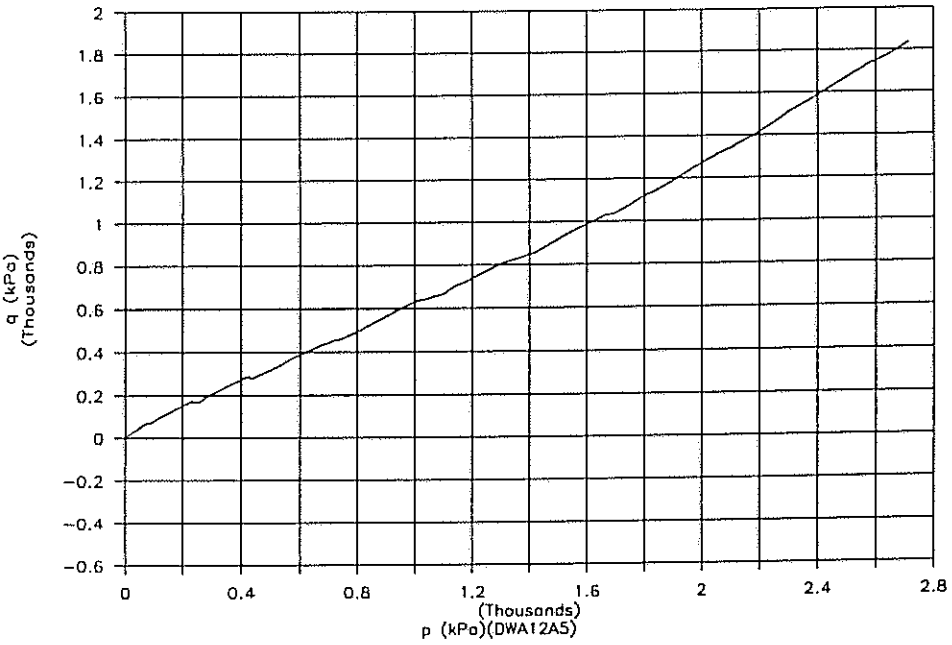

FIGURE E.1 - q AGAINST p GRAPH FOR SLIGHTLY PLASTIC SAND (MC = 10,79 %)

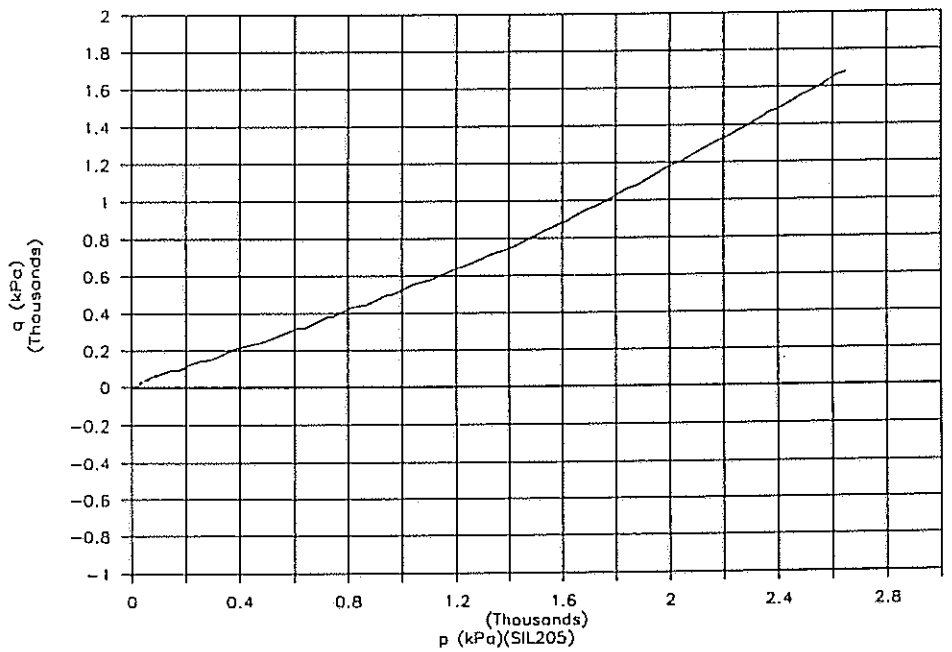

FIGURE E.2 - q AGAINST p GRAPH FOR SILTY SAND (MC = 7,67 %)

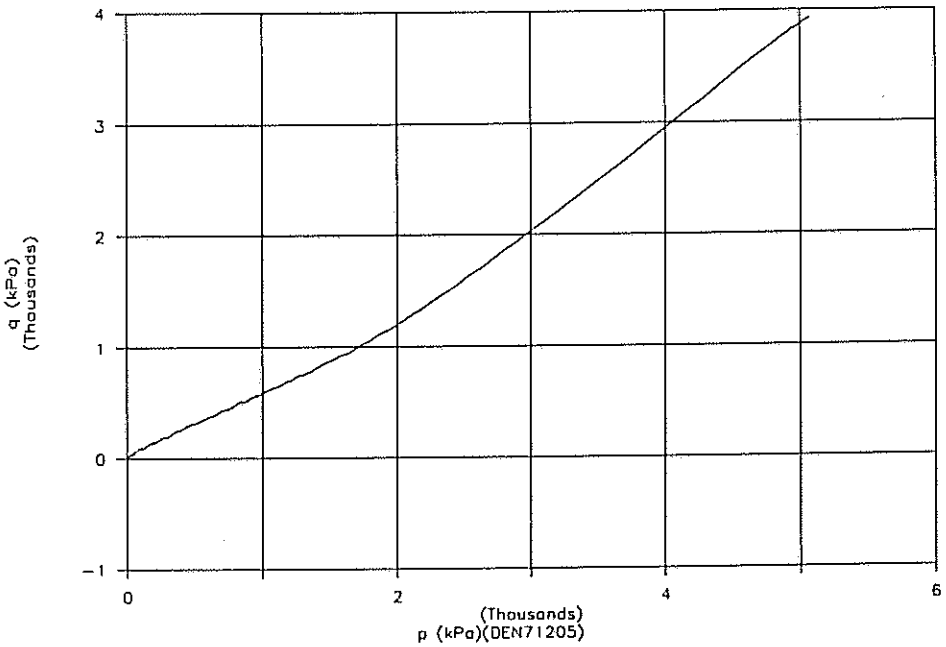

FIGURE E.3 - q AGAINST p GRAPH FOR DOLOMITIC SOIL (MC = 4,56 %)

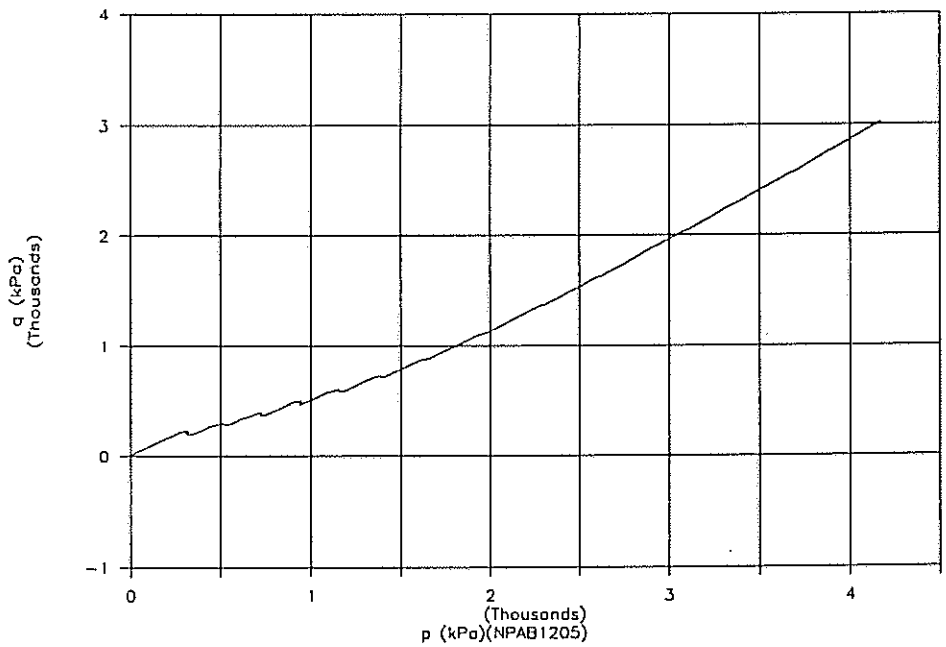

FIGURE E.4 - q AGAINST p GRAPH FOR DECOMPOSED DOLERITE (MC = 7,63 %)

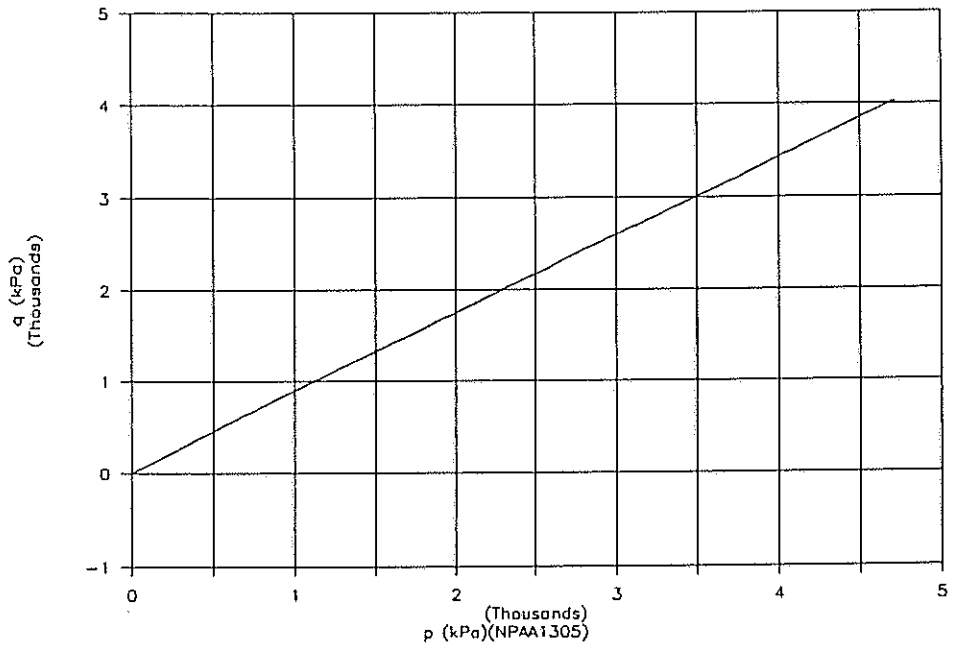

FIGURE E.5 - q AGAINST p GRAPH FOR DOLERITE CRUSHED STONE (MC = 4,51 %)

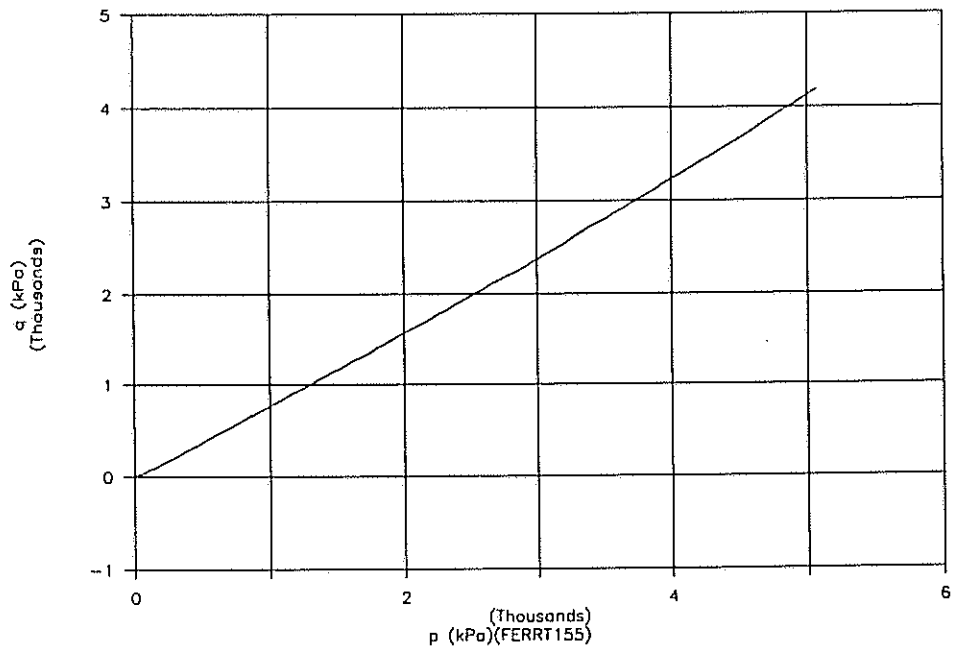

FIGURE E.6 - q AGAINST p GRAPH FOR QUARTIZITE CRUSHED STONE (MC = 5,29 %)

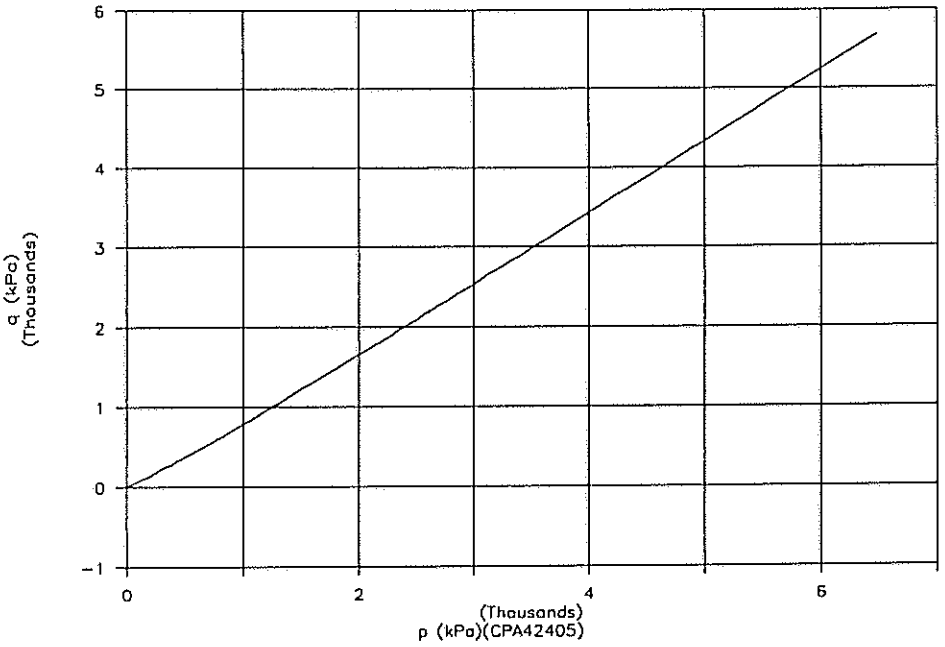

FIGURE E.7 - q AGAINST p GRAPH FOR CRUSHED ALLUVIAL GRAVEL (MC = 4,96 %)

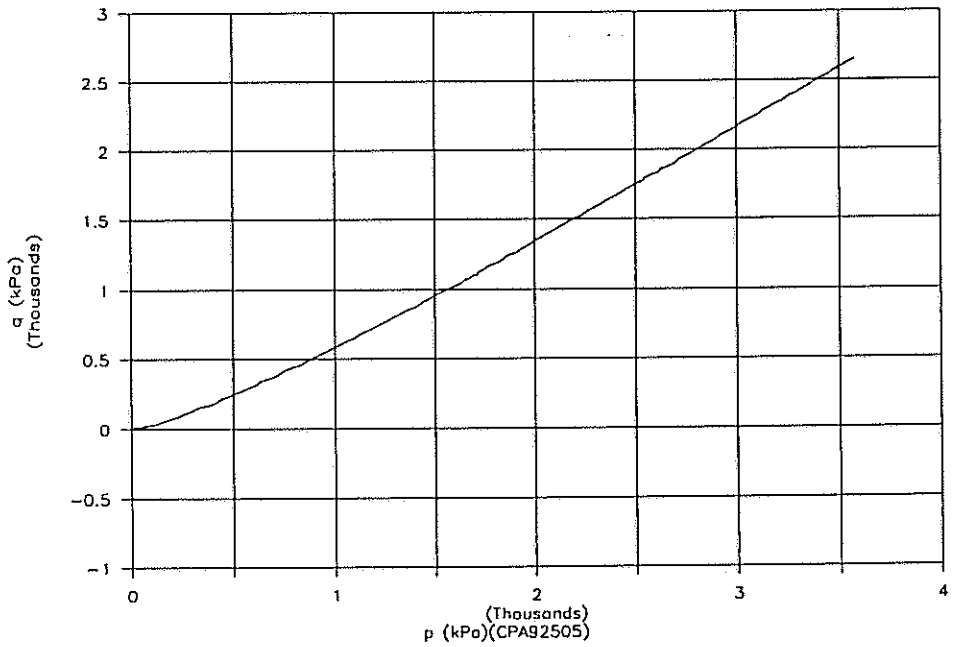

FIGURE E.8 - q AGAINST p GRAPH FOR CRUSHED HORNFELS (MC = 5,3 %)

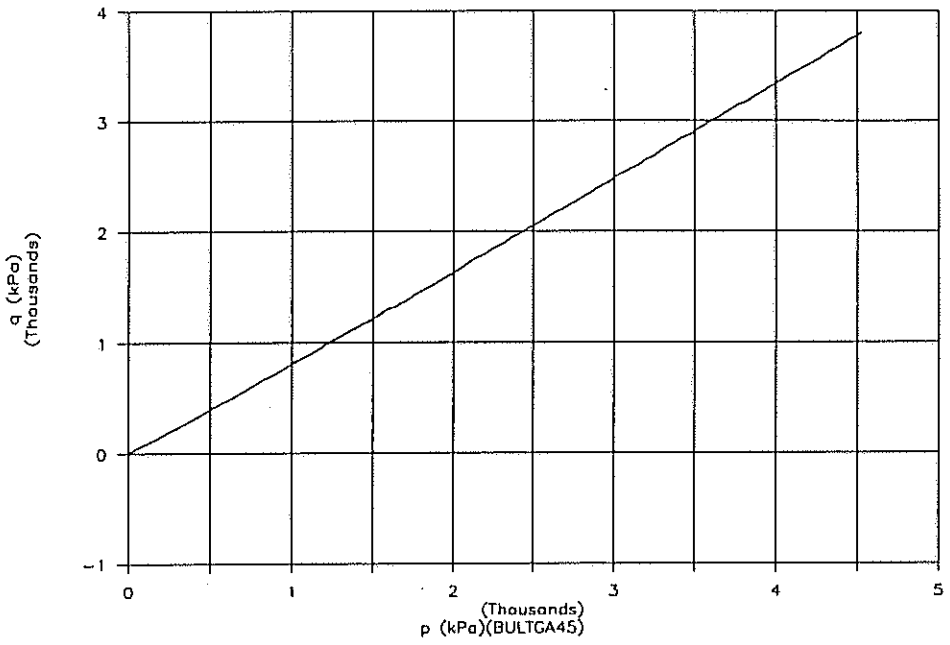

FIGURE E.9 - q AGAINST p GRAPH FOR BULTFONTEIN G1 MATERIAL (MC = 2,75 %)

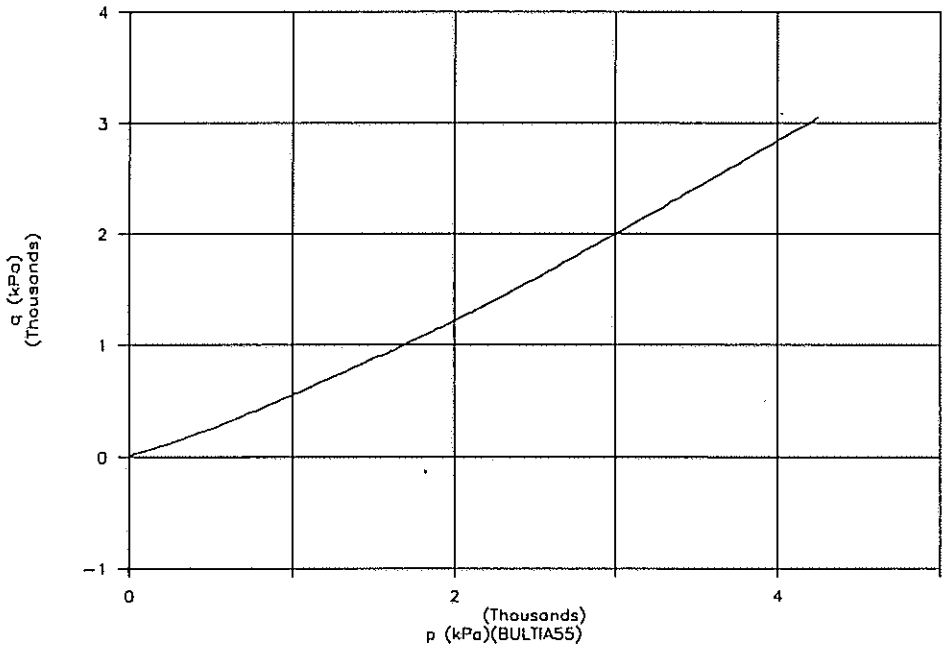

FIGURE E.10 - q AGAINST p GRAPH FOR BULTFONTEIN IN-SITU FERRICRETE MATERIAL (MC = 8,13 %)

APPENDIX F - Examples of Poisson's ratio against σ_1 for different classes of materials

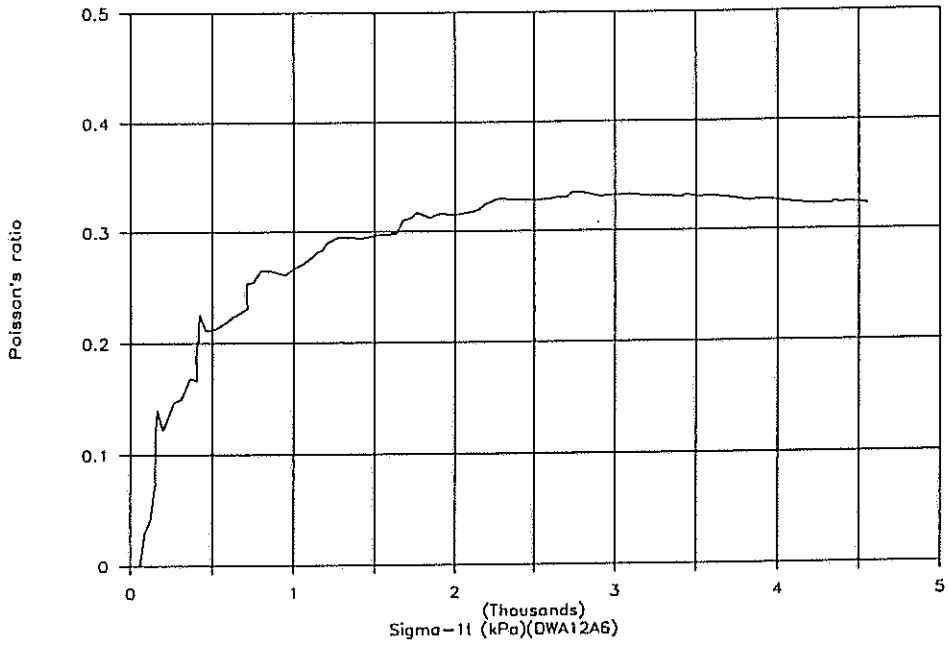

FIGURE F.1 - POISSON'S RATIO AGAINST σ_{1t} FOR SLIGHTLY PLASTIC SAND (MC = 10,79 %)

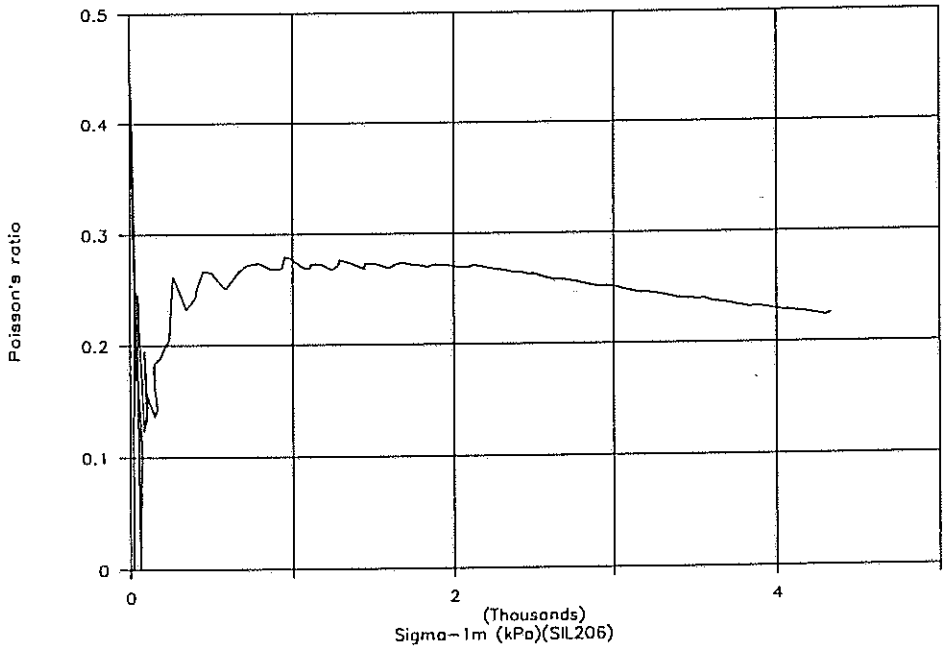

FIGURE F.2 - POISSON'S RATIO AGAINST σ_{1m} FOR SILTY SAND (MC = 7,67 %)

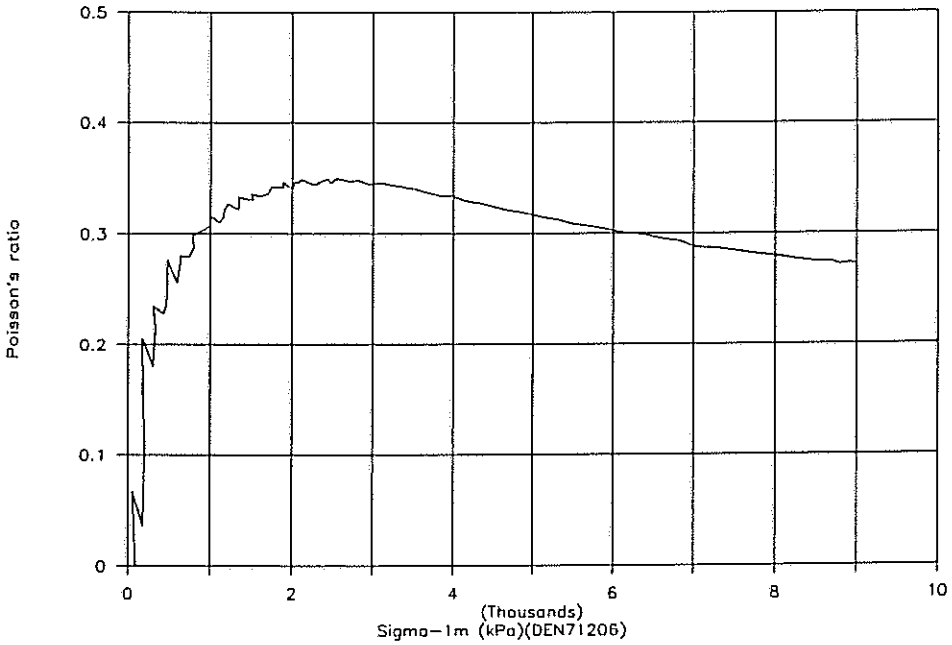

FIGURE F.3 - POISSON'S RATIO AGAINST σ_{1m} FOR DOLOMITIC SOIL (MC = 4,56 %)

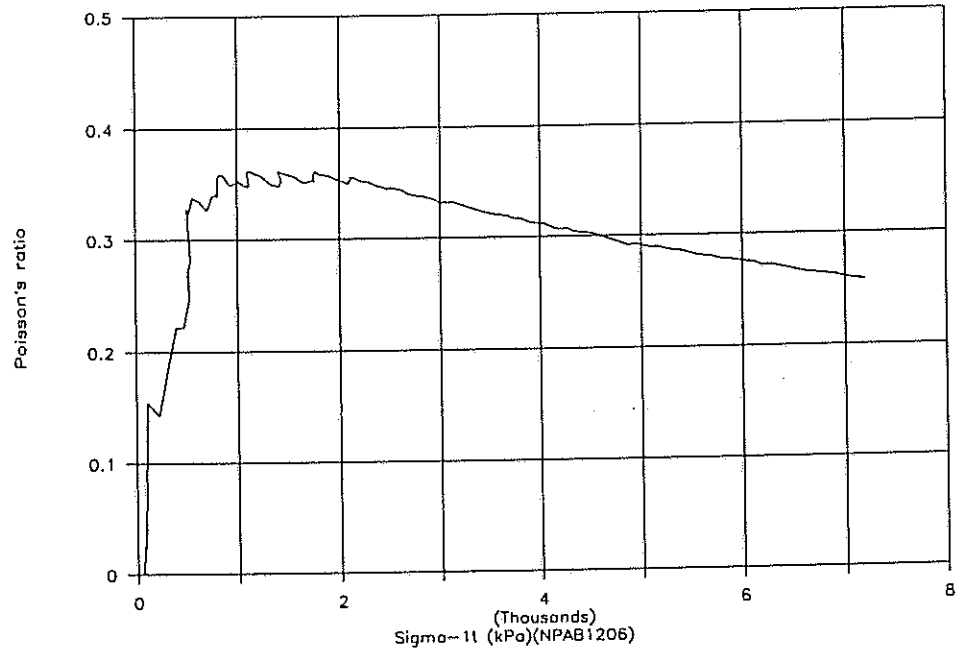

FIGURE F.4 - POISSON'S RATIO AGAINST σ_{1t} FOR DECOMPOSED DOLERITE (MC = 7,63 %)

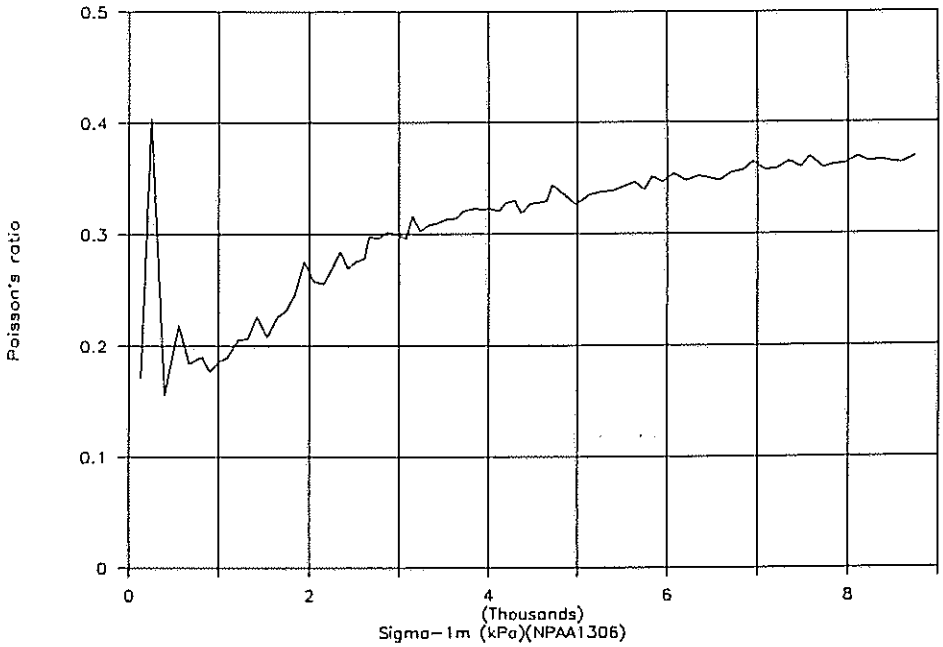

FIGURE F.5 - POISSON'S RATIO AGAINST σ_{1m} FOR DOLERITE CRUSHED STONE (MC = 4,51 %)

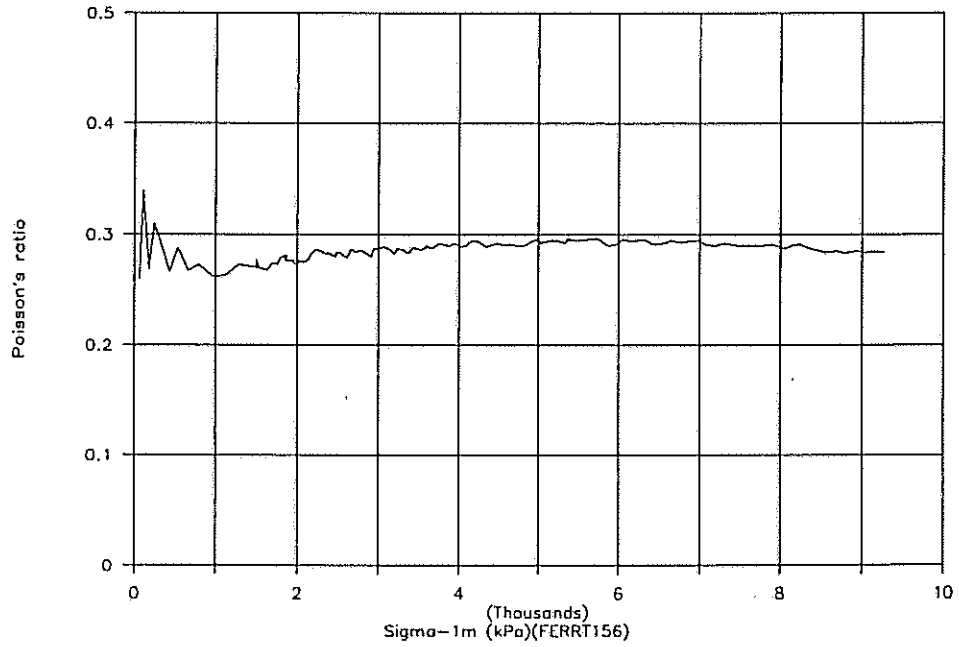

FIGURE F.6 - POISSON'S RATIO AGAINST σ_{1m} FOR QUARTZITE CRUSHED STONE (MC=5,29 %)

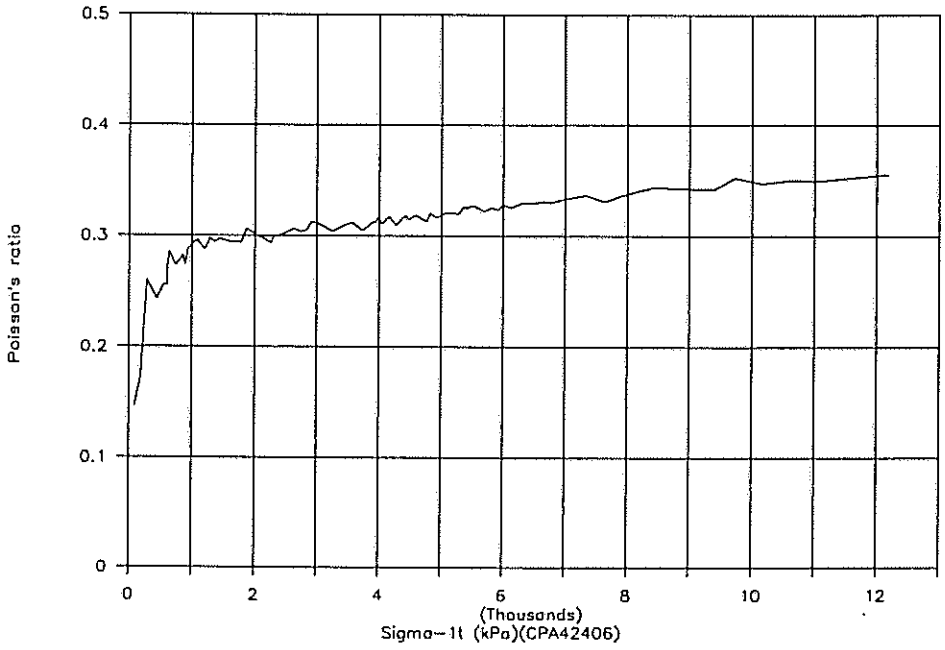

FIGURE F.7 - POISSON'S RATIO AGAINST σ_{1m} FOR CRUSHED ALLUVIAL GRAVEL (MC=4,96 %)

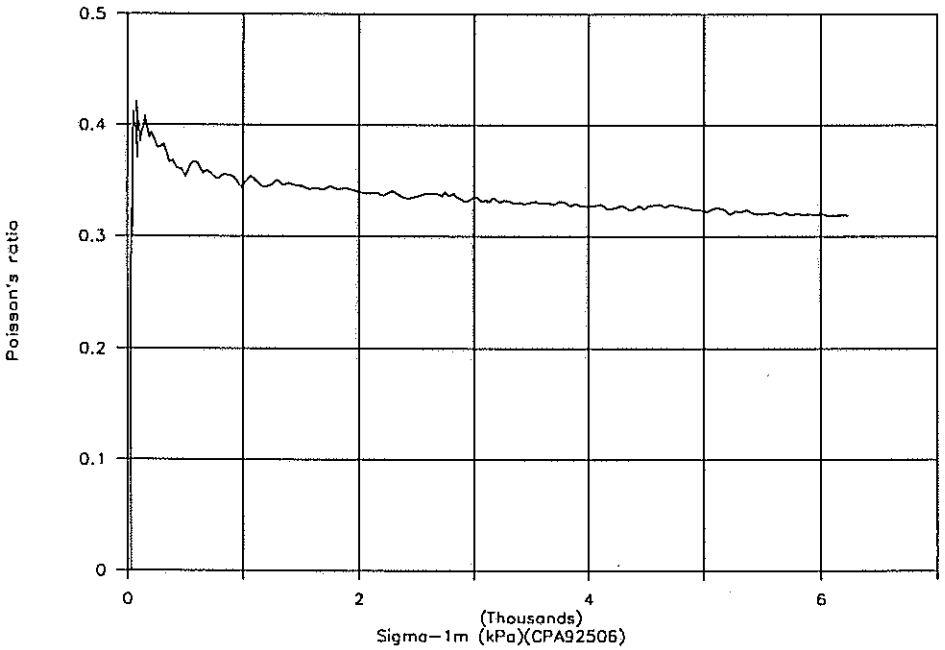

FIGURE F.8 - POISSON'S RATIO AGAINST σ_{1m} FOR CRUSHED HORNFELS (MC = 5,3 %)

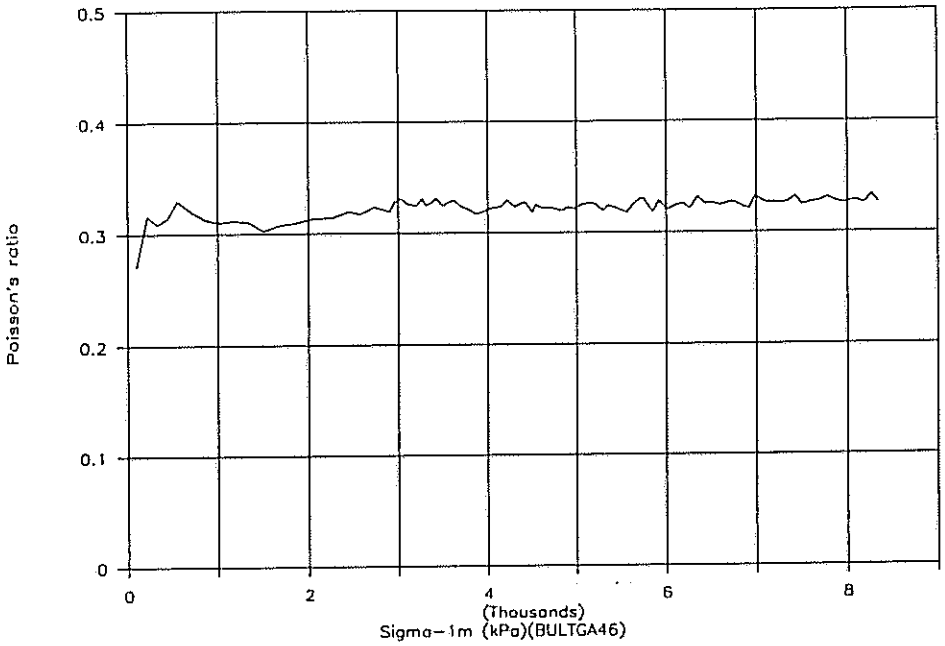

FIGURE F.9 - POISSON'S RATIO AGAINST σ_{1m} FOR BULTFONTEIN G1 MATERIAL (MC=2,75 %)

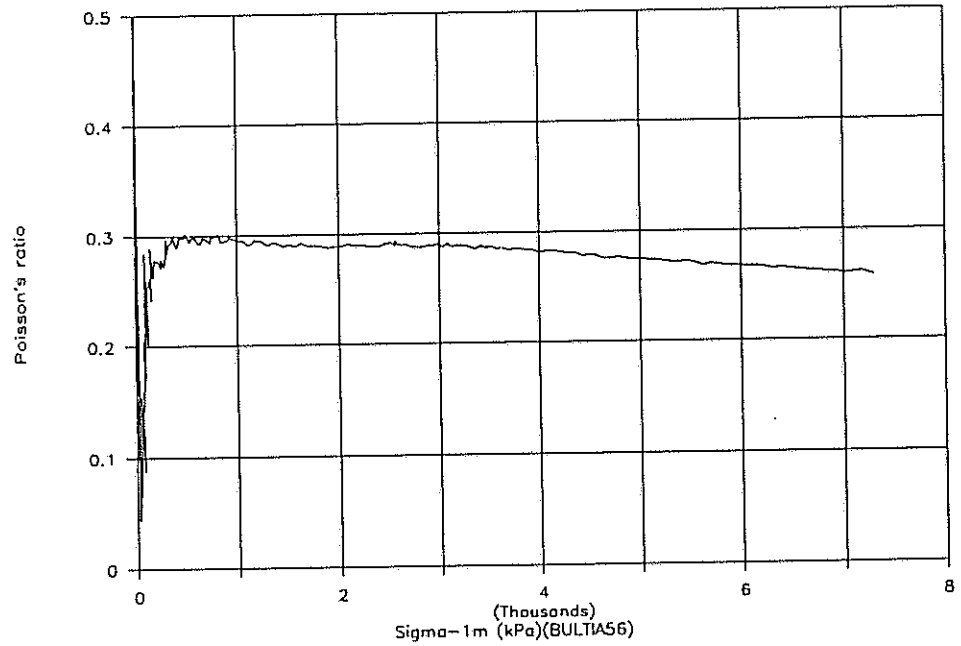

FIGURE F.10 - POISSON'S RATIO AGAINST σ_{1m} FOR BULTFONTEIN IN-SITU FERRICRETE MATERIAL (MC = 8,13 %)